

HYDRAULIC DESIGN OF LABYRINTH WEIRS

HENRY T. FALVEY

**ASCE
PRESS**

Hydraulic Design of Labyrinth Weirs

HENRY T. FALVEY

ASCE
PRESS

American Society of Civil Engineers
1801 Alexander Bell Drive
Reston, Virginia 20191-4400

Abstract: *Hydraulic Design of Labyrinth Weirs* is a comprehensive treatise on the hydraulic design of labyrinth spillways. The book begins with a section on the theory of labyrinth weirs and continues with detailed sections on significant factors that affect the discharge characteristics such as crest shape, weir height, and sidewall angle. The design of a labyrinth weir and modeling criteria is also covered. Several prototype labyrinth spillway configurations are included as examples.

Library of Congress Cataloging-in-Publication Data

Falvey, Henry T.

Hydraulic design of labyrinth weirs / Henry T. Falvey

p. cm.

Includes bibliographical references and index.

ISBN 0-7844-0631-6

1. Labyrinth weirs—Design and construction. I. Title

IV. Title.

TC555 .F35 2002

627'.883--dc21

2002027942

Any statements expressed in these materials are those of the individual authors and do not necessarily represent the views of ASCE, which takes no responsibility for any statement made herein. No reference made in this publication to any specific method, product, process, or service constitutes or implies an endorsement, recommendation, or warranty thereof by ASCE. The materials are for general information only and do not represent a standard of ASCE, nor are they intended as a reference in purchase specifications, contracts, regulations, statutes, or any other legal document. ASCE makes no representation or warranty of any kind, whether express or implied, concerning the accuracy, completeness, suitability, or utility of any information, apparatus, product, or process discussed in this publication, and assumes no liability therefore. This information should not be used without first securing competent advice with respect to its suitability for any general or specific application. Anyone utilizing this information assumes all liability arising from such use, including but not limited to infringement of any patent or patents.

ASCE and American Society of Civil Engineers—Registered in U.S. Patent and Trademark Office.

Photocopies: Authorization to photocopy material for internal or personal use under circumstances not falling within the fair use provisions of the Copyright Act is granted by ASCE to libraries and other users registered with the Copyright Clearance Center (CCC) Transactional Reporting Service, provided that the base fee of \$18.00 per chapter is paid directly to CCC, 222 Rosewood Drive, Danvers, MA 01923. The identification for ASCE Books is 0-7844-0631-6/03/ \$18.00 per chapter. Requests for special permission or bulk copying should be addressed to Permissions & Copyright Dept., ASCE.

Copyright © 2003 by the American Society of Civil Engineers. All Rights Reserved.
Manufactured in the United States of America.

Cover photo: Labyrinth weir, Tongue River Dam, Montana, USA. Photo by the author.

Preface

This book is the result of a demand for a comprehensive treatise on the hydraulic design of labyrinth spillways. Both practicing engineers and researchers should find the book useful in the hydraulic design of labyrinth weirs.

The book begins with a section on the theory of labyrinth weirs and continues with detailed sections on significant factors that affect the discharge characteristics of labyrinth weirs, such as crest shape, weir height, and sidewall angle. The most common design curves are presented in Chapter 4. From these, a recommendation was developed for a single design curve to be used in future designs. Chapter 7 is devoted entirely to design, which should lead a designer to determine the optimum configuration to meet specified hydrologic criteria. If the designer considers that the configuration is sufficiently unique that a model study is required, Chapter 11 is devoted to modeling criteria. Following these criteria will ensure that the model is conducted in a manner that will provide accurate predictions of prototype performance. To guide the designer, several prototype labyrinth spillway configurations have been included as examples of what has been studied or installed in the past.

During the preparation of this book, many long-held concepts were examined and revised in an effort to clarify them. For instance, the idea of interference was completely changed through the discovery of a paper that studied interference using an entirely new approach. Similarly, a careful examination of the original paper on nappe oscillation revealed that the problem was actually two separate problems that need separate solutions. Finally, the definition of which head to use in the computations was clarified.

The book would not have been possible without the input from many engineers and consultants. Special thanks are extended to F. Lux; Aubian Engineering Inc.; J. Paul Tullis; Utah State University; Kathy Frizell; the U.S. Bureau of Reclamation; Brian Tracy; the Corps of Engineers; John J. Cassidy, Cassidy Consultants; Sal Todaro, URS; and Michael Stevens, private consultant. Their helpful suggestions and input of additional data were extremely beneficial in completing gaps in data and guiding the direction of the book. I am grateful for the input from Professor Pinheiro on the unit costs for specific features in the metric version of the Excel spreadsheet program, as well as some of the photos of dams in Portugal. Professor Indlekofer was also a great help in guiding my thoughts on interference.

Nomenclature

A	Area
A_c	Contact Area
A_1	Coefficient for Tullis Curve
A_2	Coefficient for Tullis Curve
A_3	Coefficient for Tullis Curve
A_4	Coefficient for Tullis Curve
A_5	Coefficient for Tullis Curve
B	Length of Sidewall
B_w	Batter on Sidewall
$C(l)$	Disturbance Coefficient
C'	Discharge Coefficient with Interference
C_d	Discharge Coefficient
C_d'	Discharge Coefficient Referred to Conditions Upstream of Weir
C_{ds}	Downstream Saturation Level
C_k	Discharge Coefficient from Kindsvater and Carter
C_m	Mean value of Interference Effect
C_g	Fusegate Discharge Coefficient
C_p	Megalháes Discharge Coefficient
C_r	Reduced Discharge Coefficient
C_s	Saturation concentration
C_u	Upstream Saturation Level
C_T	Tullis Discharge Coefficient
C_w	Darvas Discharge Coefficient
C_x	Lux Discharge Coefficient
C_1	Interference Coefficient
C_2	Interference Coefficient
D	Hydraulic Depth
D_c	Depth of Cutoff Wall
D_s	Depth of Sheet Pile Wall
D_t	Throw Distance of Jet
E	Efficiency of Air Entrainment
E_f	Energy Flux
E_T	Efficiency of Air Entrainment at Any Temperature
E_w	Total Energy at Any Point on Sill
E_{20}	Efficiency of Air Entrainment at 20 degrees Celsius
F_b	Free Board Distance
F_{us}	Upstream Froude Number
H_b	Jet Breakup Length
H_d	Design Head
H_o	Total Head Upstream of Weir
H_{pL}	Piezometric Head of Lateral Flow Measured Relative to Invert

H_t	Total Head on Centerline of Channel
K	Pressure Correction Factor
K_1	Crest Radius Coefficient
K_2	Crest Radius Coefficient
L	Length along Weir
L_d	Length of Disturbance
L_{de}	Effective Length of Disturbance
L_{dim}	Ratio of Length to Upstream Head
L_e	Equivalent Crest Length
M	Apron Height
N	Total Number of Flow Depth Measurements in Main Channel
P	Weir Height
Q	Discharge
Q_L	Discharge over Side Weir
Q_N	Discharge over an Equivalent Straight Weir
Q_o	Inflow Discharge
Q_s	Submerged Discharge
R	Radius of Crest
R_h	Hydraulic Radius
S	Depth of Weir in Flow Direction
S_e	Gradient of Dissipated Energy
S_o	Bottom Slope
S_f	Friction Slope
T	Free Surface Width
T_s	Thickness of Cutoff Wall or Thickness of Floor Slab
T_w	Thickness of Weir Wall
U	Velocity of Lateral Flow
V	Average Velocity of Main Flow
V_a	Volume of Air Entrained
V_j	Jet Velocity
V_{us}	Upstream Velocity
V_x	Axial Velocity Component (With Flow Direction)
V_y	Normal Velocity Component (Perpendicular to Flow Direction)
W	Width of One Cycle of Labyrinth Weir
W_c	Width of Channel
X	Crest Coordinate in Flow Direction
Y	Crest Coordinate in Downward Vertical Direction
Y_a	Upstream or Downstream Height of Apron
Z_c	Crest Elevation
Z_w	Upstream Water Surface Elevation
Z_r	Reservoir Elevation
F	Froude Number
W	Weber Number
a	Half Apex Width
g	Gravitational Acceleration

h	Depth of Flow over Crest
h_a	Mean Depth of Flow over Weir
h_d	Submergence Depth
h_e	Equivalent Head on Weir
h_m	Measured Flow Depth over Crest
h_o	Weir Head at Steady State
h_u	Upstream Head on Weir Crest
k_t	Bulk Liquid Film Coefficient
m	Magnification
n	Number of Labyrinth Cycles
q	Lateral Flow Rate Per Unit Length Of Channel
r	Aeration Deficit Ratio
r_T	Aeration Deficit Ratio at any Temperature
r_{20}	Aeration Deficit Ratio at 20 degrees Celsius
t	Time
t_s	Time to Stabilize
t_c	Bubble Contact Time
x	Longitudinal Coordinate Along Channel Bottom Direction
y	Coordinate Perpendicular To X On A Vertical Plane
α	Sidewall Angle
α_{max}	Maximum Sidewall Angle
α_v	Velocity Distribution Factor
α_d	Aeration Deficit Ratio Constant
β	Momentum Correction Factor
β_p	Crest Pressure Coefficient
γ	Specific Weight Of Fluid
η	Pressure Head Coefficient
θ	Angle Between Channel Bottom And A Horizontal Plane
ρ	Water Density
σ	Interfacial Surface Tension
τ_{os}	Boundary Shear Stress Along The X Direction
μ_w	Magalhães Discharge Coefficient
ϕ	Acute Angle between Channel Centerline and Weir Crest
ϕ_c	Angle between Lateral Flow Vector and Channel Centerline

ΔX Distance Between Stations

Contents

Preface	iii
Nomenclature	iv
Chapter 1: Introduction	1
Purpose	1
Types of Spillways	1
Flow Characteristics	6
Other Purposes	6
Previous Installations	7
Chapter 2: Analytic Development	9
Approaches	9
Side Channel Spillways	9
Equations of Motion	9
Energy Equation	11
Momentum Equation	13
Discharge Coefficient	14
Skew Weirs	15
Labyrinth Weirs	16
Conclusions	16
Chapter 3: Nappe Interference	19
Introduction	19
Theory	20
Model Studies	24
Chapter 4: Crests Shapes	31
Types of Crests	31
Theoretical Minimum Value of the Discharge Coefficient	32
Discharge Characteristics	32
Sharp Crest and Flat Top Profile	32
Quarter-Round Profile	33
Half-Round Profile	34
Nappe Profile or Ogee Crest Profile	37
Chapter 5: Design Curves	41
Introduction	41
Basic Parameters	42
Definition of Upstream Head	43
Design Curves Derived from Model Studies	44
Taylor	44

Darvas	47
Megalhães and Lorena	49
Lux	50
Tullis et al.	53
Example Computations	54
From Hay and Taylor	55
From Darvas	55
From Megalhães and Lorena	55
From Lux	55
From Tullis et al.	55
Critique of Design Curves	56

Chapter 6: Downstream Chute61

Introduction	61
Supercritical Waves	61
Aprons	64
Submergence	67

Chapter 7: Nappe Oscillation69

Introduction	69
Nappe Vibration	69
Case Study	70
Surging Flows	74
Conclusions	75

Chapter 8: Design77

Significant Parameters	77
General Guidelines for Parameter Selection	77
Headwater Ratio	77
Vertical Aspect Ratio/Sidewall Angle	77
Magnification Ratio	78
Sidewall Angle/Magnification	78
Efficacy	79
Apex Ratio	81
Crest Shape	82
Interference Length Ratio	82
Approach Flow Conditions	82
Downstream Channel	84
Layout and Quantities	84
Dimensions	85
Quantities	86
Discharge Coefficient	87
Design Procedure	88
Steps	88
Spreadsheet	89

Chapter 9: Sedimentation and Ice95

Sedimentation Fundamentals	95
Boardman	96
Hellsgate	97
Garland Power Canal	98
Conclusions	100
Ice	100
Chapter 10: Aeration	103
Introduction	103
Theory	104
Falling Jet Types	104
Performance	106
Conclusions	107
Chapter 11: Special Cases	109
Introduction	109
Fusegates™	109
Detention Dams	113
Sheet Piling	115
Chapter 12: Modeling Procedures	119
Introduction	119
Systematic Errors	119
Scale Effects Caused by Surface Tension	119
Method of Operation	121
Random Errors	123
Conclusions	124
Application	124
Case Study	125
Appendix A	131
Appendix B	145
Bibliography	149
Index	161

This page intentionally left blank

Chapter 1

Introduction

Purpose

The purpose of this book is to present the theory, a review of past studies, and a method of designing labyrinth weirs. Although this book provides design curves, experience has shown that site-specific model studies are usually warranted. Often, site conditions vary so much from the idealized conditions that design curves are not applicable. A section on the techniques of modeling is included to give guidance in choosing model scales if a site-specific model is desired.

Types of Spillways

Most spillways consist of some form of a weir. The weirs are normally placed perpendicular to the flow direction. The most significant parameters in determining the capacity of a weir are its height relative to the upstream depth, the crest shape, and the crest length. Here, capacity refers to the flow rate or discharge for a given depth of flow over the crest of the weir. Of these parameters, the crest length has the greatest influence on the spillway capacity.

As the emphasis in dam safety has increased, many spillways must be rehabilitated to increase their capacity without changing the reservoir storage. However, for many spillways, the width of the approach channel or the downstream chute cannot be widened. To increase the crest length but keep the spillway width constant, the crest is often placed at an angle to the centerline of the chute. If the crest is placed parallel with the chute centerline, it is called a side channel spillway, as shown in Figure 1.

The length can be increased further and can still keep the downstream dimension small by folding the weir into several sections. One implementation of this idea is the duckbill spillway, as shown in Figure 2.

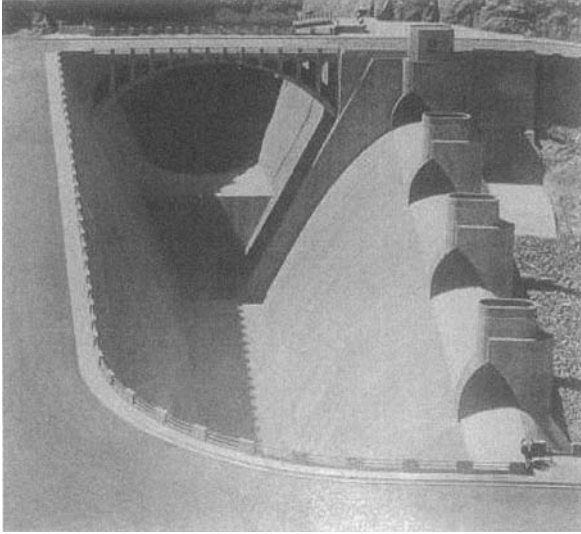


Figure 1. Side Channel Spillway - Arizona Spillway at Hoover Dam, USA. From *Dams and Control Works*, 2d Ed., Feb 1938. Permission granted to use photo from USBR.

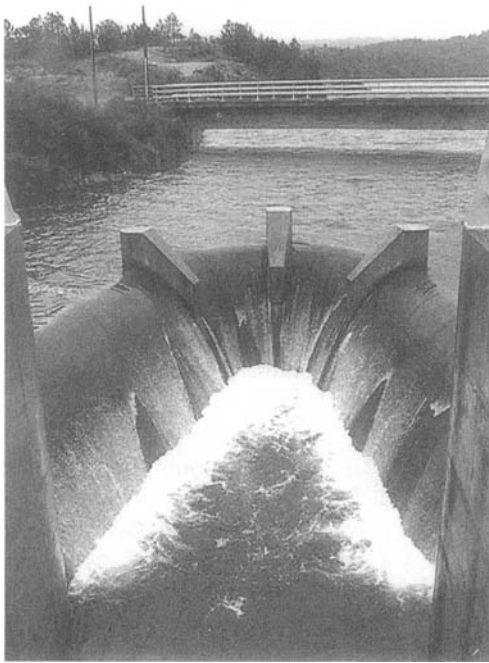


Figure 2. Duckbill Spillway - Apartadura Dam, Portugal. Permission to use photo granted by A. Pinheiro

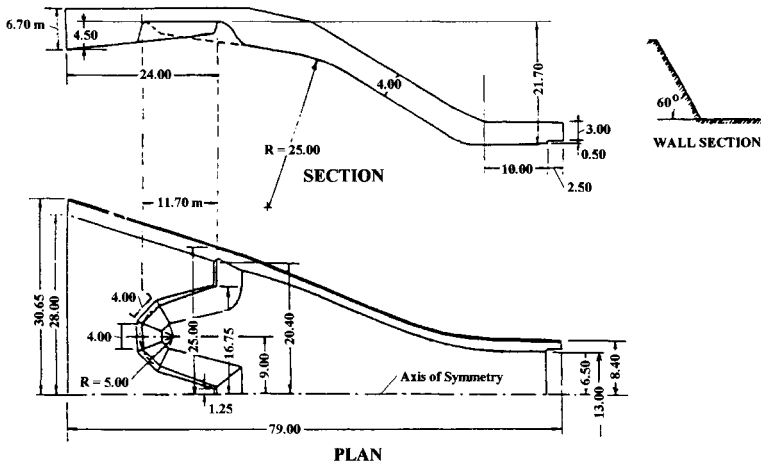


Figure 3. Symetain Hydroelectric Powerplant Spillway - Congo after Tison, G., and Franson, T., (1963), "Essais sur déversoirs de forme polygonale en plan." *Review C. Tijdschrift*, Brussels, III(3), 38-51 (in French).

Several cycles of this type of spillway can be placed together to further increase the spillway length, as shown in Figure 3.

A variation of the duckbill spillway is the bathtub spillway, as shown in Figure 4. This shape is rectangular instead of the approximately triangular shape of the duckbill.

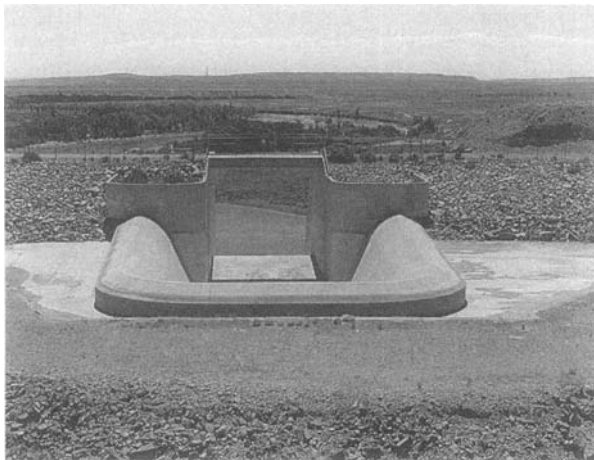


Figure 4. Bathtub Spillway - Fontenelle Dam, USA. Photo by author

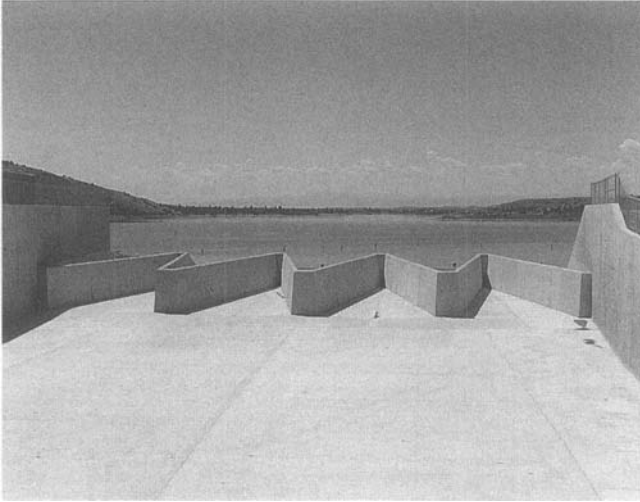


Figure 5. Labyrinth Weir - Tongue River Dam, USA, Photo by author

Several cycles of the bathtub shape can be placed side by side. These weirs are called corrugated, accordion, or folded weirs. If several cycles of the duckbill spillway are placed side by side, the weir is called a labyrinth spillway, as shown in Figure 5.

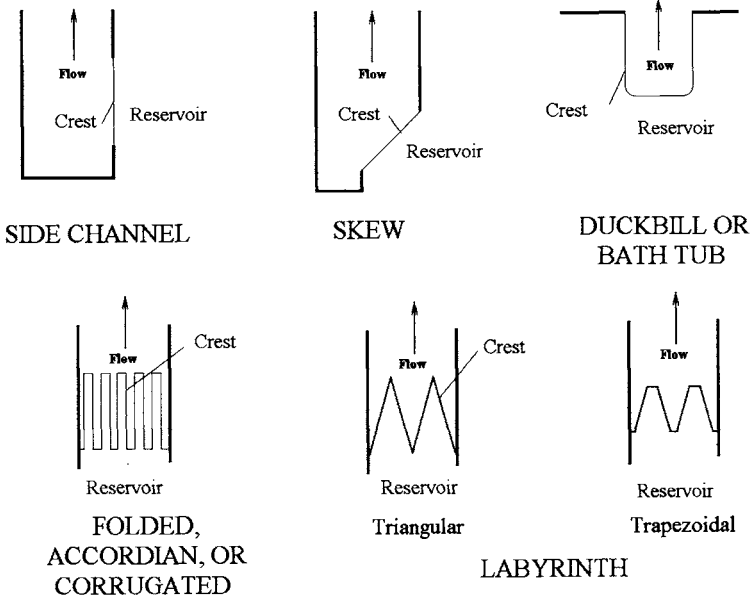
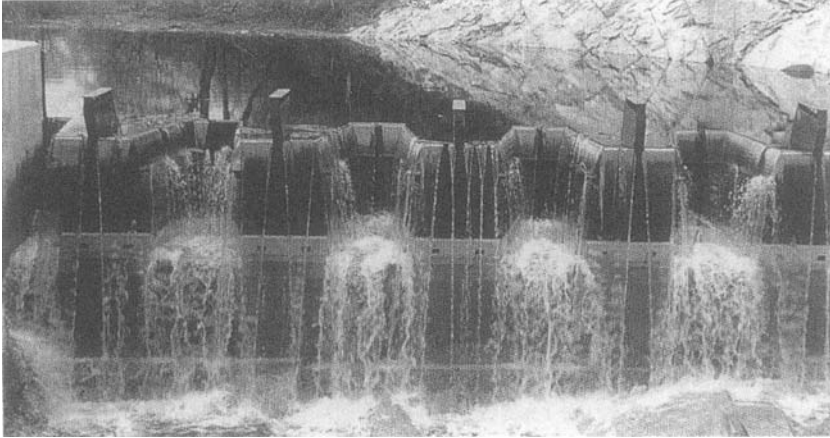
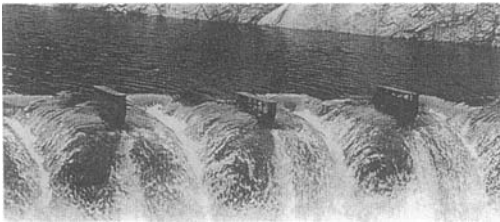


Figure 6. Classification of Spillway Shapes

Figure 6 shows the general classification of spillway shapes designed to increase capacity for a given reservoir elevation in plan view. A trapezoidal or triangular shape is more efficient than the rectangular planform. Here, the term planform refers to the shape or form of the weir crest shown in the plan view.



a. Fusegates operating as a labyrinth weir



b. Fusegate well just beginning to fill



c. Fusegate tipping

Figure 7. Fusegates™, Permission to use photos from Hydroplus International

A special type of labyrinth weir is known as a Fusegate™. This was developed in France as an alternative to fuse plugs. A Fusegate™ installation is identical in planform to that of a trapezoidal labyrinth weir, as shown in Fig. 7(a). However, as the reservoir level rises, water flows into a well beneath the gates through a well located on the lip of the gate, as shown in Fig. 7(b). The well leads to a chamber beneath the gates. When the pressure in the chamber increases sufficiently, the individual elements of the installation tip into the flow, as shown in Fig. 7(c). As the gates tip, they create a large flow area that can be used to pass extremely large flood events. Fusegates™ are constructed according to the manufacturer's standardized dimensions and can be made of either steel or concrete.

Flow Characteristics

The streamlines over weirs at an acute angle to the flow have peculiar characteristics that are not observed with flows over a straight weir. With straight weirs, all streamlines are perpendicular to the crest and are two-dimensional. However, with weirs placed at an angle to the flow, the streamlines are three-dimensional. The three-dimensional flow is one in which the streamlines under the nappe are almost perpendicular to the crest, whereas at the free water surface the streamlines are directed in the downstream direction.

The flow over labyrinth weirs is complicated further by the interference of the jets at the upstream apex of the labyrinth. That is, at high flows, the jets from adjacent crests strike each other. This creates a nappe that is not aerated and can decrease the discharge coefficient of the weir. The degree of impact increases as the angle between the crests decreases and as the flow depth over the crest increases. As a result, for most labyrinth weirs, the underside of the nappe is aerated only for low flow depths.

The interference of the jets from adjacent crests means that labyrinth weirs become less and less effective as the reservoir level rises. At some depth, the flow over a labyrinth weir is almost the same as the flow over a straight weir.

Other Purposes

Although labyrinth weirs are used to increase spillway capacity for a given downstream channel width, this is not the only purpose for them. Labyrinths are also used to control water quality by aerating the flow. For small drops, a labyrinth shape is a more efficient aerator than is a straight weir. For large drops, a labyrinth weir can cause the overflowing water to reach about 70% of the difference between the upstream dissolved air level and saturation. Thus, a labyrinth is effective in either aerating the flow or de-aerating the flow.

Labyrinth weirs are also effective as drop structures on canal systems. If used on a canal system, a set of labyrinth weirs will serve as energy dissipators and, at the same time, maintain a more constant flow depth in the canal than could be achieved with a conventional drop structure. To date, a series of labyrinth drop structures has not been implemented on a canal system.

Studies with fish ladders at low-head agricultural and municipal diversion dams show that velocities of certain sections of a fish channel were lower than with straight weirs. The lower velocities mean that the fish have an increased capability for upstream movement.

Previous Installations

Labyrinth weirs have been used for a long time. Appendix A gives a few of the prototype installations and their dimensions that have appeared in the literature. All of these installations were developed using site-specific model studies. This list is not intended to be exhaustive. It is a representative sample of the types of labyrinth weirs that have been constructed worldwide.

This page intentionally left blank

Chapter 2

Analytic Development

Approaches

The analytic development that describes the flow over labyrinth weirs follows a stepwise progression from side channel weirs, to skew weirs, and finally to labyrinth weirs. In this manner, the assumptions at each step can be examined, and the complications that are introduced by the more complex geometries can be more easily understood.

Two approaches have been used to develop the equations for flow over the various weirs: constant energy and momentum. With the constant energy approach, coefficients have to be adjusted to make the theory match the experimental results.

In the following discussions, the term head refers to the upstream water depth over the crest elevation. The term total head or reservoir head refers to the upstream water depth plus the upstream velocity head over the crest elevation.

Side Channel Spillways

Equations of Motion

The flow over side channel spillways was summarized nicely in a set of papers published by Ackers, Allen, Collinge, and Frazer in Volume 6 of the *Proceedings of the Institution of Civil Engineers* (1957). The most comprehensive treatment of spatially varied flow was developed by Yen and Wenzel (1970). Since then, others such as Ramamurthy et al. (1978), Ramamurthy and Carballada (1980), Hager (1987), and Robertson and McGhee (1993), to cite a few, have made significant contributions to the subject.

The flow over a side channel requires some simplifications in the development of an equation that describes the flow, because the direction of the jet over the weir is difficult to define. As Figure 1 shows, the direction of the jet varies from the upstream end of the weir to the downstream end. In addition to this variation, the direction of the jet also varies in the vertical plane from the weir crest to the water surface.

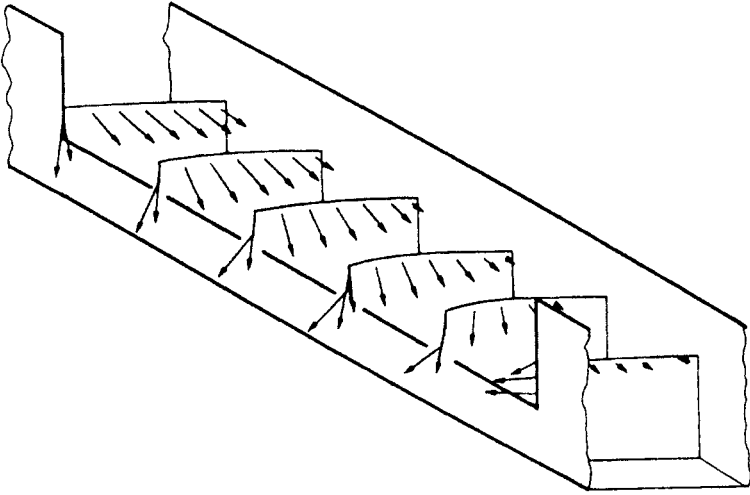


Figure 1. Velocity Vectors on a Side Channel Spillway. After Hager, W.H., (1987). "Lateral outflow over side weirs." *American Society of Civil Engineering, Journal of Hydraulic Engineering*, 113(4), 491-504, with permission of ASCE.

Ramamurthy and Carballada (1980) assumed that the axial vector component, V_x , is equal to the mean upstream velocity in the channel and that the normal component, V_y , is equal to

$$V_y = \sqrt{2 \cdot g \cdot h} \quad (1)$$

in which g = the acceleration of gravity; and h = the head on the weir. The assumption is accurate for sections in the middle portion of the weir, but does not account for end effects as shown in figure 2.

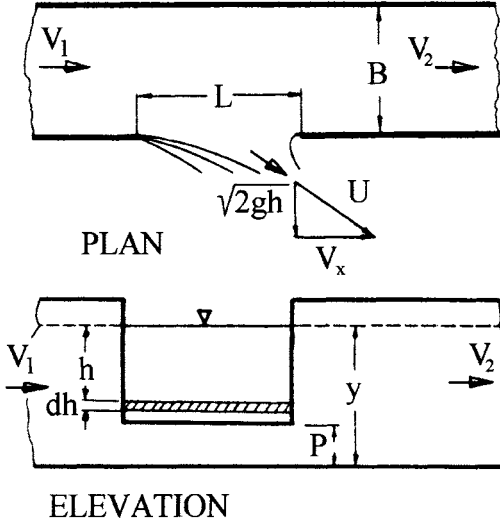


Figure 2. Side channel velocity distribution from Ramamurthy, A.S., and Carballada, L., (1980). "Lateral weir flow model," *American Society of Civil Engineering, Journal of Irrigation and Drainage*, 106(1), 9-25, with permission from ASCE.

Two approaches have been used to develop the equations for flow over a side channel weir: constant energy and momentum. Various investigators investigated the flow over side channel weirs using simplifications of the equations by Yen and Wentzel (1970). Only the momentum equation is valid when a hydraulic jump occurs in the main channel.

Energy Equation

Yen and Wentzel (1970) give the energy equation as

$$\frac{dh}{dx} = \frac{S_o - S_e + \frac{q}{VA} \left(\frac{U^2}{2g} - \frac{3\alpha_v V^2}{2g} + H_{pl} - H \cos(\theta) \right) - \frac{V^2}{2g} \frac{d\alpha_v}{dx} - H \frac{d \cos(\theta)}{dx}}{\cos(\alpha) - \frac{\alpha_v V^2}{gD}} \quad (2)$$

in which A = cross sectional area; D = hydraulic depth = A/T; E_f = energy flux; H_{pl} = piezometric head of lateral flow measured with respect to channel bottom; U = velocity of lateral flow; V = average velocity of main flow; S_e = gradient of dissipated energy defined as

$$S_e = - \frac{1}{\gamma AV} \frac{dE_f}{dx} \quad (3)$$

S_o = the bottom slope; T = free surface width; g = acceleration of gravity; H = depth of flow section measured along normal direction; x = longitudinal coordinate along channel bottom direction; y = coordinate perpendicular to x on a vertical plane; q = lateral flow rate per unit length of channel; α_v = kinetic energy flux correction factor; θ = angle between channel bottom and a horizontal plane; γ = specific weight of fluid.

Borghei et al. (1999) simplified equation (2) to

$$\frac{dh}{dL} = \frac{S_o - S_f - \frac{\alpha Q}{gA^2} \frac{dQ}{dL}}{1 - \frac{\alpha Q^2 W_c}{gA^3}} \quad (4)$$

in which W_c = the channel width; L = the length along the weir; Q = the discharge; S_f = the friction slope; and α_v = a velocity distribution factor.

Borghei (1999) gives the discharge over the weir as

$$\frac{dQ}{dL} = q = C_d \frac{2}{3} \sqrt{2g} (H_t - P)^{3/2} \quad (5)$$

in which C_d = the discharge coefficient; P = the crest height; and H_t = the total head on the centerline of the channel.

De Marchi (1943) assumed

- Uniform flow, that is, $S = S_f$,
- A uniform cross section,
- No variation in the velocity coefficient along the length of the weir,
- The discharge equation for a straight weir is applicable to the side channel weir, and
- The total energy line is parallel to the weir sill and the channel bed.

The equation that was integrated is

$$\frac{dh}{dL} = \frac{\frac{Q}{gA^2} \frac{dQ}{dL}}{\frac{Q^2 W_c}{gA^3} - 1} \quad (6)$$

The solution of this equation agreed well with empirical observations for subcritical flow.

Ackers (1957) modified De Marchi's equation by writing the total energy, E_w , at any point on the sill as

$$E_w = \frac{\alpha_v V^2}{2g} + \eta h \quad (7)$$

in which η = a pressure head coefficient.

The head corresponds to the head over the crest referred to the centerline of the channel. Using the experiments of Coleman and Smith (1923), Ackers concluded for supercritical flow that

- The discharge coefficient for straight weirs applied to side channel weirs.
- The velocity coefficient, α_v , varies between 1.15 and 1.40.
- The pressure head coefficient, η , is equal to 0.8.

Collinge (1957) used experimental studies to confirm the equation of De Marchi with both subcritical and supercritical flow. A reasonable correlation between the experiments and the equation was found. However, the discharge coefficient decreased by a few percent as the velocity of approach in the channel increased.

Momentum Equation

Yen and Wenzel (1970) give the momentum equation as

$$\frac{dh}{dx} = \frac{S_o - \frac{\tau_{ox}}{\gamma R} + \frac{q}{gA} (U \cos(\phi_c) - 2\beta V) - \frac{V^2}{g} \frac{d\beta}{dx} - h \frac{d(K \cos(\theta))}{dx}}{K \cos(\theta) \left(1 + \frac{h}{D}\right) - \frac{\beta V^2}{gD}} \quad (8)$$

in which K = pressure correction factor defined as

$$K = \frac{1}{hA} \int_0^h h(h-y) dy \quad (9)$$

R_h = hydraulic radius; β = the momentum coefficient in the flow direction; τ_{ox} = boundary shear stress along the x direction; and ϕ_c = angle between velocity vector of lateral flow and channel centerline.

In equations 2 and 8, the invert of the channel can be sloped, and the width of the channel does not have to be constant.

Robinson and McGhee (1993) obtained a good correlation between analytic and empirical results with a simplified version of equation 8 using the Runge-Kutta technique. The equation they used is given by

$$\frac{dy}{dx} = \frac{S_o - S_f + \frac{qV}{gy}}{1 - \frac{V^2}{gy}} \quad (10)$$

Robertson and McGhee (1993) also integrated the momentum equation given by equation 10 with a constant weir coefficient, C_d , of 0.6. Their results, which included examples using subcritical, supercritical flows and a hydraulic jump in the weir section, compared favorably with experimental observations.

Discharge Coefficient

For shallow depths of flow over a side weir, the discharge coefficient is similar to flow over a sharp crested weir. In this case, the discharge coefficient is a function of the weir height and the flow depth over the weir if surface tension effects are neglected. That is

$$C_d = f\left(\frac{h}{P}\right) \quad (11)$$

In this case, the flow is perpendicular to the crest of the weir. However, as the flow increases, the flow over a long crest takes on a three-dimensional form in which the streamlines at the weir crest are almost perpendicular to the crest, whereas those near the water surface are directed in the downstream flow direction. With a short crest, the streamlines at the water surface are still almost perpendicular to the weir crest.

Pinheiro and Silva (1999), using dimensional analysis, concluded that the three most important parameters are the approach flow, the ratio of the flow depth to the weir height, and the weir length to the upstream velocity head, or

$$C'_d = f\left(F_{us}, \frac{H}{P}, \frac{L}{V_{us}/2g}\right) = \frac{Q_L}{L\sqrt{2g}(H-P)^{3/2}} \quad (12)$$

in which F = the Froude number; H = the flow depth; P = the weir height; L = the weir length; V = the mean velocity; Q_L = the discharge over the side weir; and g = the acceleration of gravity. The subscript $_{us}$ refers to the conditions immediately upstream of the weir, calculated as

$$C'_c = \frac{2 \cdot C_d}{3} = 0.67 \cdot C_d \quad (13)$$

The last term in the parentheses of equation 11 is in the form of an aspect ratio, which could just as well have been expressed as the ratio of the weir length to the crest height, L/P , because

$$\frac{L}{V_{us}^2/2g} = 2\left(\frac{L}{P}\right)\left(\frac{P}{H}\right)\left(\frac{1}{F_{us}^2}\right) \quad (14)$$

The mean flow depth over the weir is given by

$$\overline{H - P} = \left[\frac{1}{L} \sum_{i=1}^{N-1} \left(\frac{H_i + H_{i+1}}{2} - P \right)^{3/2} \Delta X \right]^{2/3} \quad (15)$$

in which N = the total number of flow depth measurements in the main channel along the side weir; and ΔX = the distance between measurements H_i and H_{i+1} .

Pinheiro and Silva (1999) found that the best correlation between the three parameters is given by

$$\frac{1}{C'_d} = 1.57 + \frac{0.127}{F_{us}} + \frac{7.45}{L_{dim}} + \frac{0.52h_a}{P} \quad (16)$$

in which L_{dim} = the ratio of the length to the upstream head; and h_a = the mean depth of flow over the weir.

In a similar development, Borghei et al. (1999) developed the following relationship

$$C'_d = 0.7 - 0.48F_{us} - 0.3 \frac{P}{H_{us}} + 0.06 \frac{L}{W_c} \quad (17)$$

Note that in this equation, the total head is referenced to the upstream total head and not the average head along the weir crest.

Skew Weirs

Jain and Fischer (1981) used the momentum equation given by

$$\frac{dh}{dX} = \frac{\frac{Q}{gA^2}}{\frac{Q^2 W_c}{gA^3} - 1} \left(\frac{dQ}{dX} - \frac{Q}{W_c} \tan \theta \right) \quad (18)$$

in which X = the distance along the centerline of the channel; and θ = the acute angle between the centerline of the channel and the weir crest. This is known as the sidewall angle.

To make the equation match the data, the discharge coefficient as defined in equation 5, C_d , had to be set to between 0.34 and 0.36. This is much less than the theoretical value of about 0.6. However, the model was so small ($P = 11$ mm) that surface

tension effects must have been significant, which can explain the low values of the discharge coefficient with respect to those found by investigators using larger models.

Labyrinth Weirs

Taylor (1968) applied the theoretical approach of Nimmo (1928) to labyrinth weirs. The theory was applicable, but to obtain a high degree of accuracy, nonuniform flow conditions had to be considered. Taylor derived the following equation for a channel with converging vertical walls, negligible friction, and a flat bottom:

$$\frac{dh}{dX} = \frac{\frac{2Q}{gA^2}}{\frac{Q^2 W_c}{A^3 g} - 1} \left(\frac{dQ}{dX} - \frac{Q}{B} \tan(\theta) \right) \quad (19)$$

in which

$$\frac{dQ}{dX} = C_l \sqrt{gh}^{3/2} \quad (20)$$

The solution of this equation was solved by finite differences, in which X is taken in the opposite direction to the flow. A special set of tests was conducted, with a side channel spillway to investigate the variation in the discharge coefficient. In this study, the equation had the form of Equation 14 given by Jain and Fischer (1981). The experiments showed that the discharge coefficient, C_l , varied between 0.56 and 0.60, when calculated as

$$C_l = \frac{2\sqrt{2} \cdot C_d}{3} = 0.94 \cdot C_d \quad (21)$$

Even though the analytic description of flow over a labyrinth weir takes into account the upstream and downstream flow conditions, the effects of interference were not considered. Therefore, an analytic solution of flow over a labyrinth weir that is accurate enough to be used in design will probably never be achieved.

Conclusions

The three-dimensional flow characteristics of flow over side, skew, and labyrinth weirs make an accurate mathematical description impossible. Therefore, researchers use physical models to determine the magnitude of various coefficients in their equations. These coefficients are usually functions of many variables, such as total energy in the channel, Froude number, sidewall angle, etc. The discrepancies between the predicted water surface profile and the observed values are resolved either

through adjustments to the discharge coefficient or through additional adjustments to momentum or energy correction factors.

Because of the empirical nature involved in determining the discharge over side, skew, and labyrinth weirs, a description of the flow chosen should be as simple as possible. This book uses an empirical approach to describe the flow over labyrinth weirs. This is not to say that fundamental mathematics should be discarded. The equations provide excellent guidance in determining parameters that should be observed in analyzing the results of model studies. For example, Equations 17 and 18 show that the sidewall angle is important in describing discharge variations. Similarly, Equation 16 shows that the crest length to channel width ratio and the head to crest height ratio are important. These will be significant parameters in the development of design curves for labyrinth weirs.

This page intentionally left blank

Chapter 3

Nappe Interference

Introduction

The nappes from two weirs placed at an angle with each other will have an impact over a limited length of the weir crest, as shown in Figure 1.

This impact is called nappe interference. The effect of the nappe interference is to decrease the discharge. Interference occurs when the jets from the two sidewalls or the apex and the sidewall intersect. The throw distance of the jet, D_t , is given approximately by

$$D_t = U \cos(\alpha) \cdot t \approx U \cos(\alpha) \sqrt{\frac{2 \cdot h}{g}} \quad (1)$$

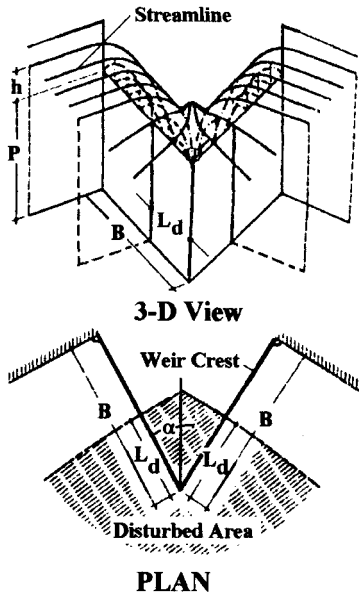


Figure 1. Nappe interference from Indlekofer, H., and Rouvé, G., (1975). "Discharge over polygonal weirs." *American Society of Civil Engineering, Journal of the Hydraulics Division*, 101(HY3), 385-401 with permission of ASCE.

in which U = the velocity at the crest; t = time; and h = the head on the crest. Because the values of V' and h vary along the weir crest, a method must be found that either predicts these variations numerically or describes the effect through an indirect method.

Theory

Indlekofer and Rouvé (1975) took the latter approach and concluded that the degree of interference or the disturbed area is a function of the head on the weir, h , the weir height, P , and the sidewall angle, α . Because the length of the corner interference is a function of the weir length, B , and the included angle, α , the interference can be written as

$$L_d = f(h, P, \alpha) = f\left(\frac{h}{P}, \alpha\right) \tag{2}$$

Indlekofer and Rouvé found that the length of the disturbance, L_d , increases linearly with flow depth. To define the problem, they used a disturbance coefficient, which is

$$C(l) = \frac{C_r}{C_d} \tag{3}$$

in which C_r = the reduced discharge coefficient for the weir caused by the interference; and C_d = the discharge coefficient for flow over a straight weir without interference. The distribution of $C_d(l)$ along the crest and the mean value of the reduced discharge coefficient, C_m , are shown in Figure 2.

The mean value of C_d is given as a function of the sidewall angle in Figure 3. An angle of 90° means that the weir has a linear planform, whereas an angle of 0°

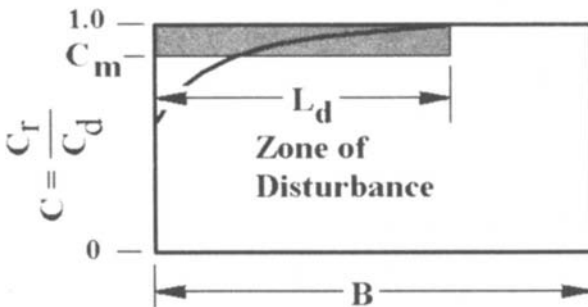


Figure 2. Distribution of $C_d(l)$ along the crest after Indlekofer, H., and Rouvé, G., (1975). "Discharge over polygonal weirs." *American Society of Civil Engineering, Journal of the Hydraulics Division*, 101(HY3), 385-401, with permission of ASCE.

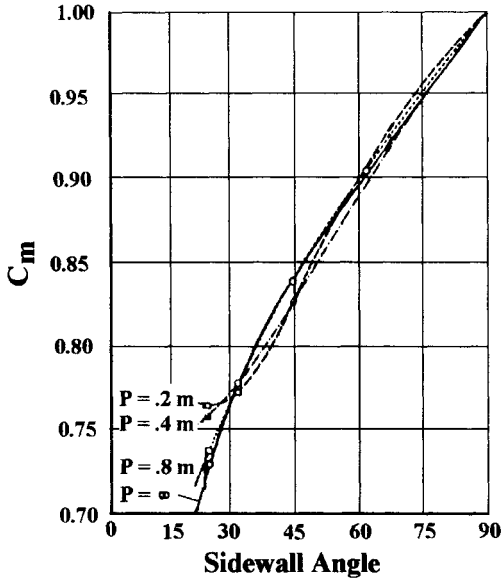


Figure 3. Dependence of the Non-Dimensional Discharge Coefficient Reduction on the Sidewall Angle from Indlekofer, H., and Rouvé, G., (1975). "Discharge over polygonal weirs." *American Society of Civil Engineering, Journal of the Hydraulics Division*, 101(HY3), 385-401, with permission of ASCE.

indicates that the sidewalls are parallel with the channel centerline. For a finite apex dimension, an angle of 0° would correspond to a rectangular weir.

Indlekofer and Rouvé used two definitions for the length of the disturbance. One is the length of the disturbance, L_d , and the other is the effective length of the disturbance, L_{de} . The relationship between the two is given by

$$L_{de} = (1 - C_m) \cdot L_d = B - \frac{3 \cdot Q}{2 \cdot C_d \sqrt{2gh_m^{3/2}}} \quad (4)$$

- The effective length can be determined from physical measurements in which the discharge coefficient is that for a straight weir using an appropriate equation for the tested crest, as given Chapter 4, Crest Shapes.
- B = the crest length.
- h_m = the measured flow depth over the weir.

The physical meaning of these lengths is shown in Figure 4.

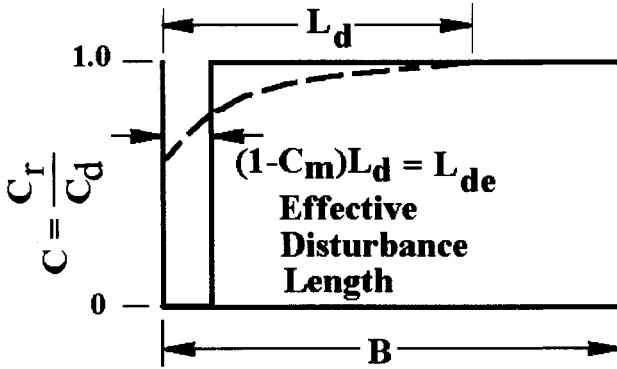


Figure 4. Definition of disturbance Lengths

The disturbance length, L_d , is the length of the crest over which the discharge is affected by the interference. The effective length, L_{de} , is the length of weir over which the discharge coefficient is equal to zero. The flow over the remaining length occurs with a discharge coefficient equal to that for a straight weir. Equation 4 is ideally suited to determine the effective disturbance length from model studies.

The effective length of the disturbance is primarily a function of the angle, as shown in Figure 5. The curve should go to zero as the sidewall angle approaches 90° ($\cos \alpha = 0$) and to infinity as the sidewall angle approaches 0° ($\cos \alpha = 1$). The data are for different sharp crested weirs with heights that correspond to P/L between 0.2 and 0.8 and different sidewall angles. Figure 5 shows that the effect of the weir height is negligible.

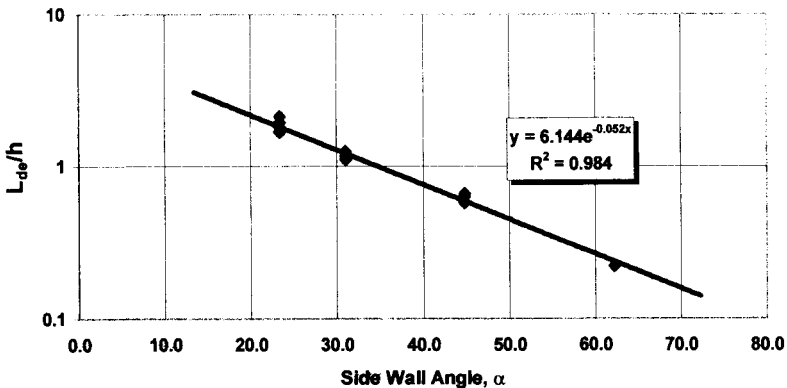


Figure 5. Dependence of Disturbance length on sidewall angle.

The experimental curve can be approximated by

$$\frac{L_{de}}{h} = 6.1 \cdot e^{-0.052\alpha} \tag{5}$$

with a correlation coefficient of 0.98. Equation 5 is approximately equal to zero as the sidewall angle goes to 90°. However, it does not approach infinity as the angle goes to 0°. Therefore, using this equation to extrapolate the effective interference length to angles less than about 10° is not recommended.

The effect of the disturbance length can be seen in Figure 6. In this figure, the magnification, L/W_c , and the sidewall angle, α , are constant. The figure depicts a labyrinth with one, two, four, and eight cycles, respectively. With eight cycles, the interference ratio, L_{de}/B , is equal to 0.5, and the interference strongly affects the discharge over the weir. As the number of cycles decreases, the interference ratio becomes smaller, thus decreasing the percentage of interference.

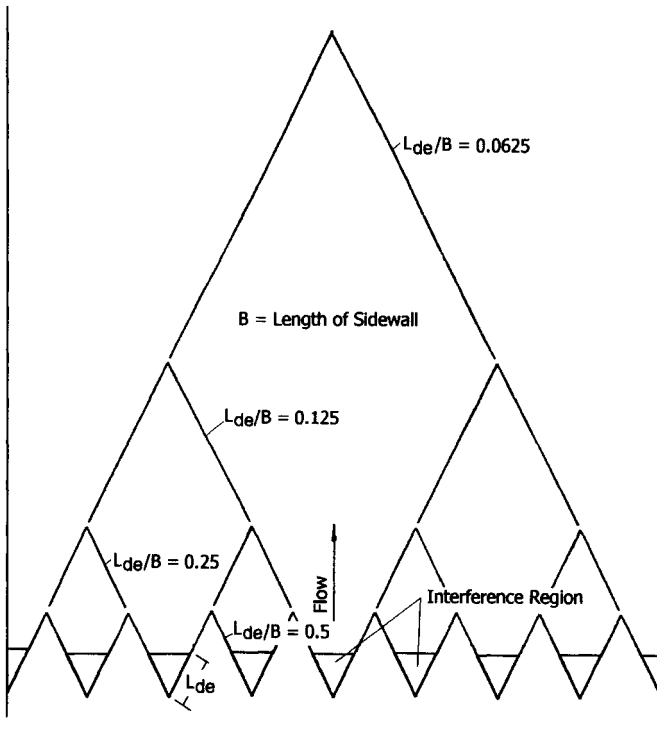


Figure 6. Graphical Representation of Interference Effects

Model Studies

The research of Indlekofer and Rouvé (1975) provides useful guidance in how to analyze the effects of interference. However, with labyrinth weirs, flow that approaches the weir is in general not perpendicular to the weir, as shown in Figure 1. Unfortunately, research has not been conducted into interference effects using the methods of Indlekofer and Rouvé. Nevertheless, some insights can be gained by examining interference on model labyrinth weirs using Equation 4. For example, at Avon and Woronora Dams, the sidewall angles are 27.5° and 22.4°, respectively. In these two cases, the interference increases linearly with the upstream total head, as shown in Figures 7 and 8. This is in agreement with the experiments of Indlekofer and Rouvé.

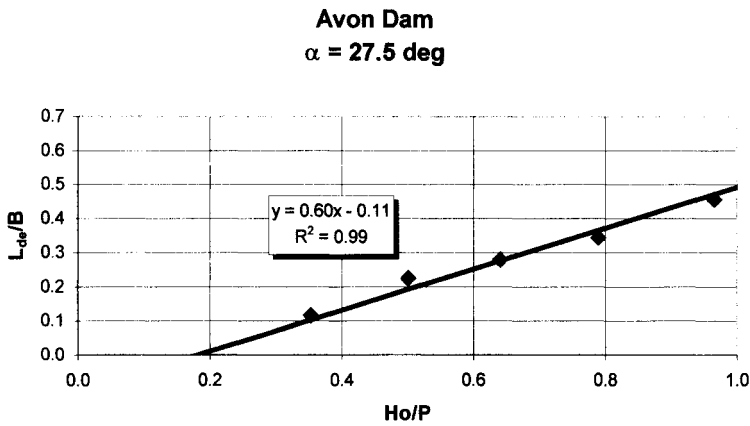


Figure 7. Avon Dam, Data from Darvas (1971)

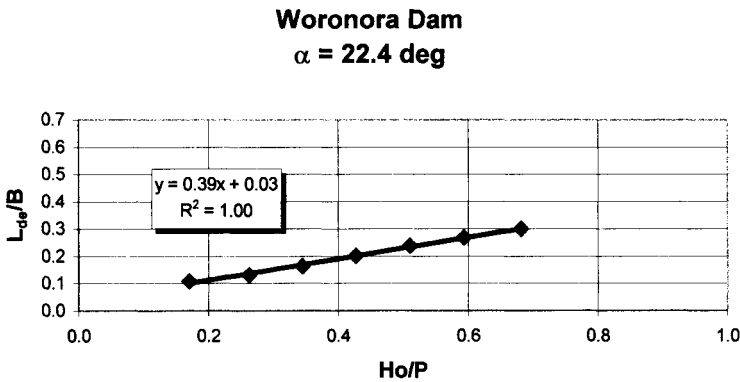


Figure 8. Woronora Dam, Data from Darvas (1971)

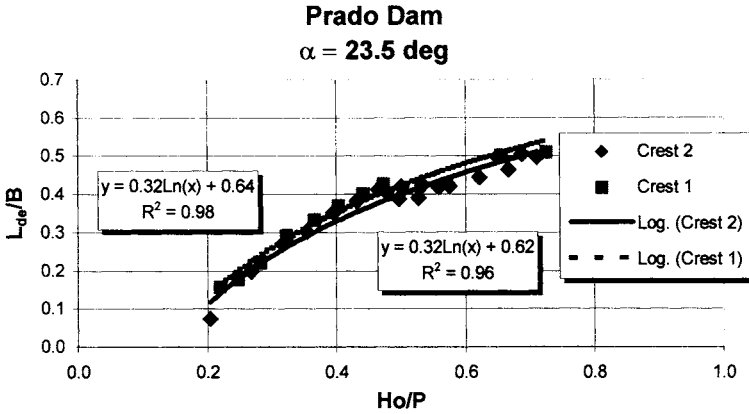


Figure 9. Prado Dam, Data from Copeland and Fletcher (2000)

The effect of the downstream channel on the effective interference length is seen from the model tests of Prado Dam. As shown in Chapter 12, Modeling Procedures, Prado Dam had a weir between the downstream apexes. The weir was not high enough to cause submersion problems, but it did influence the effective interference. Figure 9 shows that the interference is much greater than that of the Woronora Dam, although the sidewall angles are comparable.

For smaller sidewall angles, as in the Rollins Dam, the effective interference length does not vary linearly with depth, as shown in Figure 10.

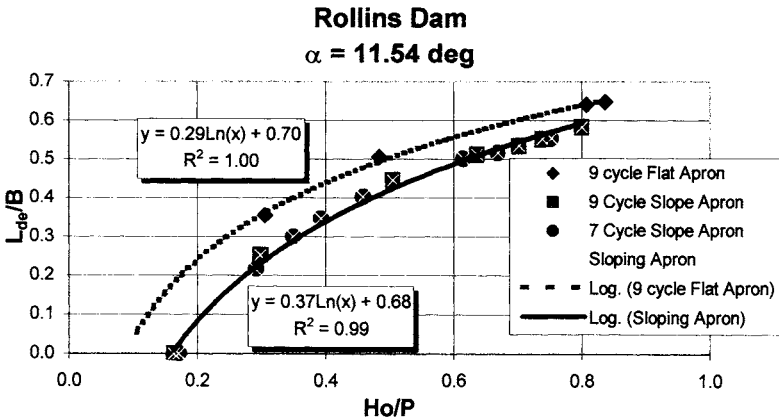


Figure 10. Rollins Dam, Unpublished data from a model study conducted at Utah Water Research Laboratory, Logan Utah by J. P. Tullis for CH2M Hill, Inc. and used with permission of Tim McCall, Chief Engineer of the Nevada Irrigation District, PO Box 1019, Grass Valley, CA.

Ute Model
 $\alpha = 12.15 \text{ deg}$

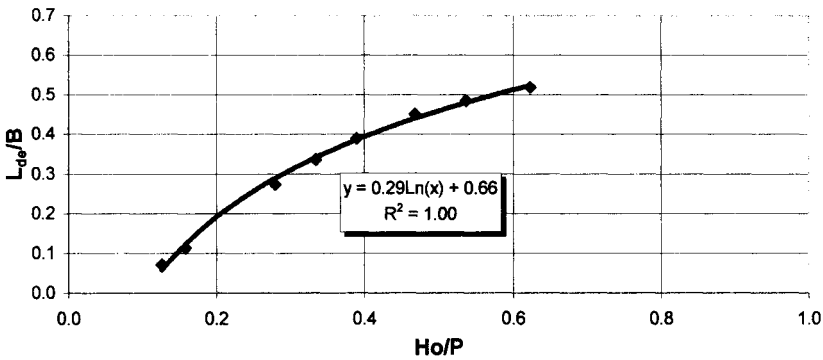


Figure 11. Ute Dam, Data from Houston (1982)

In the Rollins Dam study, the effect of the downstream submergence is evident in that the interference with a sloping apron is much less than that with a flat downstream apron. However, the variation in the effective disturbance length is logarithmic, not linear. Of particular interest is that the number of cycles does not influence the interference.

The Ute Dam model study has a slightly larger sidewall angle than the Rollins Dam, as shown in Figure 11. However, the effective interference length is roughly equivalent to the flat apron result of Rollins Dam. This indicates that the downstream apron may have had a negative influence on the discharge and interference characteristics of the Ute Dam model study.

Two model studies of Boardman Dam were conducted with identical width but with different sidewall angles. These tests indicate that the interference is less with a larger sidewall angle, as shown in Figure 12. This observation is in accordance with the theoretical studies by Indlekofer and Rouvé.

Boardman Dam

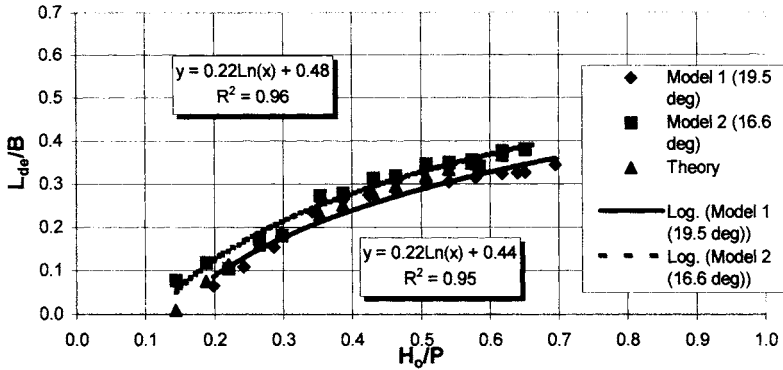


Figure 12. Boardman Dam, Data from Babb (1976)

Bartletts Ferry Dam

$\alpha = 14.04$ deg

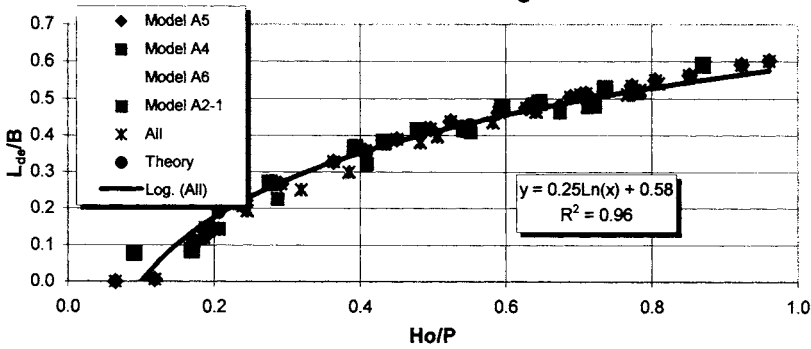


Figure 13. Bartletts Ferry Dam, Data from Mayer (1980)

Table 1. Bartletts Ferry Model Configurations
All dimensions in feet.

	Model A2-1	Model A4	Model A5	Model A6
L	12	6	6	12
W	3	1.5	1.5	3
2a	0.081	0	0	0
n	1	2	1	1

The model studies of Bartlet Dam were conducted with four different labyrinth configurations but with the same sidewall angle. The variations are shown in Table 1. These studies reveal that the width of the upstream apex, the number of cycles, and the absolute length of a side do not have an effect on the effective disturbance length, as shown in Figure 13.

Figure 14 shows the Ritschard Dam model, which has the smallest sidewall angle.

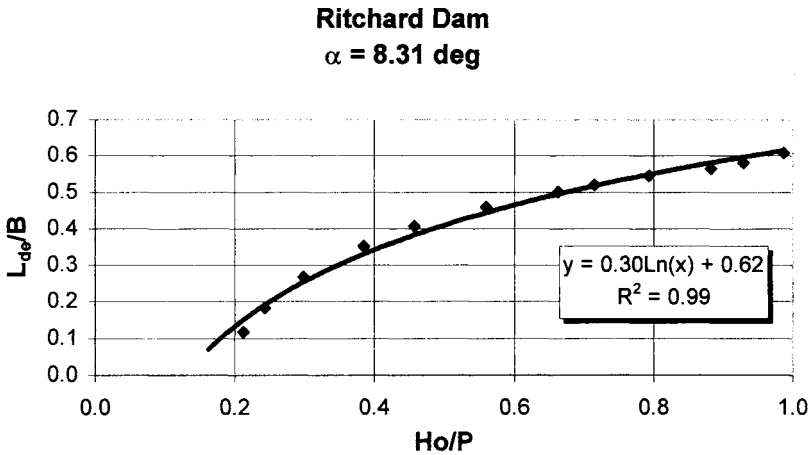


Figure 14. Ritschard Dam, Data from Vermeyen, T., (1991).

Based on these few model studies, the interference with labyrinth weirs begins only when H_o/P is greater than 0.1. The effective interference length for sidewall angles less than 20° and for values of H_o/P greater than 0.1 is given by

$$\frac{L_{de}}{B} = C_1 \cdot \ln\left(\frac{H_o}{P}\right) + C_2 \tag{6}$$

in which $C_1 = 0.224 \pm 0.053$; and $C_2 = 0.599 \pm 0.104$. The value of C_2 can be approximated by

$$C_2 = 0.94 - 0.03 \cdot \alpha \tag{7}$$

as shown in Figure 15.

Note that this relationship is based on the total upstream head, whereas Indlekofer and Rouvé used the head on the weir. Additional research is needed to determine the validity of Equations 6 and 7.

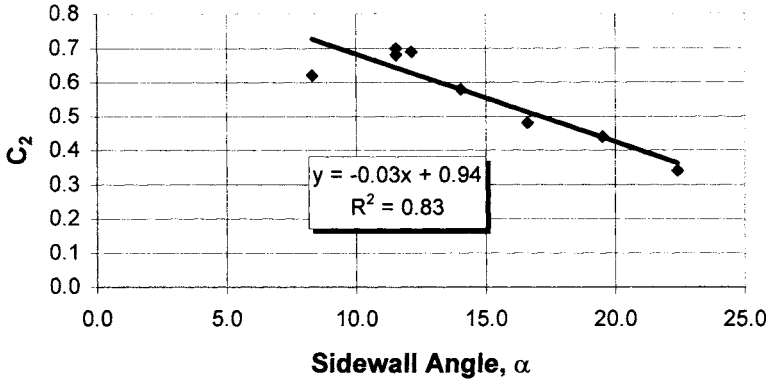


Figure 15. Variation of Coefficient C_2 with Sidewall angle, α

Taylor (1968) also studied interference. From his studies, he concluded that the depth ratio, h/P , should be less than or equal to 0.7 and that the height aspect ratio, W_c/P , should be greater than 2. Because W_c/P can be written as $(W_c/h)(h/P)$, the criteria established by Taylor essentially mean that the depth aspect ratio, h/W_c , should be less than 0.35. The depth aspect ratio is a measure of the sidewall friction effect on the flow over the weir. For depth aspect ratios of large value, the boundary layer that develops on the sidewalls becomes significant. However, for depth aspect ratios of small value, the effect of the boundary layer on the sidewalls is small. Neither W_c/h nor h/P affect the interference. Breaking the height aspect ratio, W_c/P , into its two components shows that this parameter is *not* a significant parameter affecting interference. Instead, the significant parameter that more accurately describes interference is the ratio of the effective disturbance length to the length of the wall.

This page intentionally left blank

Chapter 4

Crest Shapes

Types of Crests

The crests on labyrinth weirs consist of everything from a sharp crest profile to the so-called nappe profiles. Figure 1 shows the crest shapes used with most labyrinth weirs.

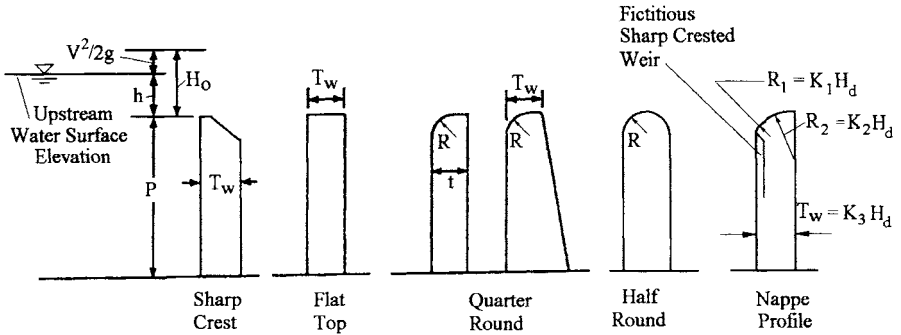


Figure 1. Crest Shapes

Knowledge of the discharge coefficients for each of these shapes is important because they can be used to determine the flow rate over a labyrinth operating with low heads. As shown in Chapter 12, Modeling Procedures, the discharge coefficients of most labyrinth weir model studies have significant errors at low heads. Therefore, a method is needed to estimate the flow rates at small heads over the labyrinth.

This chapter discusses linear weirs. An understanding of the parameters that govern linear weirs is important to understand the complexities of labyrinth weirs. The question of whether to use the head on the weir ($Z_w - Z_c$) or the total head ($Z_w + V_{us}^2/2g - Z_c$) or ($Z_r - Z_c$) is discussed in Chapter 5, Design Curves. In any case, use the discharge coefficients associated with the head definition for which they were derived. Here, Z_c = the crest elevation; Z_w = the upstream water surface elevation; Z_r = the reservoir elevation; and V_{us} = the mean upstream water velocity.

Theoretical Minimum Value of the Discharge Coefficient

The discharge equation can be written in terms of the total upstream head, H_o , as

$$Q = C_d \frac{2}{3} \sqrt{2g} L H_o^{3/2} \quad (1)$$

This equation is usually used for flow over flat, broad-crested, quarter-round, half-round, and nappe (ogee) profile weirs. It is useful when the elevation of the reservoir is known relative to the elevation of the weir.

The minimum value of the discharge coefficient is the value of the coefficient for a very small P/H_o in which P and H_o are shown in figure 1. It can be estimated by assuming the flow is at critical depth on the weir crest. This assumption ignores viscous and surface tension effects, such as those included in the last term of the Rehbock coefficient. At critical depth, the discharge is given by

$$Q = \left(\frac{2}{3}\right)^{3/2} \sqrt{g} L H_o^{3/2} \quad (2)$$

Equating these two expressions gives the minimum value of the discharge coefficient, C_d , as

$$C_d = \frac{3}{2} \left(\frac{2}{3}\right)^{3/2} \frac{1}{\sqrt{2}} = 0.58 \quad (3)$$

This value is equivalent to a P/H_o of zero, i.e., the flow over a sudden drop with a weir height of zero.

At the other end of the spectrum, as H_o/P approaches zero, the coefficient should also approach this minimum (neglecting surface tension and viscous effects), because the flow is essentially at critical depth for small flow depths over the weir.

Discharge Characteristics

Sharp Crest and Flat Top Profile

For a linear weir, the discharge is given in terms of head on the weir by

$$Q = C_d \frac{2}{3} \sqrt{2g} L h^{3/2}$$

(4)

in which C_d is given by the Rehbock coefficient

$$C_d = 0.605 + 0.08 \frac{h}{P} + \frac{1}{305h(ft)} \quad (5)$$

or, in the metric system, by

$$C_d = 0.605 + 0.08 \frac{h}{P} + \frac{1}{h(mm)} \quad (6)$$

This form of the discharge equation is useful when the weir is to be used as a measuring device. In this case, the upstream water depth over the weir is measured; Equation 4 gives the discharge directly. If Equation 1 were used, an iterative procedure would be necessary, because the upstream velocity head is dependent on the discharge.

Quarter-Round Profile

Tullis et al. (1995) conducted tests with a quarter-round profile. The results were presented using Equation 1. The discharge coefficient for the quarter-round profile is shown in Figure 2. In this figure, the discharge coefficient should also approach the minimum value, because the flow should approach critical depth as the upstream head becomes small. This curve is for a radius equal to 1/12 of the weir height, and the wall thickness is 1/6 of the weir height.

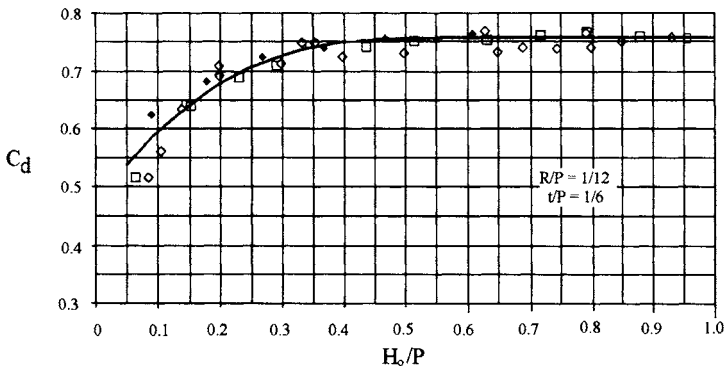


Figure 2. Discharge Coefficient for a Quarter-Round Profile. from Tullis, J.P., Nosratollah, A., and Waldron, D., (1995). "Design of labyrinth spillways." *American Society of Civil Engineering, Journal of Hydraulic Engineering*, 121(3), 247-255., Permission ASCE.

Half-Round Profile

The discharge coefficient for the half-round profile is influenced by the flow over the crest. Four flow conditions are possible: pressure, atmospheric, subatmospheric, and

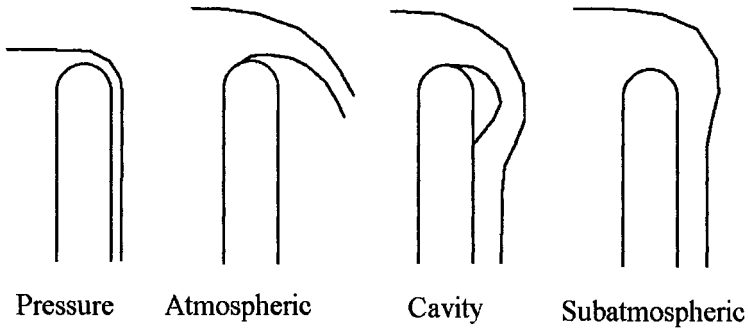


Figure 3. Definition of crest flow conditions.

cavity. Mathematically, these are defined as the pressure on the crest with the coefficient

$$\beta_p = \frac{\left(\frac{P_c}{\gamma}\right)}{Y_o} \quad (7)$$

in which P_c = the pressure at the crest; and Y_o = the water depth at the crest. The various conditions are thus $\beta > 0$, pressure; $\beta = 0$, atmospheric; and $\beta < 0$, subatmospheric or cavity. These conditions are shown in Figure 3.

Pressure flow is analogous to discharge over an ogee crest with a head that is less than the design head. The pressure on the entire crest is positive (above atmospheric). As the head increases, a point is reached in which the head on the crest is atmospheric. Atmospheric flow is analogous to the design head on an ogee crest. At higher heads, the pressure on the crest becomes subatmospheric. If the downstream nappe can be aerated, the pressure at the crest will become atmospheric, and the jet will spring free from the crest, as shown in Figure 3. However, if the nappe cannot be aerated, then subatmospheric flow forms, in which the nappe will cling to the downstream face of the weir. Between these two extremes, an enclosed air pocket or air cavity may form. This is called cavity flow. The cavity flow is usually unstable. That is, depending on the downstream water level, the cavity flow will transition between atmospheric and subatmospheric conditions.

The discharge coefficient given by Equation 1 should be a function of the radius of curvature, the weir height, and the head on the weir. Mathematically, the relationship is

$$C_d = f\left(\frac{H_o}{R}, \frac{H_o}{P}\right) \tag{8}$$

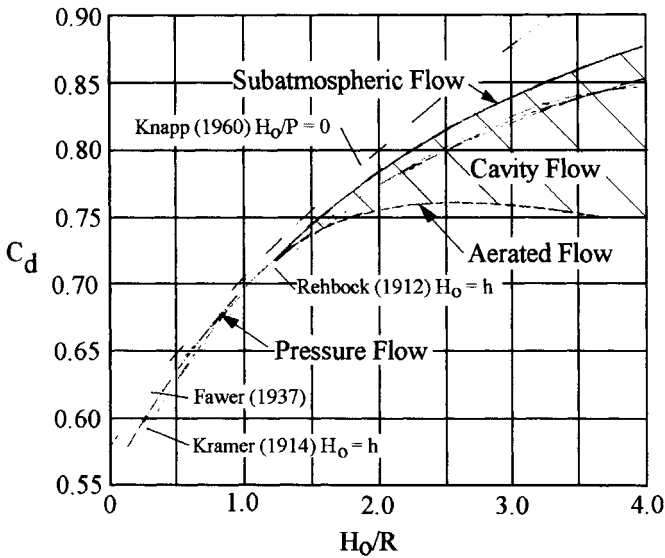


Figure 4. Discharge Coefficient - Half-Round Profile After Rouvé, G., and Indlekofer, H., (1974), "Abfluß über geradlinige Wehre mit halbkreisförmigem Überfallprofil," Der Bauingenieur 49,250-256, (in German), with permission ASCE.

This indicates that the results should be presented as a three-dimensional curve in which the Z-axis is C_d , the X-axis is H_o/P , and the Y-axis is H_o/R . For pressure flow and subatmospheric flow, H_o/R is the most significant parameter. With aerated flow, the nappe separates from the rounded crest. The point of separation moves upstream, and the discharge over the crest is analogous to flow over the quarter-round crest. For this case, H_o/P is more important than H_o/R . Unfortunately, most investigators do not make these distinctions.

Indlekofer and Rouvé (1975) measured the discharge coefficients for half-round profiles. Their results are expressed as a function of H_o/R , as shown in Figure 4. The borderline between pressure flow and subatmospheric or aerated flow occurs with a value of H_o/R of approximately 1.3.

In the model studies of Boardman labyrinth, Babb (1976) found that the pressure flow occurred for an H_o/P of less than 0.3. This is equivalent to an H_o/R of less than 3.6. This difference between this value and those determined by Indlekofer and Rouvé can

be explained by the angle for which the flow passes over the weirs. The angle with Indlekofer and Rouvé was 90° , whereas that with Babb was approximately 20° .

With the tests of Babb (1976), for H_o/R values greater than 3.6, the nappe sprung free and the crest became aerated. At heads with an H_o/P greater than 0.5, which corresponds to an H_o/R greater than 6, the tail water effects became large enough to submerge the nappe, causing it to become subatmospheric.

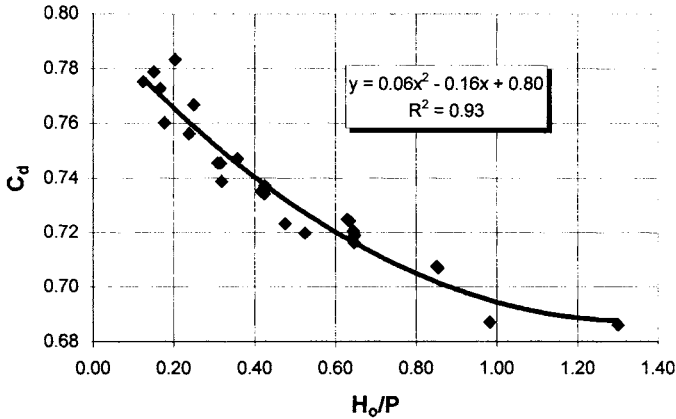


Figure 5. . Discharge Coefficients for Aerated Flow from Amanian (1987), "Performance and design of labyrinth spillways." MSc thesis, Utah State University, Logan, Utah.

Amanian (1987) determined the discharge coefficient for half-round profiles. All of the tests used values of H_o/R greater than 2, which are in the aerated, subatmospheric, or cavity flow range. The point of transition from pressure to aerated flow was not determined. The results for the aerated flow are shown in Figure 5 as a function of H_o/P . Comparison of these coefficients with those of the quarter-round profile shows that both have similar but not identical coefficients. With small values of H_o/P , the half-round profile has a higher discharge coefficient and a smaller value for large values of H_o/P . The results for the subatmospheric flow are shown in Figure 6.

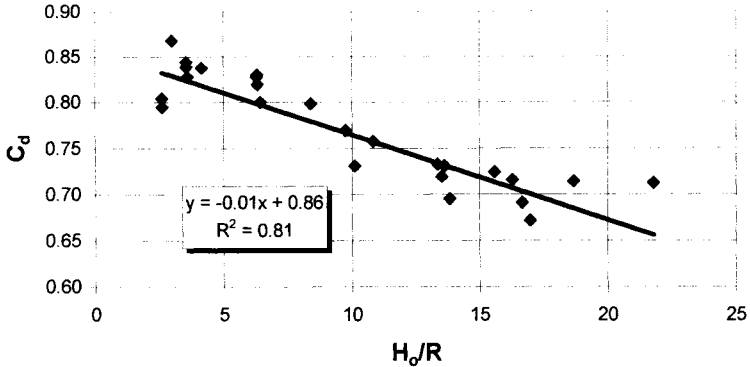


Figure 6. Discharge Coefficients for Sub atmospheric Flow from Amanian (1987), "Performance and design of labyrinth spillways." MSc thesis, Utah State University, Logan, Utah.

These tests were performed with weir heights of 102, 152, and 204 mm. As shown in Chapter 12, Modeling Procedures, surface tension effects are large for an H_o/P of less than 0.3 with weir heights of less than 150 mm. Therefore, surface tension effects present in the model studies will not be present in the prototype. The effect of surface tension is to create a higher discharge than will be present in nature. The Boardman tests by Babb (1976) were probably also influenced by surface tension at low heads because they were conducted with a weir height of only 92 mm.

Nappe Profile or Ogee Crest Profile

The nappe profile is defined by the lower nappe of a fictitious sharp crested weir placed on the upstream face, as shown in Figure 1. The area beneath the nappe can be filled with concrete without affecting the flow over the weir. In fact, the pressure on the crest will be atmospheric even though the air/water boundary is replaced with a concrete/water boundary. Model studies with sharp crested weirs were used to develop the Corps of Engineers and the U.S. Bureau of Reclamation charts for ogee crests. The ogee crest is an approximation to the aerated nappe profile. However, the nappe profile varies as the upstream head varies. Therefore, the concrete crest will be atmospheric only for one upstream head. This head is called the design head for that particular crest. If the upstream head is less than the design head, the pressure on the crest will be positive. Conversely, if the head is greater than the design head, the pressure will be negative. This effect is probably small if only the section of the profile from the fictitious weir to the weir crest is filled with concrete.

The shape of the nappe, upstream of the crest, can be approximated by two circular curves. The coefficients for the curves are a function of the approaching velocity head, the total upstream head, and the slope of the upstream face of the weir. The values of the coefficients shown in Figure 1 for a vertical upstream face and no

upstream velocity head are $K_1 = 0.530$, $K_2 = 0.235$, and $K_3 = 0.284$. Hoffman (1974) gives the values of the coefficients for other approach conditions. Comparison of the wall-thickness ratio given by K_3 with the wall-thickness ratio given by Tullis (1995) for quarter-round profiles results in a design head of H_o/P of about 0.59 for the tests with the quarter-round profiles.

A power law gives the profile downstream of the crest. The Corps of Engineers recommends the following relationship:

$$Y = \frac{X^{1.85}}{2 \cdot H_d^{0.85}} \tag{9}$$

The U.S. Bureau of Reclamation (1974) gives the discharge for a nappe profile as

$$Q = CLH_o^{3/2} \tag{10}$$

In this case, the discharge coefficient is dimensional. The coefficient is equivalent to

$$C = \frac{2}{3} \sqrt{2g} C_d \tag{11}$$

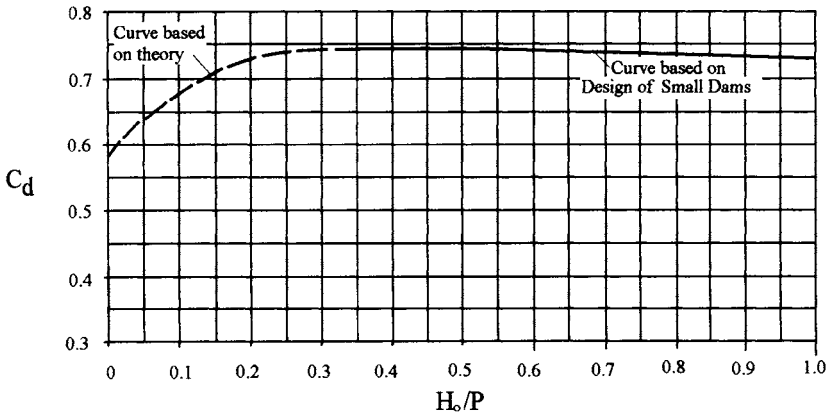


Figure 7. Discharge Coefficient for a Nappe Profile

The value of the coefficient, C_d , for various design heads is shown in Figure 7. These coefficients have been computed from the curves given by Hoffman (1974). Note: the curves by Hoffman are plotted as a function of P/H_o , not H_o/P . For values of H_o/P less than 0.35, the shape of the curve was approximated, with a curve whose minimum value is equal to 0.59, with H_o/P equal to zero.

Megalhães and Lorena (1989) recommended that the nappe crest shape be extended beyond the apex of the crest, as shown in Figure 8. Even with this extension, the discharge coefficient should be the same as in Figure 7. The use of the Megalhães and Lorena profile requires that the apex width be greater than for the crest shapes in

Figure 1. Therefore, the discharge from a labyrinth with this shape will probably be less than that from a nappe crest without the extension because of the increased nappe interference caused by supporting the jet further downstream.

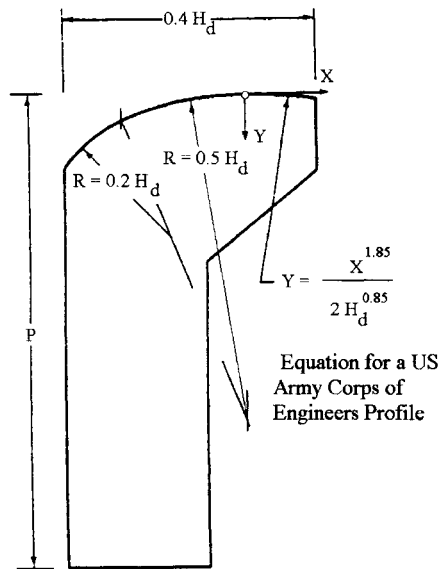


Figure 8. Ogee Crest Profile from Megalhães, A.P., (1985). "Labyrinth weir spillway." *Transactions of the 15th Congress ICOLD, Vol. VI, Q59-R24*, Lausanne, Switzerland, 395-407, with permission of ICOLD.

This page intentionally left blank

Chapter 5

Design Curves

Introduction

As the water level rises with a labyrinth weir having a quarter-round crest, the flow goes through several stages. With very small heads, if the weir height is large enough, the nappe breaks up, and the underside of the nappe is aerated. This can be seen in Figure 3 of Chapter 9, Sedimentation and Ice, in which the nappe is on the verge of breakup where it falls into the downstream pool. With further increases in depth, the nappe becomes thick enough that subatmospheric pressure develops under the nappe. Hinchliff and Houston (1984) call this stage the subatmospheric phase. Lux (1989) includes both of these two stages into the aerated phase.

If the head continues to rise, the water surface profile on the centerline between two walls, section A-A, exhibits a noticeable dip from the reservoir level. Further downstream, the profile increases again and then drops at the downstream apex, as shown in Figure 1. However, the downstream level rise never reaches that of the reservoir. Hinchliff and Houston call this stage the aerated phase because the nappe periodically aerates from the downstream apex. Lux calls this the transitional phase.

With higher reservoir levels, the nappe thickens, and the tail water becomes high enough to preclude any aeration. Hinchliff and Houston call this stage the nonaerated, solid nappe phase. Lux calls it the suppressed phase.

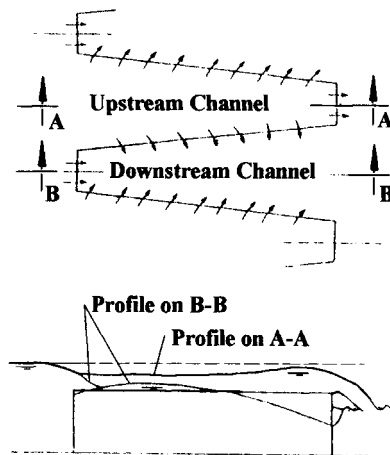


Figure 1. Water Surface Profile on the Centerline between the Walls

The various stages can be seen in some of the design curves based on the discharge. The curves of Lux, are one example. However, the noticeable changes in the slope of the curve cannot readily be detected in the curves based on the discharge coefficient. The curve by Tullis et al. (1995) is an example.

Basic Parameters

The discharge characteristics of labyrinth weirs are primarily a function of the weir height, P , the depth of flow upstream of the weir, h , the width of the weir, W , the developed length of the labyrinth, L , and its shape. Thus, the discharge can be expressed as

$$Q = f(h/P, L/W, Shape) \tag{1}$$

The shape of a labyrinth can be rectangular, trapezoidal, or triangular. The dimensions of these various shapes are defined in Figure 4.

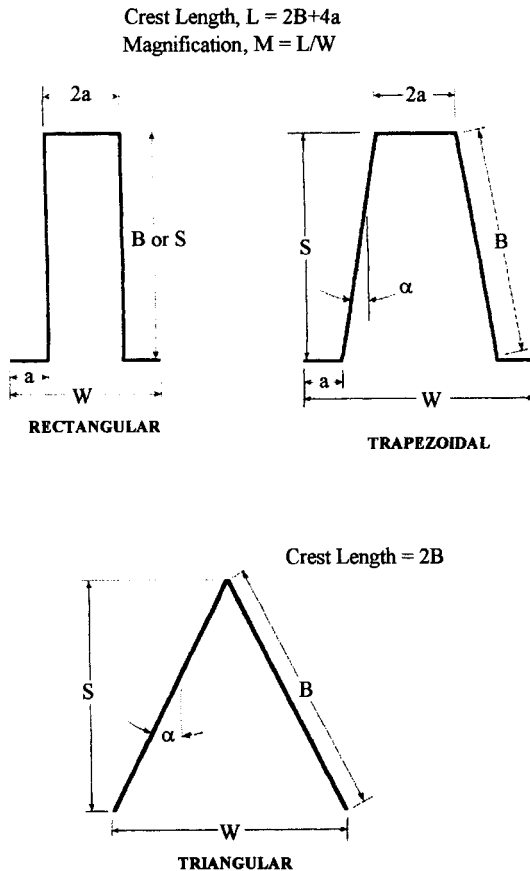


Figure 2. Labyrinth Weir Shapes

Chapter 2, Analytic Development, showed that the flow over a skew weir is strongly influenced by the angle the weir forms with the upstream flow direction. For a triangular weir, the angle is related to the L/W ratio by

$$\alpha_{\max} = \arcsin(W / L) \tag{2}$$

The angle given by this relationship is the maximum value that can be achieved for a labyrinth weir. For a trapezoidal plan form, the angle is given by

$$\alpha = \arcsin\left(\frac{W - 4a}{L - 4a}\right) \tag{3}$$

Definition of Upstream Head

Model investigations of some site-specific labyrinth weir installations showed that for a given reservoir elevation, the curves of Hay and Taylor (1970) predicted a greater discharge over the labyrinth spillway than the discharge measured in the model. For example, Megalhães (1985) found that the predicted flow rate was greater than what he observed in his studies. Houston (1982) also found that the predicted discharge was greater than that observed on a physical model test of Ute Dam. Cassidy et al. (1983) also shows that the Hay and Taylor curves predicted a larger discharge than that measured in a model. In an effort to explain the difference, Houston (1982) hypothesized that the difference was that Hay and Taylor used the head on the crest, *h*, whereas for a labyrinth spillway that is connected directly to a reservoir, the total upstream head, *H₀*, must be used. The definition of these heads is shown in Figure 3.

Rouse (1936) showed that the flow over a weir takes place under conditions of minimum energy. Hence, the total elevation of the energy grade line is determined by the ratio of the head on the weir to the total depth, and the velocity of approach is not

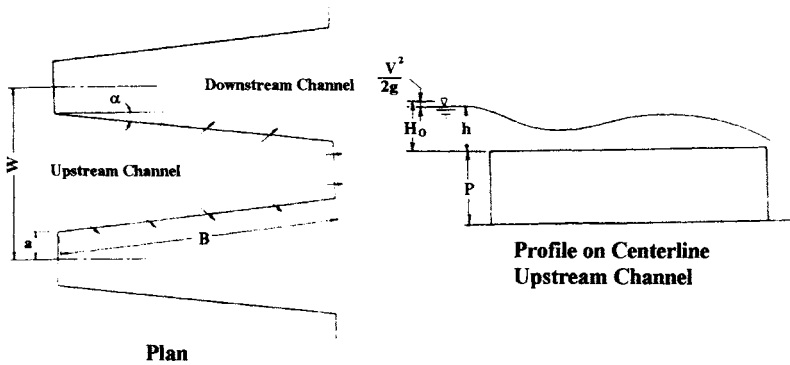


Figure 3. Head Definition

an independent variable. As such, the velocity of approach does not need to be treated as an independent variable in the discharge relationship. Therefore, the difference between the model observations is not related to the definition of the upstream head. Instead, the observations with site-specific models and the arguments of Rouse can be reconciled by realizing that the discharge over a weir or a spillway is dependent on the approach flow conditions. That is, the geometry of the channel upstream of the weir is a significant parameter, not the magnitude of the velocity of approach. This means that the discharge curves for a labyrinth placed in a channel are expected to be different from those in which the labyrinth extends into the reservoir. To reiterate, the difference is the result of the geometry of the approach flow and not the definition of the upstream head. Cassidy et al. (1985) clearly demonstrated that either the upstream head or the head on the weir could be used to define a discharge coefficient. When using a discharge coefficient curve, care must only be taken to select the appropriate head to determine the discharge.

Many researchers have developed discharge curves for labyrinth weirs. Some use the head on the weir, and some use total upstream head or reservoir head. Some curves are for a labyrinth in a channel, and some are for a labyrinth located at the beginning of a channel. Be careful that the areas of application for each design curve are clearly understood. Several of the more common design curves are given in the following sections.

Design Curves Derived from Model Studies

Taylor

In the experiments by Taylor (1968), the discharge was made dimensionless by dividing the labyrinth weir flow by the discharge of a linear weir that has the same channel width. This is a clever method of removing the effects of surface tension in the model tests. In this manner, a family of curves that represent the characteristics is given by

$$\frac{Q_L}{Q_N} = f(h/P, Shape) \quad (4)$$

in which Q_L = the total discharge of the labyrinth weir; Q_N = the discharge of a linear weir having the same width of the labyrinth weir; and h = the head on the weir.

Design charts prepared by Hay and Taylor (1970) are shown in Figures 4a and 4b. These curves are for a labyrinth located in a channel.

Triangular

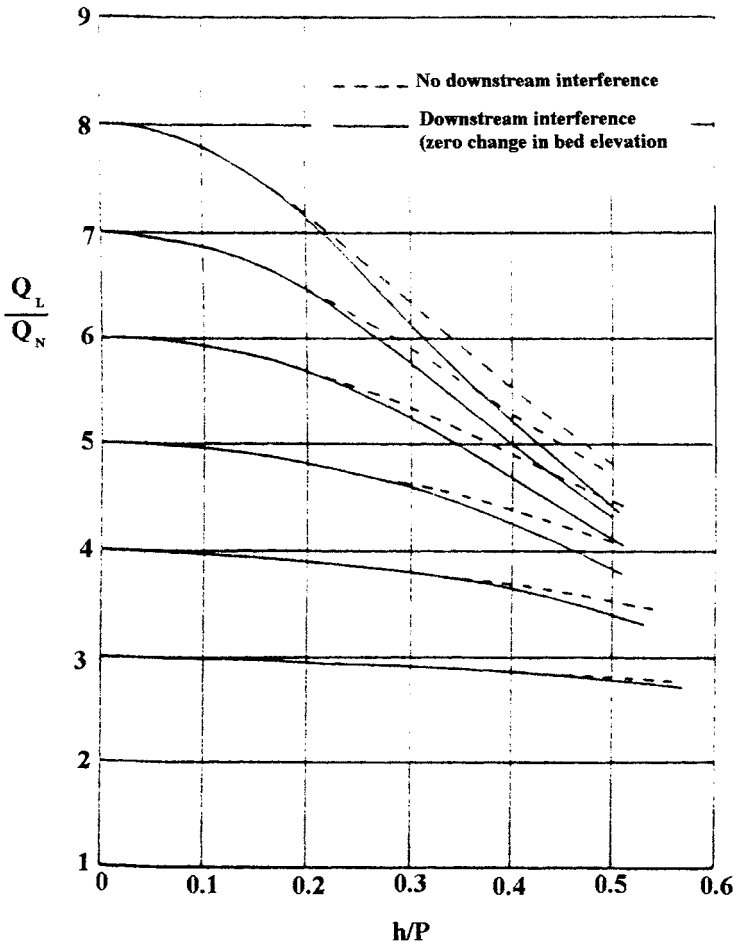


Figure 4a. Design Curve - Triangular -Sharp Crested Weir from Hay, N., and Taylor, G., (1970). "Performance and design of labyrinth weirs." *American Society of Civil Engineering, Journal of Hydraulic Engineering*, 96(11), 2337-2357., permission from ASCE.

Trapezoidal

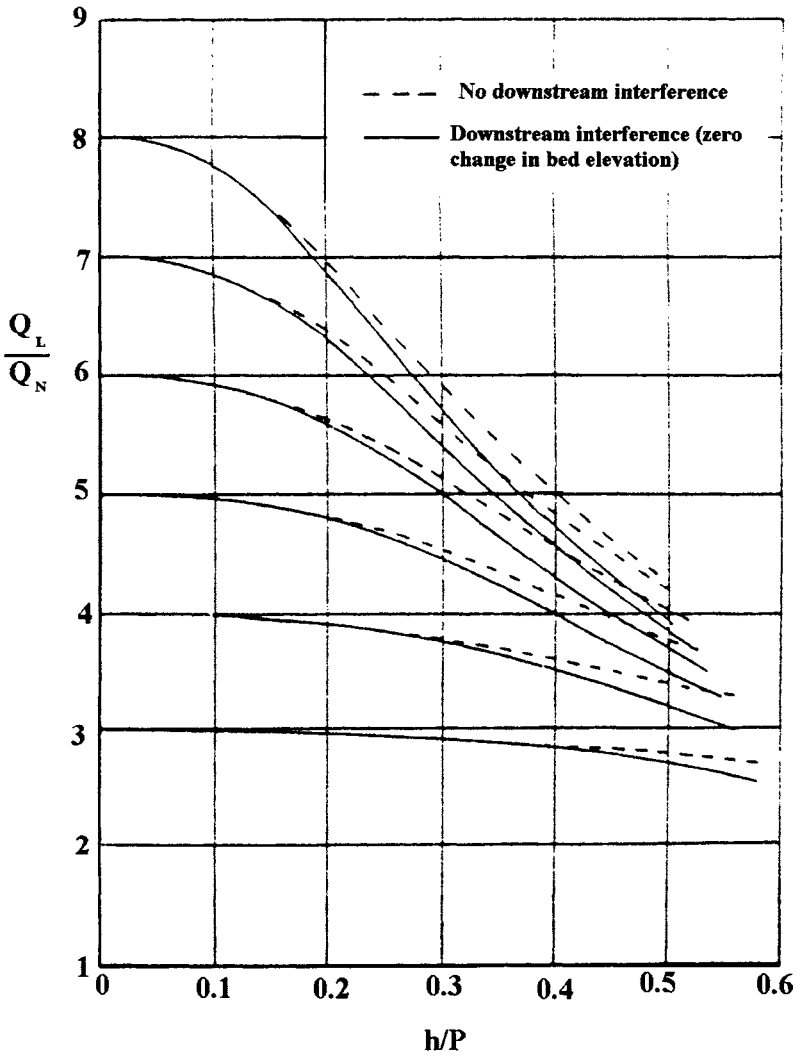


Figure 4b. Design Curve - Trapezoidal - Sharp Crested Weir from Hay, N., and Taylor, G., (1970). "Performance and design of labyrinth weirs." *American Society of Civil Engineering, Journal of Hydraulic Engineering*, 96(11), 2337-2357., permission from ASCE.

The discharge for a linear weir in these studies was determined from the weir equation of Kindsvater and Carter (1959):

$$Q_k = C_s \cdot L_e \cdot h_e^{3/2} \quad (5)$$

in which the discharge coefficient C_s is given by

$$C_k = 3.22 + 0.40 \cdot \frac{h}{P} \quad (6)$$

or, in English units, by

$$3.22 = 0.6 \cdot \frac{2}{3} \cdot \sqrt{2 \cdot 32.2} \quad (7)$$

The equivalent crest length, L_e , is given by

$$L_e = L - 0.003 \text{ ft} \quad (8)$$

And the head on the weir is given by

$$h_e = h + 0.003 \text{ ft} \quad (9)$$

in which L_e = the equivalent crest length; and h_e = the equivalent head on the crest. Note that Equation 6 is in English units and is not dimensionally homogeneous. The corrections to the length and the head make a difference only for small values of h/P that might be observed in physical models. For prototype dimensions, these corrections are negligible, but in a model with small heads, the corrections are significant.

With submerged flow, the author corrected the flow over the linear weir using the Villemonte (1947) equation for submerged flow. The Villemonte relation is given by Equation 1 in Chapter 6, Downstream Chute, and in Figure 12 in Chapter 11, Special Cases.

Darvas

Darvas (1971) introduced the concept of a discharge coefficient defined as

$$C_w = \frac{Q_L}{W \cdot H_o^{1.5}} \quad (10)$$

in which Q_L = the total discharge; W = the total width of the labyrinth weir; and H_o = the total head on the weir. This coefficient has the units of $\text{ft}^{0.5}/\text{sec}$. The plots of Darvas are given as a family of curves in which

$$C_w = f(H_o / P, L / W) \quad (11)$$

in which L = the developed length of the labyrinth weir. These curves are shown in Figure 5.

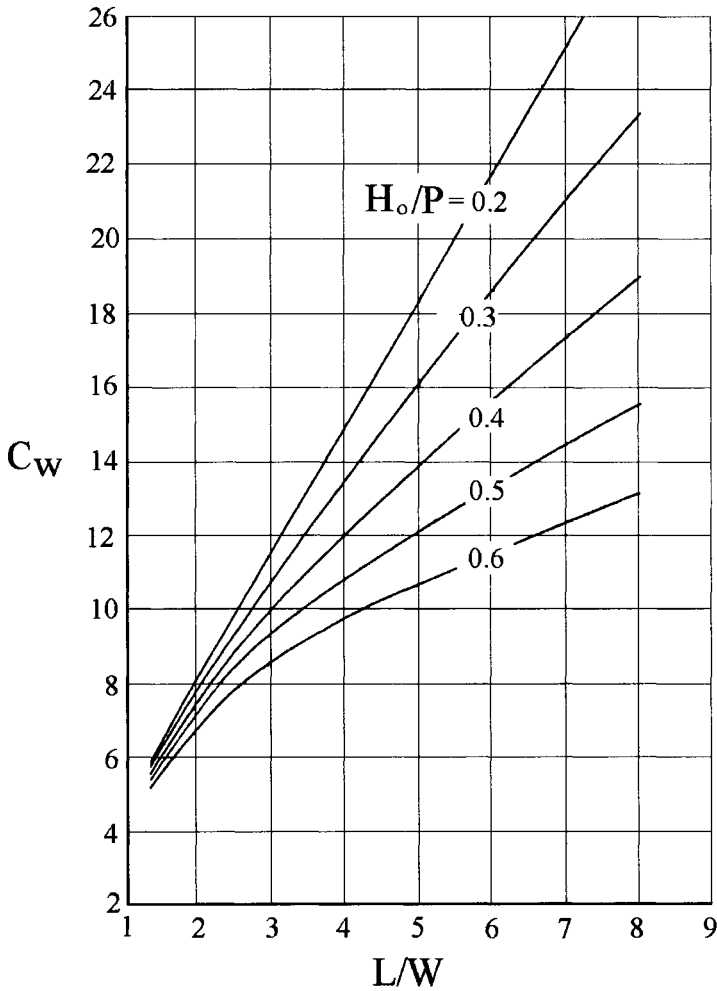


Figure 5. Design Curves from Darvas, L.A., (1971). "Discussion of 'Performance and design of labyrinth weirs,' by Hay and Taylor." *American Society of Civil Engineering, Journal of Hydraulic Engineering*, 97(80), 1246-1251., permission from ASCE.

Megalháes and Lorena

Megalháes and Lorena (1989) developed curves similar to that of Darvas (1971), except their curves are for a nappe or ogee crest, and the discharge coefficient is given in dimensionless terms by

$$C_p = \frac{Q_L}{W\sqrt{2gH_o^{1.5}}} \quad (12)$$

These curves are shown in Figure 6.

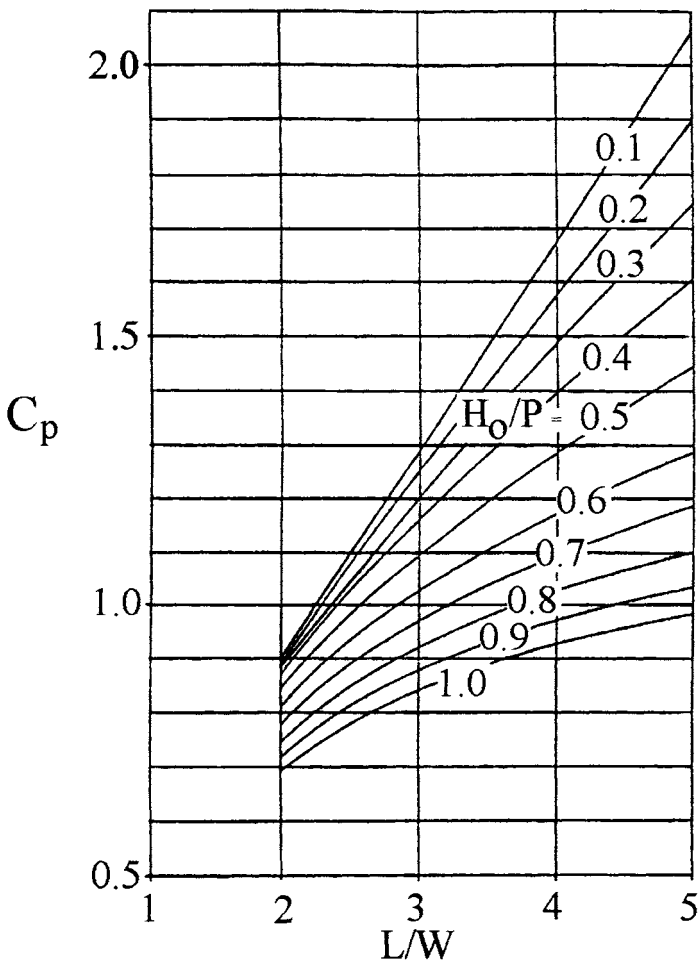


Figure 6. Design Curves for an ogee crest from Megalhães, A.P., (1985). "Labyrinth weir spillway." *Transactions of the 15th Congress ICOLD, Vol. VI, Q59-R24*, Lausanne, Switzerland, 395-407., permission from ICOLD.

Lux

Lux (1989) introduced another discharge coefficient based on the total upstream head. His relationship for the discharge of one cycle is given by

$$Q_x = C_w \left(\frac{W_c/P}{W_c/(P+k)} \right) W_c \cdot H_o \cdot \sqrt{g \cdot H_o} \quad (13)$$

in which k = a shape constant; H_o = the total upstream head; and g = the acceleration of gravity.

Lux found that k is 0.18 for triangular plan forms and is 0.1 for trapezoidal plan forms when a/W_c was equal to 0.0765, in which a is the half width of the upstream face of the labyrinth, as shown in Figure 2. The subscripts refer to a single cycle and not the entire width of the labyrinth. For multiple cycles, the discharge given by this equation must be multiplied by the number of cycles, n , or

$$Q_L = Q_c \cdot n \quad (14)$$

The curves of Lux and Hinchliff (1985) are given in Figure 3 for triangular and trapezoidal plan form shapes.

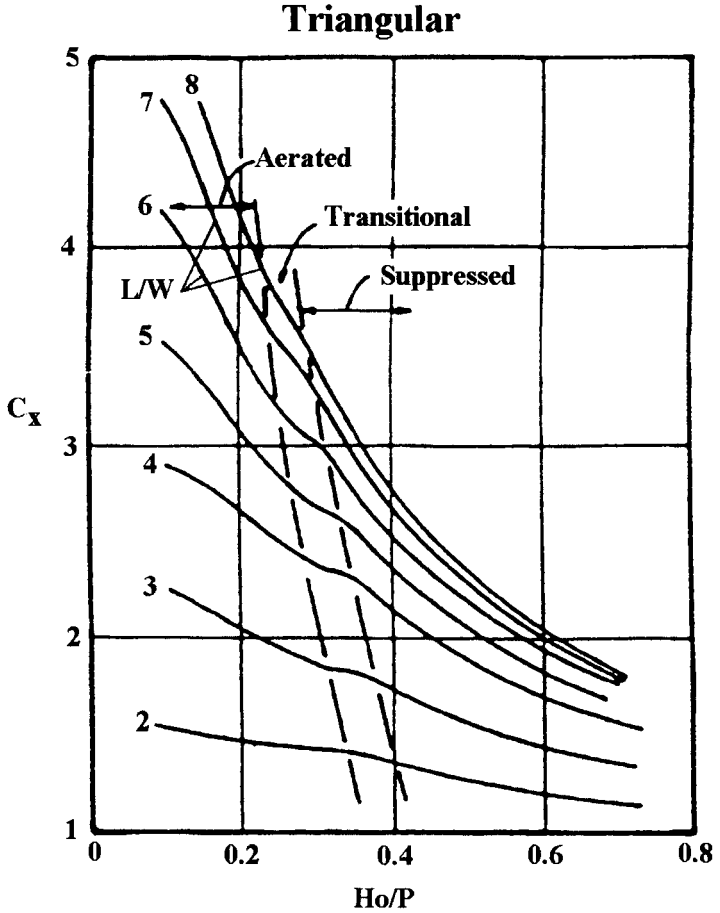


Figure 7a. Design Curve - Triangular Weir from Lux, F., and Hinchliff, D.L., (1985). "Design and construction of labyrinth spillways." *15th Congress ICOLD, Vol. IV, Q59-R15*, Lausanne, Switzerland, 249-274. permission from ICOLD.

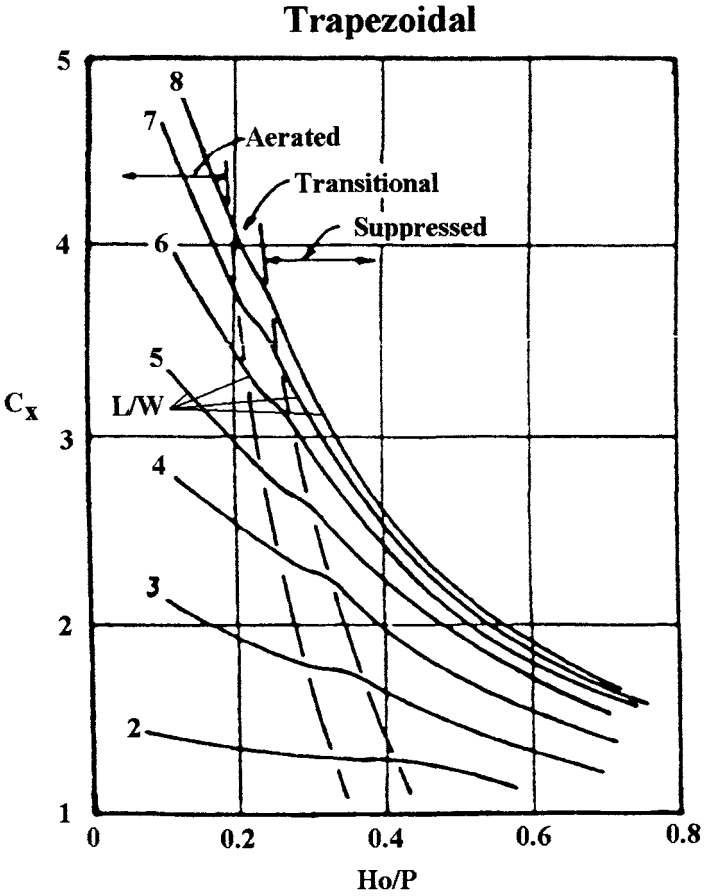


Figure 7b. Design Curve - Trapezoidal Weir from Lux, F., and Hinchliff, D.L., (1985). "Design and construction of labyrinth spillways." *15th Congress ICOLD, Vol. IV, Q59-R15*, Lausanne, Switzerland, 249-274, permission from ICOLD.

Tullis et al.

Tullis et al. (1995) defined a coefficient that used the total upstream head on the weir. Their equation is

$$Q_L = C_T \cdot L \cdot \frac{2}{3} \cdot \sqrt{2 \cdot g} \cdot H^{1.5} \tag{15}$$

This is similar to the conventional weir discharge equation (Equation 1 in Chapter 4, Crest Shapes), except that the head is the total upstream head and not the head on the weir crest. All of the tests were performed in a channel similar to the investigations of Taylor (1968).

The crest coefficients for a triangular weir with a quarter-round crest are shown in Figure 8 as a function of the angle that the weir makes with the flow.

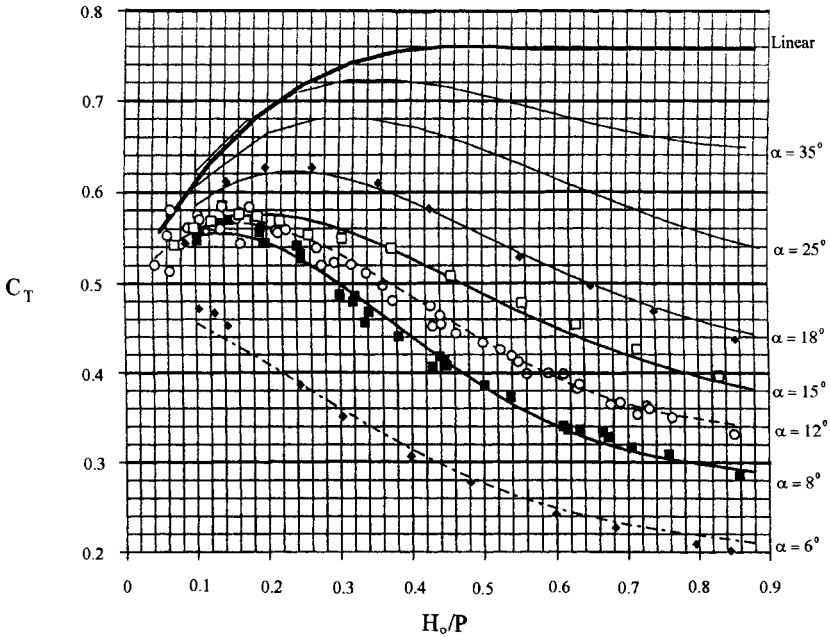


Figure 8. Design Curves with Quarter-round Crest and a Triangular Weir from Tullis, J.P., Nosratollah, A., and Waldron, D., (1995). “Design of labyrinth spillways. ” *American Society of Civil Engineering, Journal of Hydraulic Engineering*, 121(3), 247-255.

The data were fit with an equation of the form

$$C_T = A_1 + A_2 \left(\frac{H_o}{P} \right) + A_3 \left(\frac{H_o}{P} \right)^2 + A_4 \left(\frac{H_o}{P} \right)^3 + A_5 \left(\frac{H_o}{P} \right)^4 \quad (16)$$

The coefficients are given in the following matrix

Table 1. Coefficients for Design Curve

α	A_1	A_2	A_3	A_4	A_5
6	0.49	-0.24	-1.20	2.17	-1.03
8	0.49	1.08	-5.27	6.79	-2.83
12	0.49	1.06	-4.43	5.18	-1.97
15	0.49	1.00	-3.57	3.82	-1.38
18	0.49	1.32	-4.13	4.24	-1.50
25	0.49	1.51	-3.83	3.40	-1.05
35	0.49	1.69	-4.05	3.62	-1.10
90	0.49	1.46	-2.56	1.44	0

To determine intermediate values of α , compute the discharge coefficient for the two adjacent angles and then interpolate between the values. Do not interpolate between the coefficients. The coefficients for a labyrinth weir are valid only up to H_o/P of 0.9. With a linear weir, the coefficients are valid only up to H_o/P of 0.7. For larger depths, use a C_r of 0.76. These limits are not restrictive, because the design is generally limited to H_o/P less than 0.7.

Example Computations

The discharge as computed by the various methods can be illustrated with a practical example. Assume the following

- One cycle whose width, W , is 6 m;
- Crest length, L , is 24 m, or four times the width of a cycle;
- Weir height, P , is 3 m;
- Reservoir head over the crest, H_o , is 1.5 m; and
- A trapezoidal weir with an upstream width, a , is 0.45 m.

The pertinent parameters are

- Aspect ratio, W/P , is 2;
- Magnification ratio, L/W , is 4;
- Depth ratio, H/P , is 0.5;
- Blockage ratio, a/W , is 0.075; and
- Angle of wall, a , is $\arcsin((W-4a)/(L-4a))$, or 10.9° .

From Hay and Taylor (1970)

$$Q_L/Q_N = 3.7$$

$$Q_N = (0.6 \cdot 2/3 \cdot (2 \cdot 9.81)^{1/2} + 0.4 \cdot 0.5)(6)(1.22)^{3/2} = 16 \text{ m}^3/\text{sec}$$

$$V^2/2g = (59.3/(6 \cdot (3+1.22)))^2/(2 \cdot 9.81) = 0.28 \text{ ft}$$

$$h \text{ (by trial and error)} = 1.5 - 0.28 = 1.22 \text{ ft}$$

$$h/P = 0.41$$

$$Q_L = 16 \cdot 3.7 = 59.3 \text{ m}^3/\text{sec}$$

From Darvas (1971)

$$C_w = 10.9 \cdot 0.552 = 6.01$$

Note: the 0.522 is to convert the coefficient to metric units

$$Q_L = 6.01 \cdot 6 \cdot 1.5^{3/2} = 66.2 \text{ m}^3/\text{sec}$$

From Megalhães and Lorena (1989)

$$C_m = 1.29$$

$$Q_L = 1.29 \cdot 6 \cdot (2 \cdot 9.81)^{1/2} \cdot 1.5^{1.5} = 63 \text{ m}^3/\text{sec}$$

From Lux (1989)

$$C_c = 1.7$$

$$k = 0.18$$

$$Q_L = 1.8 \cdot (2/2.1) \cdot 6 \cdot 1.5 \cdot (9.81 \cdot 1.5)^{1/2} = 59.2 \text{ m}^3/\text{sec}$$

From Tullis et al. (1995)

$$C_T = 0.42$$

$$Q_L = (2/3) * 0.42 * 24 * (2 * 9.81)^{1/2} * 1.5^{1.5} = 55 \text{ m}^3/\text{sec}$$

Critique of Design Curves

As shown in Table 2, the mean of all the curves is $60.5 \text{ m}^3/\text{sec}$ with a standard deviation of $\pm 4.2 \text{ m}^3/\text{sec}$. The two outliers from the mean are the curves of Darvas and Tullis. Considering that the values are taken from interpolations of curves and that the experimental error in developing the curves is on the order of at least $\pm 5\%$, the agreement between the five curves is remarkable. However, the variation among these values means that the design curves must be examined in more detail.

Table 2
Comparison of Design Curves

Design Curve	Discharge	% Difference from Mean
Darvas	66.2	9.4
Hay	59.3	-2.0
Lux	59.2	-3.1
Tullis	55.0	-9.1
Megalhães	63.0	4.1
Mean	60.5	

The design curves of Hay and Taylor (1970) are applicable for sharp crested spillways that are located in a straight chute. They should not be used for rounded crests or for spillways that are not located well within a straight chute. The curves of Darvas (1971) are dimensional. However, they are applicable for crests with a quarter-round shape. The curves of Megalhães and Lorena (1989) were developed for an ogee crest, and they are nondimensional. Lux (1989) developed nondimensional curves for quarter-round crests. His equation takes into account the aspect ratio, W/P . However, the studies of Hay and Taylor (1970) showed that the aspect ratio does not have a significant effect if it is larger than 2. Therefore, the equation of Lux is more complicated than necessary. In addition, if the k value in the equation of Lux corrects for the trapezoidal shape, then only one set of design curves is needed, not two. The curves of Tullis (1995) are for quarter-round crests with a triangular shape. With these curves, the angle of the crest and not the magnification is the significant parameter. The advantage of the curves by Tullis is that they show when interference

becomes significant. This can be seen in the deviation of each curve from the linear weir, as shown in Figure 8.

Because all the design curves are computed with different definitions of the discharge coefficient, a comparison of them can be made only if a constant definition is chosen. A discharge coefficient of the form given by Equation 15 appears to be a logical parameter for comparing the different design curves.

To illustrate the comparison, the model data on Avon and Woronora labyrinth spillways, as reported by Darvas (1971), and the model data of Boardman, as reported by Babb (1976), are compared with the tests by Tullis (1995). These curves are shown in Figures 9, 10, and 11. They all agree relatively well with the design curves of Tullis (1995).

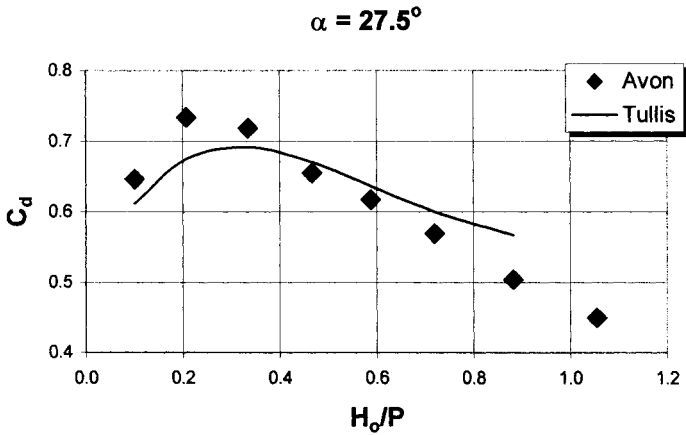


Figure 9. Avon Labyrinth Spillway, Data from Darvas (1971)

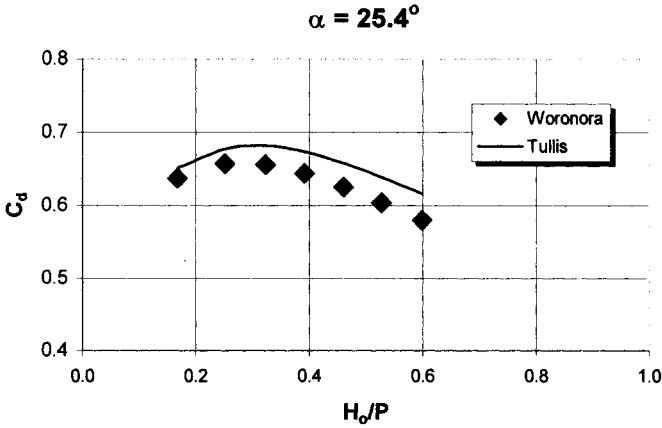


Figure 10. Woronora Labyrinth Spillway, Data from Darvis (1971)

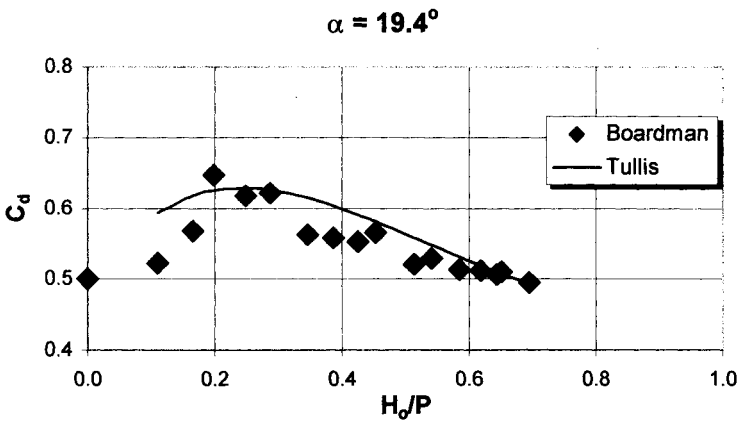


Figure 11. Boardman Labyrinth Spillway, Data from Babb (1976)

Plotting the data of Megalhães with the same definition of the discharge coefficient shows that a labyrinth with an ogee crest has a lower coefficient than does the quarter-round shape for heads with an H_0/P greater than 0.2, as shown in Figure 12. The percentage difference between the two curves is greater with the larger crest angles and may be the result of increased interference with the larger ogee crest.

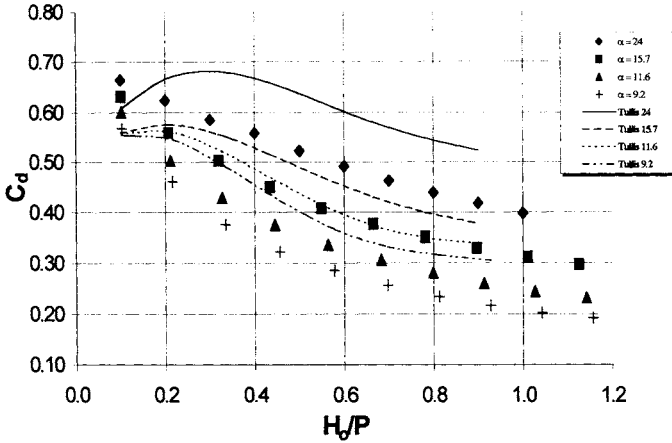


Figure 12. Curves for an ogee crest, Data from Magalhães and Lorena (1989)

Appendix B shows a comparison of the Tullis (1995) curves with published data from several labyrinth spillways. For these computations, the discharge coefficient for the spillway was determined using Equation 15. The values for the Tullis coefficient were determined by interpolating discharge coefficients between adjacent sidewall angles using Equation 16. The difference indicates the percentage that the published data are either greater or less than the Tullis coefficient. The average deviation from the Tullis curves is about -1%, with a standard deviation of about 10%. These values are well within the values that would be expected from experimental error. The major deviations are caused by spillways with nonsymmetrical inlet flow conditions, possible errors in the published dimensions and flow properties, or cases in which the invert slopes in a downstream direction. In this latter case, the weir height varies along the crest, and H_o/P is not well defined.

The excellent agreement indicates that the Tullis curves can be used for initial computations for both trapezoidal and triangular shaped labyrinth spillways. Because the curves are developed in terms of the angle of the sidewalls, they take into account the difference between the trapezoidal and the triangular shapes. The difference between the trapezoidal and the triangular shapes is in the amount of flow that passes over the upstream and downstream apex sections of the trapezoidal weir. Because this length is a small proportion of the total weir length, the difference in discharge between the two shapes is generally less than 10%.

This page intentionally left blank

Chapter 6

Downstream Chute

Introduction

The purpose of the downstream chute is to convey the water from the weir back to the original streambed. Several items need to be considered in the design of the downstream chute. If the chute is not as wide as the spillway, then a transition is placed between the spillway and the chute. To accelerate the flow and prevent submergence of the spillway, the chute is usually placed on a hydraulically steep slope. Any changes in alignment on steep chutes will create supercritical waves. Even if the width does not change, supercritical waves can form downstream from each apex of the labyrinth.

If the downstream chute is on a subcritical slope, submergence can become a problem with high tailwater elevations. Some designers have considered the use of aprons between the downstream walls to accelerate the flow away from the labyrinth. Therefore, the effect of these aprons must also be considered.

Supercritical Waves

Because of the similarity in the equations that describe the formation of supercritical waves and the formation of shock waves with high-speed compressible flows, supercritical waves are often referred to as shock waves. The formation of supercritical waves with converging flow from a wide spillway to a narrow chute is clearly evident in the tests of the Boardman spillway, as shown in Figure 1.

Depending on the design of the chute, the supercritical waves can propagate downstream with a resulting overtopping of the chute sidewalls. The supercritical waves can be eliminated or reduced by proper design of the transition. Many authors have written on this subject, so supercritical waves are not covered in this book. A good summary reference is by Hager (1992) in Bulletin No. 81 of the International Committee on Large Dams. Of particular interest is the use of a curved invert geometry to eliminate the shockwaves.

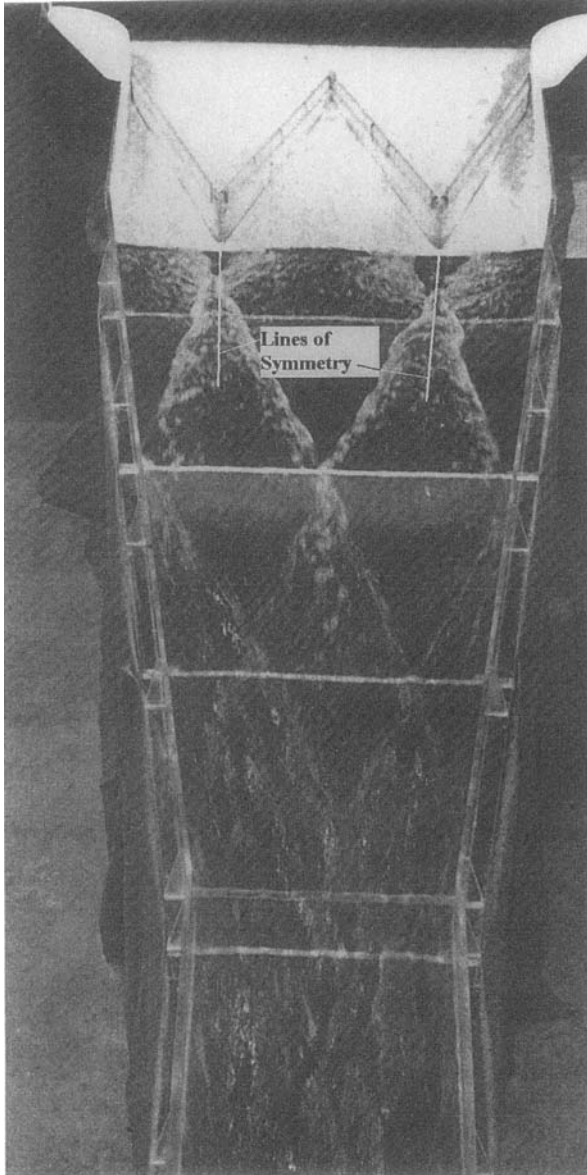


Figure 1. Supercritical Waves in Downstream Transition Section - Boardman Spillway from Babb, A.F., (1976). "Hydraulic model study of the Boardman Reservoir spillway." R.L. Albrook Hydraulic Laboratory, Washington State University, Pullman, Wash., May. Permission from Albrook Hydraulic Laboratory.

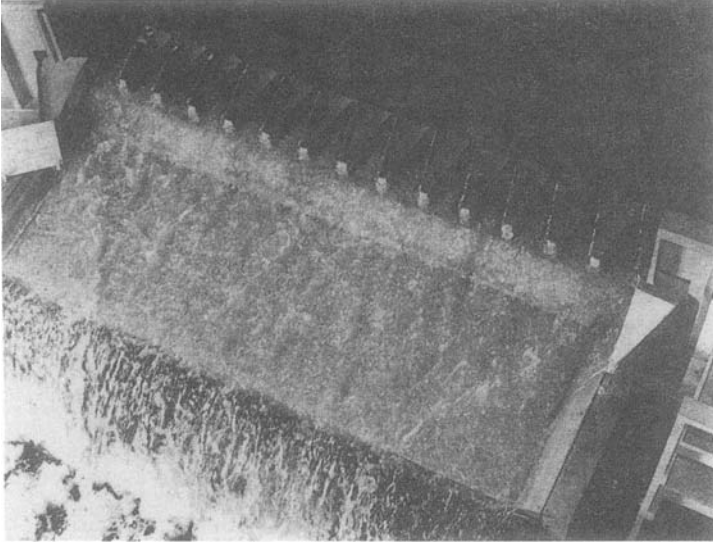


Figure 2. Ute spillway from Houston, K.L., (1982). "Hydraulic model study of Ute Dam labyrinth spillway." *Report No. GR-82-7*, U.S. Bureau of Reclamations, Denver, Colo. Permission from USBR.

If the number of cycles relative to the chute width is large, then the supercritical waves interact, and the flow in the downstream chute is almost uniform. An example of this is the 14-cycle model of the Ute spillway, as shown in Figure 2.

Flow splitter walls have been used in an attempt to control the formation of the supercritical waves. For instance, flow splitters were placed downstream of the apexes on the Quincy spillway in an effort to control the supercritical waves, as shown in Figure 3.



Figure 3. Splitter walls at Quincy Spillway

However, as shown in Figure 1, the splitter walls are located in the zone where the flow is symmetrical, and they will have little or no effect on the supercritical waves. Therefore, the use of splitters attached to the downstream apex of steep slopes is not recommended to reduce supercritical waves.

Aprons

Taylor (1968) studied the effect of a downstream apron, as shown in Figure 4.

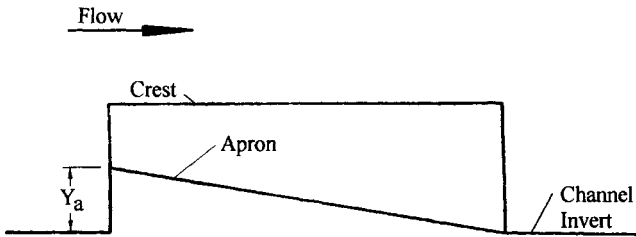


Figure 4. Downstream Apron from Taylor, G., (1968). "The performance of labyrinth weirs." PhD thesis, University of Nottingham, Nottingham, England.

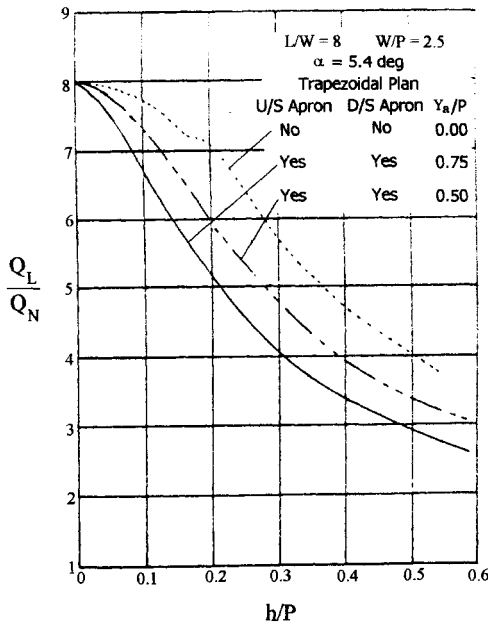


Figure 5. Effect of aprons on Labyrinth Discharge Apron from Taylor, G., (1968). "The performance of labyrinth weirs." PhD thesis, University of Nottingham, Nottingham, England.

He found that the apron decreases the discharge over the weir, as shown in Figure 5. In this figure, aprons were installed both upstream and downstream. Y_a is the height of the apron above the invert, and P is the weir height. This configuration could simulate sediment in the upstream channel and an intentional installation of a downstream apron. The results clearly show that attempts to direct the flow over a labyrinth through the use of aprons are not effective.

One example of a downstream apron is that of the Arnwell Magna spillway in the United Kingdom, as shown in Figure 6. The ideas behind this design were evidently for dissipation of the energy of the downstream flow before it entered the stilling basin and for aesthetics. However, the effect of the downstream apron is to increase the submergence on the crest; absence of the apron will decrease the capacity of the structure over that of a spillway.

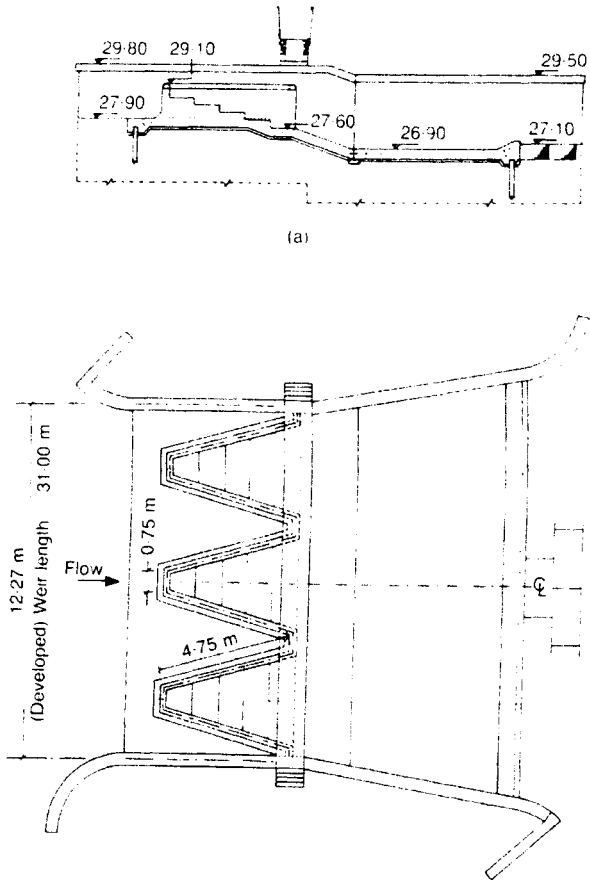


Figure 6. Arnwell Magna (River Lee)- UK from Van Beesten, (1992), "Hydraulic structures in flood control systems," *Proceedings of the Institution of Civil Engineers, Civil Engineering*, 92, Feb., 30-38, permission from ICE.

To reduce the effect of the downstream apron and to assist the movement of water downstream from the spillway, the floor on which the labyrinth is placed often slopes downward, as shown in Figure 7. When possible, this configuration should be used. The downward sloping apron decreases the tendency for submergence and improves the aeration of the crest.

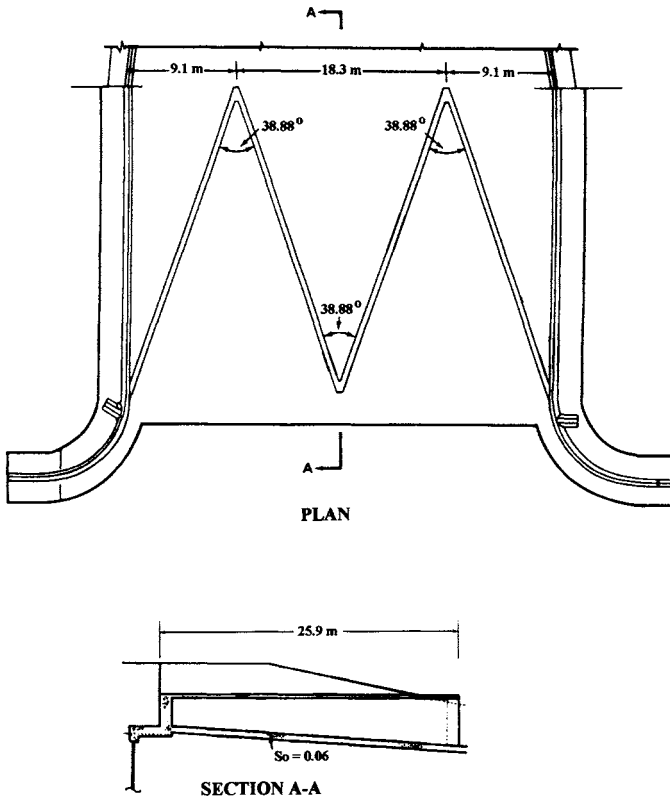


Figure 7. Boardman Spillway from Babb, A.F., (1976). "Hydraulic model study of the Boardman Reservoir spillway." R.L. Albrook Hydraulic Laboratory, Washington State University, Pullman, Wash., May, permission from Albrook Hydraulic Laboratory.

Submergence

If the water level in the space between the labyrinth weirs exceeds the crest elevation, the weir is submerged. Submergence decreases the flow rate over the weir. The submergence, h_d , of weirs is described by the height of the tailwater above the crest of the weir. With sharp crested weirs, the submerged discharge, Q_s , is given by the Villemonte (1947) equation:

$$Q_s = Q \left[1 - \left(\frac{h_d}{h_u} \right)^{3/2} \right]^{0.385} = Q \left[1 - \left(\frac{h_d P}{P h_u} \right)^{3/2} \right]^{0.385} \quad (1)$$

in which Q = the discharge, as determined from the upstream head, h_u ; and h_d = the downstream head on the weir crest. If the depth is measured far enough downstream, Equation 1 gives good results whether the jet plunges or not.

Taylor (1968) found that the effect of submergence with labyrinth weirs is similar, as shown in Figure 8. With the tailwater elevation equal to the elevation of the weir crest, no effect was noted on the design curve. Falvey and Treille (1995) observed the same result with flow over fuse gates. Only when the tailwater becomes higher than the crest does the discharge begin to decrease. Taylor shows that as the submergence (defined in this case as the ratio of the downstream water level over the crest to the weir height) increases, the flow over the weir decreases. The curves in Taylor's thesis are a bit confusing because he calculated the linear weir characteristics using Equation 1. Figure 8 shows the effect of submergence relative to a nonsubmerged linear weir. The theoretical lines in the figure are determined using Equation 1. When h_d/P equals h/P , the curves must go to zero. The trends indicate that Equation 1 may describe the effects of submergence for large values of h/P . However, when h_d/P approaches h/P , Equation 1 deviates from the observed data. These results indicate that more research is needed on the submergence effects with labyrinth weirs.

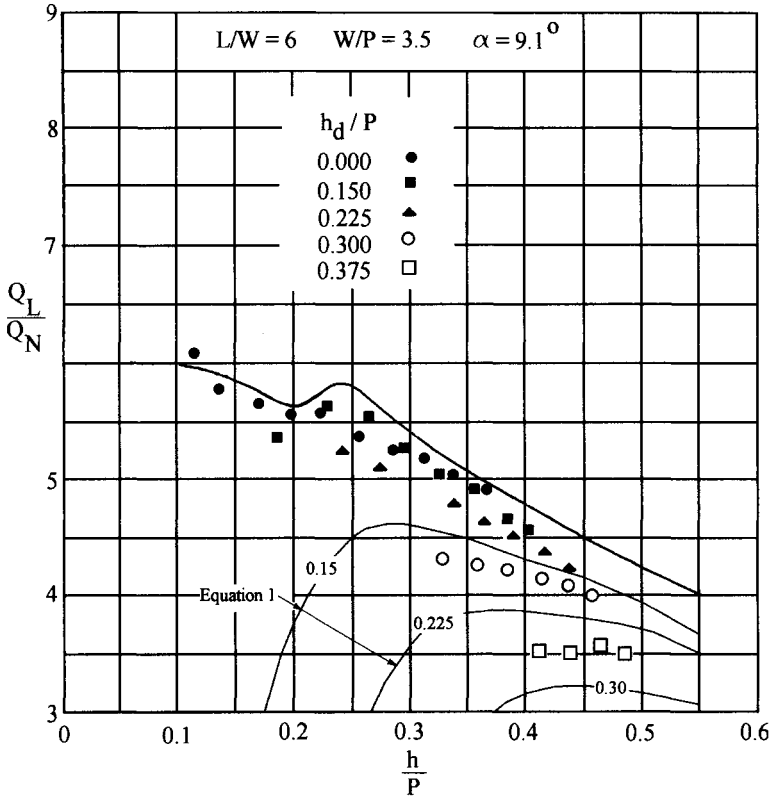


Figure 8. Effect of Submergence on Discharge after Taylor, G., (1968). "The performance of labyrinth weirs." PhD thesis, University of Nottingham, Nottingham, England.

As noted in Chapter 3, Nappe Interference the configuration of the downstream channel can have an important influence on the performance of the labyrinth weir. As Figure 9 in that chapter shows, the use of a sloping instead of a flat downstream channel can decrease the effective interference by a factor of 2.5. This effect was noted even when the crest was far from being submerged.

Chapter 7

Nappe Oscillation

Introduction

For a small water level depth over a labyrinth weir having a quarter-round or a sharp crest, the nappe is aerated. It is for these flows that nappe vibration occurs. With nappe vibration, the nappe sustains waves along its trajectory. With further increases in flow depth, the nappe becomes thicker, nappe vibration stops, and aeration of the underside of the nappe is suppressed. When this happens, an air pocket forms beneath the nappe. As air is evacuated from the pocket, the pressure in the air pocket becomes subatmospheric. If it becomes low enough, air will be entrained through the nappe, and the pressure in the pocket will suddenly rise. However, the process then begins again. This flow condition is known as transitional flow in that the nappe alternates between aerated flow and nonaerated flow. The transitional flow phenomenon is called surging. Surging is accompanied with increases and decreases in the discharge, as well as fluctuations in the downstream water level. The distinction between nappe vibrations and surging is significant because the remedy for one may not be the remedy for the other.

Nappe Vibration

Nappe vibration can occur when the labyrinth is operating under low heads ($h/P \approx 0.01$ to 0.06). The lower figure corresponds approximately to the fall height for which the solid nappe will break up into individual clumps of water. Using the data from Ervine and Falvey (1987), the breakup length ratio, L_b/h , can be estimated to be between 50 and 100. This corresponds to a head ratio, h/P , of between 0.01 and 0.02.

Nappe vibration can cause objectionable noise and pressure fluctuations on the labyrinth sidewalls. At Avon Dam in Australia, nappe vibration created irritating noise that shook the windows of residents living near the dam, as shown in Figure 1.

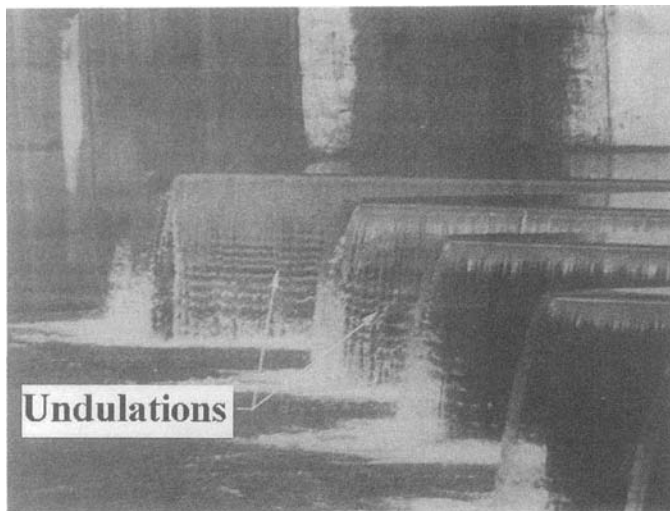


Figure 1. Vibrating Nappe - Avon Dam, after Australia Metropolitan Water, Sewerage and Drainage Board, (1980). "Investigation into spillway discharge noise at Avon Dam." *ANCOLD Bulletin No. 57*, 31-36. Permission requested.

Naudascher and Rockwell (1994) attribute the vibrations to inadequate aeration under the nappe. However, the root cause for the vibrations still has not been completely described. The fall height is a significant parameter. In addition, the thickness of the boundary layer and the three-dimensionality of the flow at the detachment point appear to be important. These facts indicate that the real cause of the vibrations may be a flow instability that is generated by the three-dimensional flow over the crest. Specific frequencies in the instability are amplified as the thin jet sheet falls over a critical height. Perhaps the air under the nappe contributes to this amplification. However, Falvey (1980) reports on nappe vibrations with fully aerated jets.

Case Study

The investigations of nappe vibration by the Metropolitan Water, Sewerage and Drainage Board (1980) on the Avon labyrinth spillway are particularly enlightening. The Board conducted studies on a 1:8-scale model, a full-scale model having a half-size drop, and a full-scale model with the prototype drop height. The crest profile of the Avon labyrinth spillway was compared with the crest profile of the Woronora spillway, which did not exhibit nappe vibration. The two crests are markedly different, as shown in Figures 2 and 3.

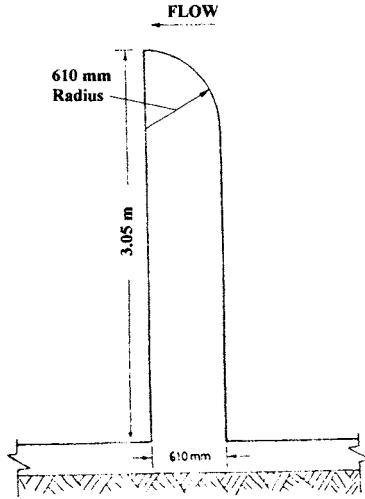


Figure 2. Avon Spillway, after Metropolitan Water, Sewerage and Drainage Board, (1980). "Investigation into spillway discharge noise at Avon Dam." *ANCOLD Bulletin No. 57*, 31-36.

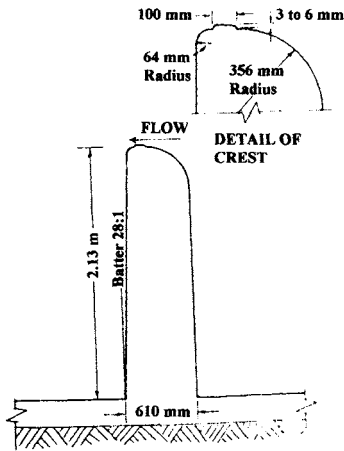


Figure 3. Woronora Spillway, after Metropolitan Water, Sewerage and Drainage Board, (1980). "Investigation into spillway discharge noise at Avon Dam." *ANCOLD Bulletin No. 57*, 31-36.

The crest on the Woronora spillway was eroded, and aggregate was exposed. In addition, it had a raised section just upstream of the 64-mm radius. The sidewall height is about 2/3 that of the Avon spillway.

Nappe vibration was produced in the 1:8-scale model. However, the vibrations did not arise naturally. Placing a stick in the nappe and then quickly withdrawing it would excite the nappe to oscillate for about 14 to 35 seconds. The width of the test channel was 610 mm, and the range of heads for which vibrations occurred was 60 to 74 mm. The frequency of vibrations was 48 Hz.

Several modes of vibrations were observed with the half-height, full-scale model. These were produced over a head range of 16 to 120 mm. These correspond to a head ratio, h/P , of 0.008 to 0.056. The width of the full-scale models was 4.27 m. With the full-height, full-scale model, the vibrations were observed to grow and decay, as shown in Figure 4. The depth aspect ratio, h/B , for this condition was 0.015

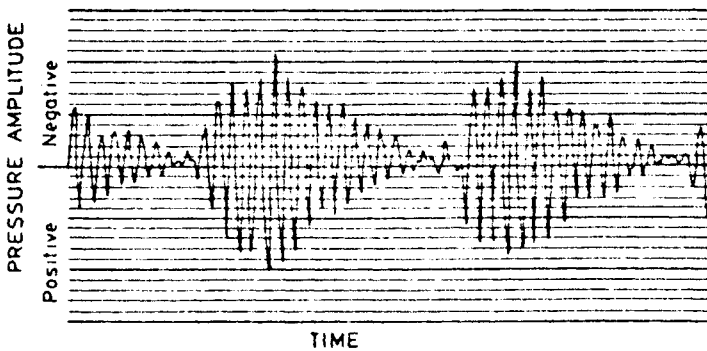


Figure 4. Growth and decay of Vibrations with a head of 63 mm from Metropolitan Water, Sewerage and Drainage Board, (1980). "Investigation into spillway discharge noise at Avon Dam." *ANCOLD Bulletin No. 57*, 31-36, Permission requested.

Several modifications to the crest were studied. These included a radius on the downstream face of the crest, a bulbous nose on the downstream face, an angle iron on the crest, splitters, and roughening the crest, as shown in Figure 5.

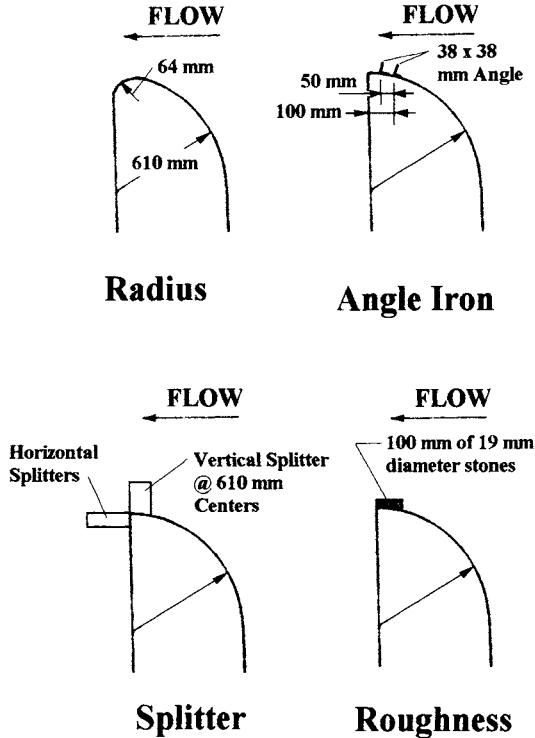


Figure 5. Modifications of crest after Metropolitan Water, Sewerage and Drainage Board, (1980). "Investigation into spillway discharge noise at Avon Dam." *ANCOLD Bulletin No. 57*, 31-36.

The radius required a higher head for the nappe to spring free. In the case of the half-height model, this was beyond the range at which vibrations developed. However, for the full-height model, it was not sufficient to prevent vibrations. The bulbous nose (not shown) also caused the napped to cling to the downstream face. The construction of this feature was deemed to be too expensive.

The angles on the crest were either 50 or 100 mm from the downstream face, not both. The tests showed that this modification had promise; however, it was not used because of difficulties in attaching the angles to the crest.

The splitters were effective in significantly reducing the vibrations. They were observed to thicken the nappe near the splitters. The proportion to which the thickened nappe intruded into the overflowing nappe had a significant effect on the degree to which the vibrations were suppressed. This observation indicates that a splitter consisting of a flat plate placed normal to the flow will be more effective than a right-angle splitter whose apex is oriented in the upstream direction. The height aspect ratio, h/B , for which the splitters were effective, varied between 1:5 for the

maximum depth and 1:38 for the minimum depth at which vibrations were observed. Because so many splitters were required to eliminate the vibrations, this solution was not recommended.

The roughened crest completely eliminated the vibrations. The only disadvantages were that the crest height was increased by 15 mm and that the discharge was decreased by about 2%. This modification was achieved by gluing the stones to the crest with an epoxy cement. Falvey (1980) also noted that a roughened surface to the upstream face of a flip bucket spillway eliminated vibrations. In both cases, the roughness is not sufficient to cause breakup of the jet.

Surging Flows

Surging flows occur with a much higher head on the crest than that with nappe vibrations. For example, the Boardman spillway has a semicircular crest. With this crest profile, the water clings to the downstream side of the crest until the head ratio, H_o/P , reached a value of about 0.3. Then the flow became transitional. When the head ratio reached a value of about 0.5, the surging stopped. A part of the model study was to investigate the magnitude of the oscillations to ensure that their frequency did not correspond to the natural resonance frequency of the sidewalls. The fluctuations were somewhat random, but they had a predominant frequency in the range of 0.1 to 0.6 Hz. Note that this is much lower than the 48-Hz frequency observed at Avon Dam. Crests with a semicircular profile have similar characteristics, with the exception that the surging starts at a somewhat smaller head ratio.

The remedy for surging flow is the installation of a flow splitter near the downstream end of the weir crest. Hinchliff and Houston (1984) recommend that flow splitters be located at a distance equal to 8% to 10% of the wall length upstream of the downstream apex. These types of splitters were placed on the Flamingo spillway, as shown in Figure 6.

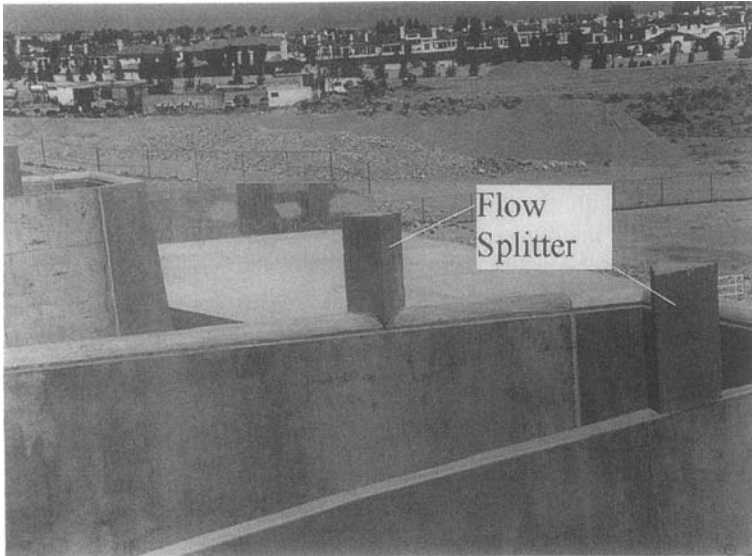


Figure 6. Flow Splitters on the Downstream Walls.

None of the remedial measures used to suppress nappe vibration will be effective in reducing surging. Yildiz and Üzücek (1996) recommend the use of aerators located in the sidewalls as an effective means to suppress surging. They argue that this approach does not have the negative aspect of reducing spillway length that occurs with flow splitters. If aerators are used, the vents should be located high on the wall, as close to the downstream crest as possible. However, no guidance is presently available as to the size or horizontal location of the vents.

Conclusions

Nappe vibration a flow instability and a lack of aeration are important considerations in the design of a labyrinth spillway. One remedy that has been suggested in the literature to eliminate nappe vibration is the provision of air vents within the sidewalls of the labyrinth weir. Obviously, these will not be effective if the true cause of the vibrations is a function of either the turbulence or the boundary layer thickness of the flow over the crest as it forms into a free jet.

The head ratio, h/P , for which nappe vibrations occur, is very small. At Avon Dam, the ratio was in the range 1:100 to 1:17. To stop vibrations with flow splitters, the jet was broken up into segments with an aspect ratio of flow depth to crest length between 1:5 and 1:38.

The Avon Dam tests show that even a 1:8-scale model has difficulty in reproducing the nappe vibration that was observed in the prototype. Observations in models in which surface tension is significant will certainly produce erroneous results.

If the function of the roughness is to increase the boundary layer thickness, then the roughness does not need to be placed on the weir crest. In fact, placing the roughness further upstream on the curved crest may be more effective, and a smaller roughness could be used.

As opposed to nappe vibration, which creates noise, the most important consideration with surging deals with the fluctuating pressures on the walls. Frequencies of oscillation are usually measured in a model study to ensure that the surging frequency does not coincide with the natural frequency of the wall.

Chapter 8

Design

Significant Parameters

Studies on labyrinth weirs have shown that the most significant parameters are the length to width ratio, L/W ; the total head to crest height ratio, H_o/P ; and the sidewall angle, α . The aspect ratio, W/P , which others found to be important, has been replaced by a disturbance to sidewall length ratio, L_d/B . Rounding the crest has only a minor effect on improving the discharge coefficient ($< 3\%$). Finally, the number of weir cycles, n , is not a significant parameter on the discharge characteristics of labyrinth weirs. The approach flow conditions to the labyrinth weir are significant in determining the discharge coefficient for the spillway.

General Guidelines for Parameter Selection

Headwater Ratio

The headwater ratio is the total head on the weir divided by the weir height, H_o/P . Because the discharge coefficient decreases with increasing head, labyrinth weirs have the greatest application where the head is small. Lux (1989) recommends that the maximum headwater ratio be in the range of 0.45 to 0.50. Nevertheless, some labyrinth spillways have been designed with headwater ratios as large as 1. The maximum headwater ratio is more a question of the range over which the model discharge coefficients were determined rather than some absolute value. For example, the maximum headwater ratio for the Tullis et al (1996) tests is an H_o/P of 0.9. Because the equations to be used in the analysis are only valid up to an H_o/P of 0.9, this is the upper headwater limit. If higher values are necessary, then a physical model study of the structure is required.

Vertical Aspect Ratio/Sidewall Angle

The vertical aspect ratio is the width of a weir cycle divided by the weir height, W/P . Taylor (1968) recommends that to minimize the effect of nappe interference, the vertical aspect ratio should be larger than 2. For design purposes, a value between 2.0 and 2.5 is recommended by Lux (1989) for initial computations. As shown in Chapter 3, Nappe Interference, this ratio does not have a significant effect on nappe interference, as has been thought up until now. This criterion has been superseded by the disturbance length concept described below

Magnification Ratio

The magnification ratio is the length of the labyrinth crest divided by the cycle width, L/W . The limit for the curves of Tullis (1994) is an angle of 6° , which corresponds to a magnification ratio of about 9.5. As shown below, the effectiveness of a labyrinth weir decreases rapidly as the magnification ratio exceeds 10. With a magnification ratio of less than 2, consideration should be given to widening the intake or using an ogee crest that is curved in plan rather than using a labyrinth weir.

Sidewall Angle/Magnification

With a triangular labyrinth, the sidewall angle and the magnification are interrelated. The angle is given by

$$\alpha = \sin^{-1}\left(\frac{W}{2 \cdot B}\right) = \sin^{-1}\left(\frac{1}{m}\right) \quad (1)$$

in which m = the magnification ratio.

Limits for Triangular Labyrinths

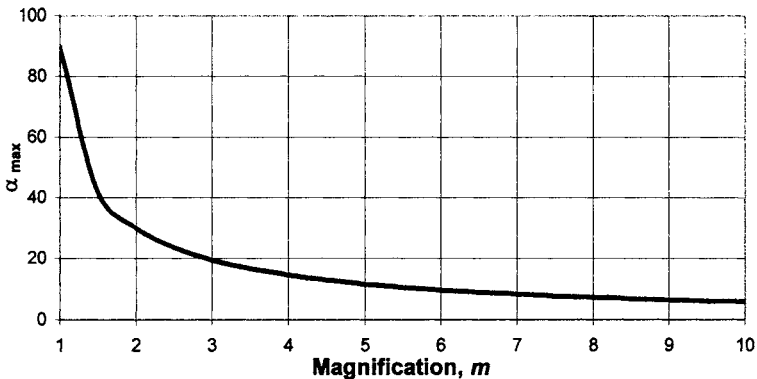


Figure 1. Maximum Angle for Triangular Labyrinth Weirs

Figure 1 gives the maximum angle for a triangular labyrinth weir. With a trapezoidal labyrinth, the angle of the sidewall will be less than that shown in Figure 1 for a given magnification. That is, the relationship between the magnification and the sidewall angle will lie below the curve with a trapezoidal labyrinth.

Efficacy

Actually, the magnification that is chosen applies only to small values of head. As the head increases, the discharge coefficient decreases. Thus, if a labyrinth is to pass the maximum discharge for a given reservoir elevation, then the product of the discharge coefficient and the magnification should be a maximum. Dividing this product by the discharge coefficient for a straight weir is called the efficacy. Efficacy is given by

$$\varepsilon = \frac{C_d(\alpha) \cdot M}{C_d(90^\circ)} \tag{2}$$

in which $C_d(\alpha)$ indicates that the discharge coefficient is a function of the sidewall angle.

Efficacy is essentially the same as the Q_L/Q_N parameter used by Taylor (1968). However, efficacy incorporates the magnification and the effect of the sidewall angle into one parameter. Thus, with this parameter, the benefits of changes in the labyrinth geometry can be estimated quickly during the design process.

The effects of head on the weir and the sidewall angle are clearly shown in Figure 2. The discharge coefficient for different angles is obtained from Figure 8 in Chapter 5, Design Curves.

The magnification parameter for a triangular labyrinth as a function of the sidewall angle is obtained from Figure 1 or Equation 1 above. For example, with an H_o/P of 0.7 and a sidewall angle of 18° , the discharge coefficient is 0.485, the magnification is

Efficacy

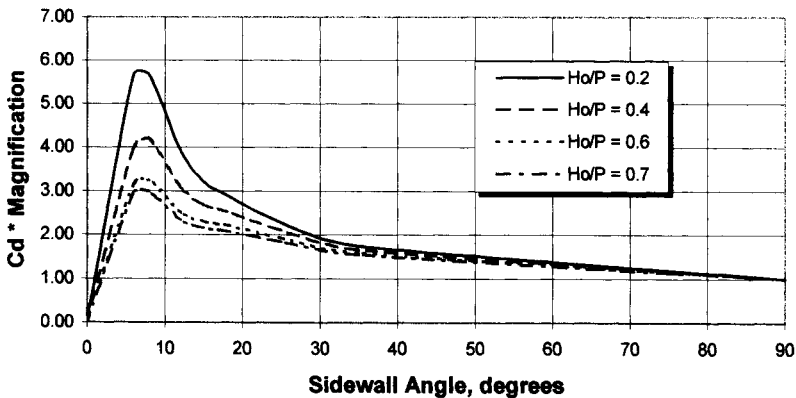


Figure 2. Efficacy for triangular weirs

3.24, and the discharge coefficient for the straight weir is 0.76. This gives an efficacy equal to 2.1. This means that the labyrinth can pass a little more than twice the flow for a given head than can a straight weir. However, if the sidewall angle is decreased to 8° , the efficacy increases to 3 because $C_d(\alpha)$ is 0.315, m is 7.18, and $C_d(90^\circ)$ is 0.76. Thus, the weir can pass three times the flow for a given head than can a straight weir.

The efficacy reaches a maximum value for all head ratios at a sidewall angle of about 8° . This angle corresponds to a magnification of 7.2. The efficacy decreases rapidly as the angle becomes smaller than 8° . In addition, Figure 2 shows that the efficacy decreases as the head over the weir increases.

The effects for a trapezoidal weir are similar to those for a triangular weir except that the efficacy does not approach zero as the sidewall angle approaches zero. With a trapezoidal or rectangular weir, the apex distance separates the two walls. For example, with a rectangular weir, a zero sidewall angle means that the two walls are parallel.

Taylor (1968) studied the decrease in the discharge for trapezoidal and rectangular weirs and presented his data in the form of Q_L/Q_N , as shown in Figure 3. This figure shows that the sidewall angle of 9.5° has a higher discharge than does the 7° angle. Unfortunately, the data are too incomplete to show the effect at larger angles. Note that Figure 2 is for a quarter-round crest, whereas the curves in Figure 3 are for a sharp crest. In addition, Figure 2 contains both the magnification and the angle effects in one curve. This is an area in which more research is needed.

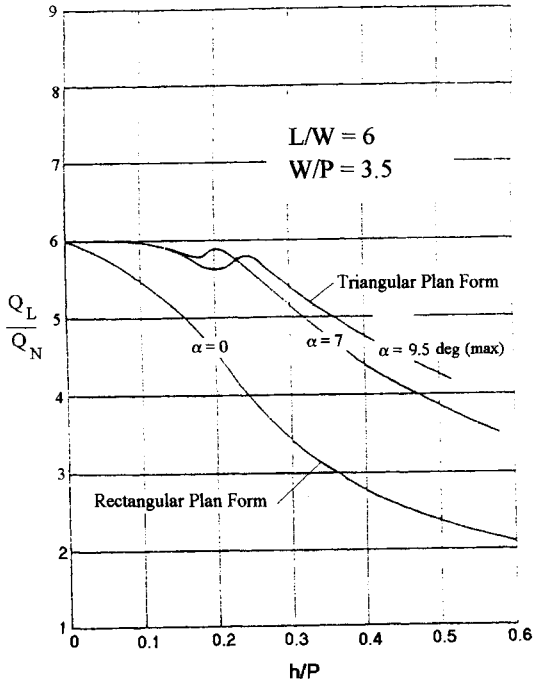


Figure 3. Effect of sidewall angle on discharge from Taylor, G., (1968). "The performance of labyrinth weirs." PhD thesis, University of Nottingham, Nottingham, England.

Apex Ratio

The apex ratio is the width of the apex divided by the cycle width, $2a/W$. The most efficient labyrinth weir is the triangular plan form. Interference increases with an increase in the apex ratio. However, construction considerations often dictate the use of a finite apex width. Values of the apex ratio that are less than 0.08 will not have a significant effect on the performance of a labyrinth weir. This is because of two effects. One is interference at the upstream apex. With interference, the upstream section of the sidewall does not convey a significant amount of water. Therefore, replacing the sharp corner of the triangular labyrinth with a blunt apex has little effect on the overall performance of the labyrinth. Similarly, the downstream end of a triangular labyrinth is essentially a stagnation zone. This is made evident by the rise in the water surface profile at the downstream end of the channel between the sidewalls, as shown in Figure 1 in the Chapter 5, Design Curves. Because of the stagnant zone, the downstream end of the labyrinth can also be replaced with a blunt apex with little effect on the overall performance of the weir.

Crest Shape

As the discharge coefficients show, the crest shape does not have a significant effect on the performance of the labyrinth weir. The quarter-round and the half-round shapes are commonly found in prototype structures. An ogee shape that is not thicker than the wall width may have a slightly higher coefficient at small heads. This shape is not more difficult to form than are the quarter-round and the half-round shapes, and it may stay aerated at higher heads. The full ogee shape used by Megalhães and Lorena (1989) is not recommended. It has a lower discharge coefficient at high heads because of nappe interference. In addition, the mass on the top of the wall requires much more attention to the wall design. This configuration will be more susceptible to vibration as the head over the crest increases. The effect of the crest shape on the discharge coefficient is given in Chapter 4, Crest Shapes.

Interference Length Ratio

As shown in Chapter 3, Nappe Interference, the ratio of the disturbance length to the sidewall length is an important consideration to limit the effects of interference. The disturbance length is determined from

$$\frac{L_{de}}{h} = 6.1 \cdot e^{-0.052 \cdot \alpha} \quad (3)$$

in which α = the sidewall angle in degrees. Here, the equation of Indlekofer and Rouvé (1975) is used instead of the suggested equations based on model studies of labyrinth weirs. When research has been completed on the interference with labyrinth weirs, this equation will be replaced with a more accurate relationship.

The ratio of the disturbance length to the sidewall length, L_{de}/B , should be less than or equal to 0.3. This can be written as

$$\frac{L_{de}}{B} = \frac{h}{B} \cdot 6.1 \cdot e^{-0.052 \cdot \alpha} \leq 0.3 \quad (4)$$

Approach Flow Conditions

Houston (1983) made a very important study of the effect of placement of the labyrinth weir relative to the reservoir. As shown in Figure 4, the labyrinth can be placed within the chute in either the normal or the inverted position, at the entrance to the chute, or extending into the reservoir. With a magnification of 5 and the orientation of the labyrinth in the normal position, the discharge was 9% greater than it was in the inverted position. In the normal position, the friction on the chute walls is a minimum.

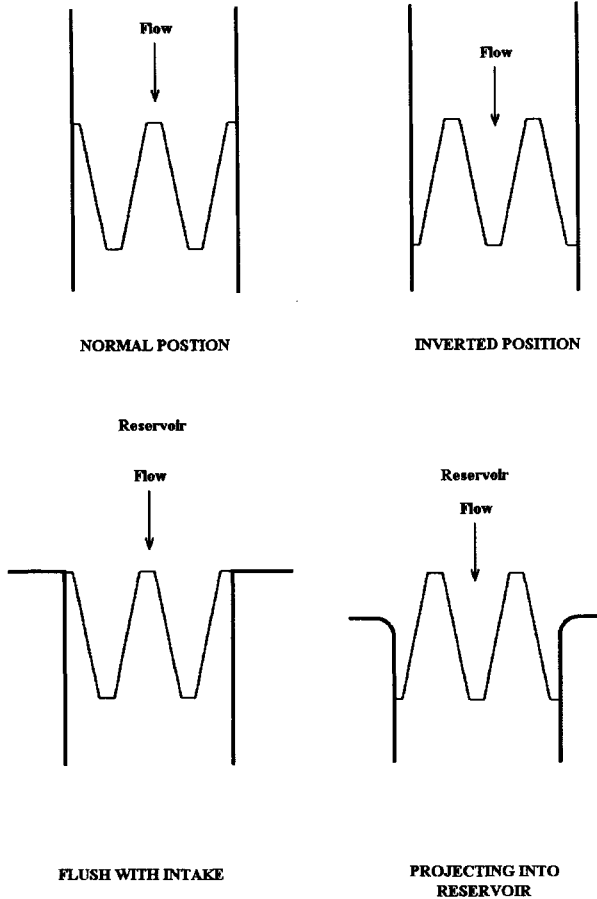


Figure 4. Labyrinth weir locations and orientations after Houston (1983)

As the labyrinth is moved into the reservoir, its capacity increases. The discharge with the labyrinth projecting into the reservoir is 20% greater than it is when in the normal position. However, a labyrinth projecting into the reservoir must use the less-efficient inverted position to tie the weir into the abutment. The curves used in the Excel spreadsheet, described below, are for a labyrinth weir placed in the normal position.

If a greater length of labyrinth is needed to pass a given discharge, the width of the approach section can be increased. For example, the width of the Avon spillway was made about 5.5 times wider than the downstream channel by creating a wide approach section. Similarly, the labyrinth width of the Kizilcapinar and Sarioglan spillways were made wider through the use of an expanded upstream approach channel. The alignment of the Avon and the Kizilcapinar spillways were curved, whereas that of the Sarioglan labyrinth was straight. Details of the alignments of these three spillways are given in Appendix A.

Downstream Channel

Considerations concerning the effects of the downstream channel geometry are given in Chapter 6, Downstream Chute.

Layout and Quantities

The dimensions of a labyrinth weir are shown in Figure 5. Stevens developed an Excel spreadsheet for URS¹ to be used in the design of labyrinth spillway installations. His spreadsheet was extensively modified to include the curves of Tullis (1994) and all the updated design limits. The spreadsheet is available in both English and metric units from falvey@members.asce.org.

¹ M. A. Stevens, PO Box 3263, Boulder, CO, 80307. Tel (303) 444-7120.

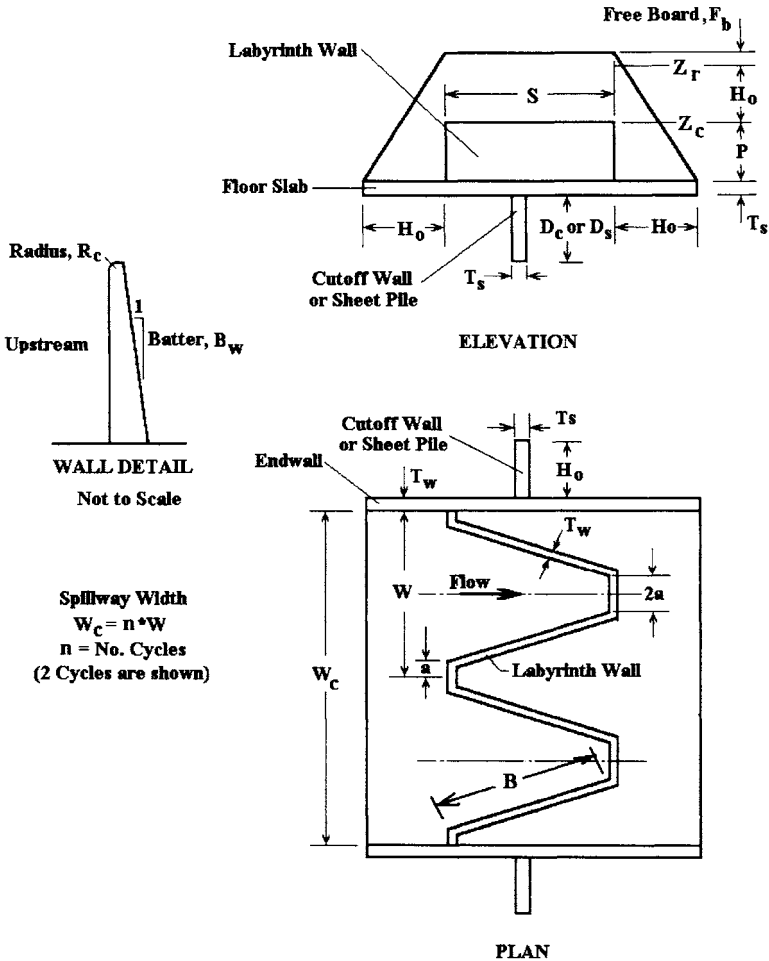


Figure 5. Definition Sketch for Labyrinth Spillway Geometry

Dimensions

The dimensions of the labyrinth weir are determined as follows:

Width of each cycle

$$W = \frac{W_c}{n} \tag{5}$$

Crest length of weir

$$L_w = \left(\frac{L}{W} \right) \cdot W = m \cdot W \tag{6}$$

Sidewall angle

$$\alpha = \tan^{-1} \left(\frac{W - 4 \cdot a}{2 \cdot S} \right) \quad (7)$$

Length of one leg of weir crest

$$B = \frac{L - 2 \cdot (2 \cdot a)}{2} \quad (8)$$

Depth of labyrinth weir

$$S = \sqrt{B^2 - \left(\frac{W - 2 \cdot a}{2} \right)^2} \quad (9)$$

Head on weir

$$H_o = Z_r - Z_c \quad (10)$$

Quantities

The volume computations to estimate the materials and costs are as follows:

Weir walls

$$V_w = n \cdot L \cdot P \cdot T_w \quad (11)$$

End walls

$$V_e = (P + H_o + F_b) \cdot (S + H_o) \cdot 2 \cdot T_w \quad (12)$$

Slab

$$V_s = (S + 2 \cdot H_o) \cdot W_s \cdot T_s \quad (13)$$

Concrete cutoff wall

(Without sheet piles)

$$V_c = [W_s \cdot D_c + 2 \cdot (D_c + T_s + P + H_o + F_b)] \cdot T_s \quad (14)$$

(With sheet piles)

$$V_c = W_s \cdot 2 \cdot D_c \quad (15)$$

Sheet piles

$$A_s = (W_s \cdot D_s) + D_s \cdot (P + H_o + F_b) \quad (16)$$

Reinforcing bars

$$M(lb) = \frac{\gamma_s}{3.5} \cdot (V_w + V_e + V_s + V_c) \quad (17)$$

in which γ_s = the unit weight of steel.

Discharge Coefficient

The discharge coefficients are obtained from Table 1 based on the design curves of Tullis (1994). In this table, the discharge coefficient is computed from

$$C_d = A_1 + A_2 \frac{H_o}{P} + A_3 \left(\frac{H_o}{P} \right)^2 + A_4 \left(\frac{H_o}{P} \right)^3 + A_5 \left(\frac{H_o}{P} \right)^4 \quad (18)$$

in which the discharge is given by

$$Q = C_d \cdot \frac{2}{3} \sqrt{2 \cdot g} \cdot L \cdot H_o^{3/2} \quad (19)$$

Interpolation for other angles should be done by first determining the coefficient for the adjacent angles and the given head ratio. Then, use linear interpolation between the two adjacent angles. Do not interpolate between the coefficients!

The discharge curves of Tullis (1994) are valid for an H_o/P of less than or equal to 0.9, for interference ratios less than those shown in Figure 7, and for sidewall angles greater than or equal to 6°.

Because the head ratio, H_o/P , should be less than 0.9, a maximum interference criterion of L_{do}/B equals 0.35 is recommended for use in the spreadsheet.

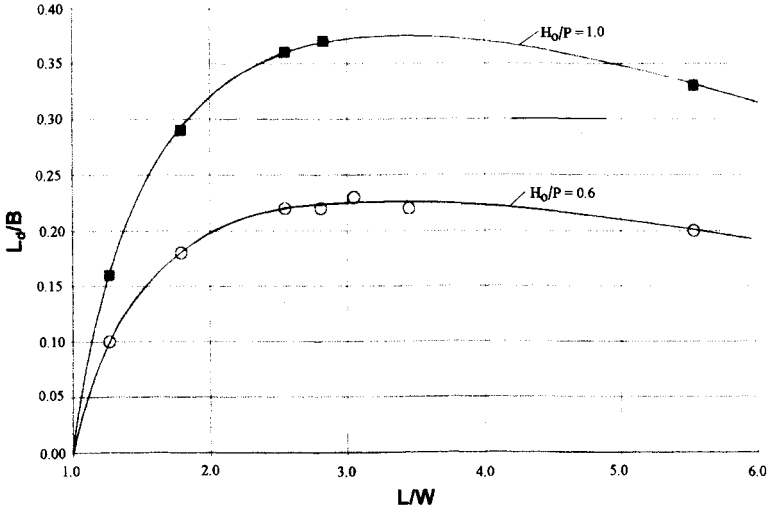


Figure 6. Maximum interference ratios for the design curves based on data from Tullis, J.P., Nosratollah, A., and Waldron, D., (1995). "Design of labyrinth spillways." *American Society of Civil Engineering, Journal of Hydraulic Engineering*, 121(3), 247-255.

Design Procedure

Steps

The steps in the design procedure are based on the availability of a spreadsheet that facilitates the process.

- Determine the labyrinth's location and channel alignment based on site conditions.
- Define the maximum allowable operating head on the weir that will satisfy operational specifications.
- Define the maximum discharge to be passed at the maximum allowable operational head.
- Use the spreadsheet to determine the spillway configuration that will pass the discharge at the specified operational head. Varying the floor elevation, the magnification, and the number of cycles will determine the most economical configuration. Figure 5 in Chapter 3, Nappe Interference, shows that the

smallest slab to support a labyrinth weir is the one that has the largest number of cycles. Therefore, the most economical design will be one with the smallest magnification ratio and the maximum number of cycles that does not violate the head and interference criteria. Violation of the interference criteria means that experimental conditions for which the discharge equations were developed are being exceeded. Thus, the discharge values may be in error. If the economics of the structure indicate that higher interference values are desirable, then a model study of the structure should be conducted to verify the performance at higher heads. As shown in Chapter 3, Nappe Interference, structures with interference values as high as 0.6 have performed satisfactorily.

- The designer must pay close attention to the estimated wall and slab thickness, as well as to the depth of the cut off wall. In addition, the unit prices should be as accurate as possible. These variables have a significant influence on the cost of the structure.
- Perform reservoir routing to verify that the selected design will meet the specified maximum head and discharge requirements.
- Analyze the approach flow conditions for high-velocity concentrations that may decrease the capacity of the spillway. For this analysis, a mathematical or a physical model study may be necessary.
- If either the reservoir routing or the approach flow conditions are not satisfactory, redesign the spillway by revising the approach flow width, changing the alignment, and varying the spillway input parameters using the spreadsheet.

Spreadsheet

For the Excel spreadsheet shown on the following pages, the required input is listed under the section "User Input." All other items are filled in automatically. The spreadsheet calculates the pertinent spillway dimensions, the maximum discharge, the estimated cost of the installation, a detailed discharge curve, and the labyrinth dimensions. The coordinates for one cycle are computed and plotted.

LABYRINTH WEIR DESIGN
No Approach Velocity

PROJECT: Hyrum
PROJECT NO. 1
FLOOD CRITERIA: PMF

TIME: 16:50:51
DATE: 02-Sep-02
BY: HTF

USER INPUT					
Max. Res	Zr	4678.0 ft	Thickness		
Crest el.	Zc	4672.0 ft	Wall	Tw	1 ft
Floor el.	Zf	4660.0 ft	Slab	Ts	1 ft
Spillway width	Ws	60.0 ft	Cutoff Depth		
Apex Width	2a	4 ft	Sheet Pile	Ds	0 ft
No. of cycles	n	2	Conc Wall	Dc	4 ft
Magnification	L/W	4.95			

CHECK ON RATIOS
Ld/B = 0.33 Ld/B RATIO IS OK
Ho/P = 0.50 Ho/P RATIO IS OK
L/W RATIO IS OK
Note: Lq/B must be <= 0.35
Ho/P must be <= 0.9
α must be >= 6 deg

LABYRINTH DIMENSIONS (Per Cycle)

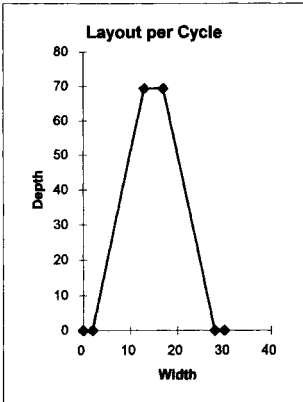
Wall Height	P	12 ft
Width	W	30.00 ft
Length	L	148.50 ft
Wall Length	B	70.25 ft
Depth	D	69.38 ft
Head max	H	6.00 ft
Wall Angle	α	9.01 deg
Length of	Lb	22.99
Interference		

CREST LAYOUT
(One Cycle)

X	Y	
0	0	Weir wall, cy
2.00	0	Abutment walls, cy
13.00	69.38	Slab, cy
17.00	69.38	Concrete cutoff, cy
28.00	0	Sheet pile, sf
30.00	0	Reinforcement, lb

COST CALCULATION

Unit price \$/unit	Units	Cost \$
	350	132
	350	106
	225	181
	200	86
	20	0
0.65	70,682	45,943



ESTIMATED COST
\$187,154

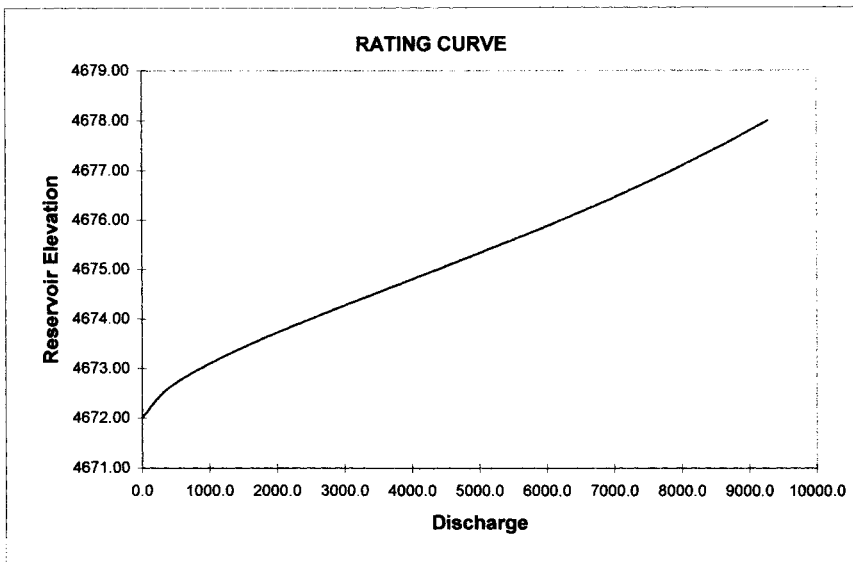
DISCHARGE
Qmax 9,285 cfs

COEFFICIENTS

Column	2.00
Cd lower	0.38
Cd Upper	0.44
Cd	0.40
Efficacy	2.59

RATING CURVE

HEAD	H _o /P	C _{lower}	C _{upper}	C _d	Q	RES
6.00	0.50	0.38	0.44	0.40	9285	4678.00
5.40	0.45	0.41	0.46	0.42	8455	4677.40
4.80	0.40	0.44	0.49	0.45	7559	4676.80
4.20	0.35	0.47	0.51	0.48	6580	4676.20
3.60	0.30	0.50	0.53	0.51	5518	4675.60
3.00	0.25	0.53	0.55	0.53	4394	4675.00
2.40	0.20	0.54	0.56	0.55	3247	4674.40
1.80	0.15	0.55	0.57	0.56	2140	4673.80
1.20	0.10	0.55	0.56	0.55	1155	4673.20
0.60	0.05	0.53	0.53	0.53	393	4672.60
0.00	0.00	0.49	0.49	0.49	0	4672.00



Discharge Coefficient Table Tullis et al. (1995)

	Angle wall makes with centerline α							
	6	8	12	15	18	25	35	90
A0	0.49	0.49	0.49	0.49	0.49	0.49	0.49	0.49
A1	-0.24	1.08	1.06	1.00	1.32	1.51	1.69	1.46
A2	-1.20	-5.27	-4.43	-3.57	-4.13	-3.83	-4.05	-2.56
A3	2.17	6.79	5.18	3.82	4.24	3.40	3.62	1.44
A4	-1.03	-2.83	-1.97	-1.38	-1.50	-1.05	-1.10	

LABYRINTH WEIR DESIGN

PROJECT: Serne
 PROJECT NO. 1
 FLOOD CRITERIA: PMF

TIME: 16:54:16
 DATE: 02-Sep-02
 BY: HTF

USER INPUT					
Max. Res	Zr	79.6 m	Thickness		
Crest el.	Zc	78.5 m	Wall	Tw	0.5 m
Floor el.	Zf	76.0 m	Slab	Ts	1 m
Spillway width	Ws	15.0 m	Cutoff Depth		
Apex Width	Za	3 m	Sheet Pile	Ds	0 m
No. of cycles	n	1	Conc Wall	Dc	2 m
Magnification	L/W	4			

CHECK ON RATIOS
 $L_d/B = 0.15$ L_d/B RATIO IS OK
 $H_o/P = 0.44$ H_o/P RATIO IS OK
L/W RATIO IS OK
 Note: L_d/B must be ≤ 0.30
 H_o/P must be ≤ 0.9
 α must be ≥ 6 deg

LABYRINTH DIMENSIONS (Per Cycle)

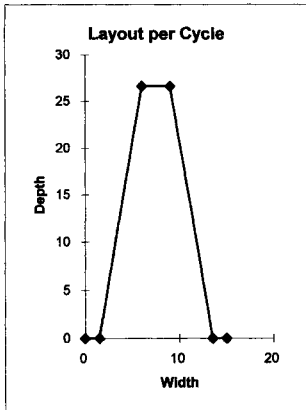
Wall Height	P	2.5 m
Width	W	15.00 m
Length	L	60.00 m
Wall Length	B	27.00 m
Depth	D	26.62 m
Head max	H	1.10 m
Wall Angle	α	9.59 deg
Length of	L_d	4.09 m
Interference		

CREST LAYOUT (One Cycle)

X	Y	
0	0	Weir wall, m ³
1.50	0	Abutment walls, m ³
6.00	26.62	Slab, m ³
9.00	26.62	Concrete cutoff, m ³
13.50	0	Sheet pile, m ²
15.00	0	Reinforcement, kg

COST CALCULATION

Unit price Euros/unit	Units	Cost Euros
150	75	11,250
140	128	17,853
125	432	54,042
300	508	152,400
200	0	0
3.4	94,807	322,344



ESTIMATED COST
 557,889 Euros

DISCHARGE

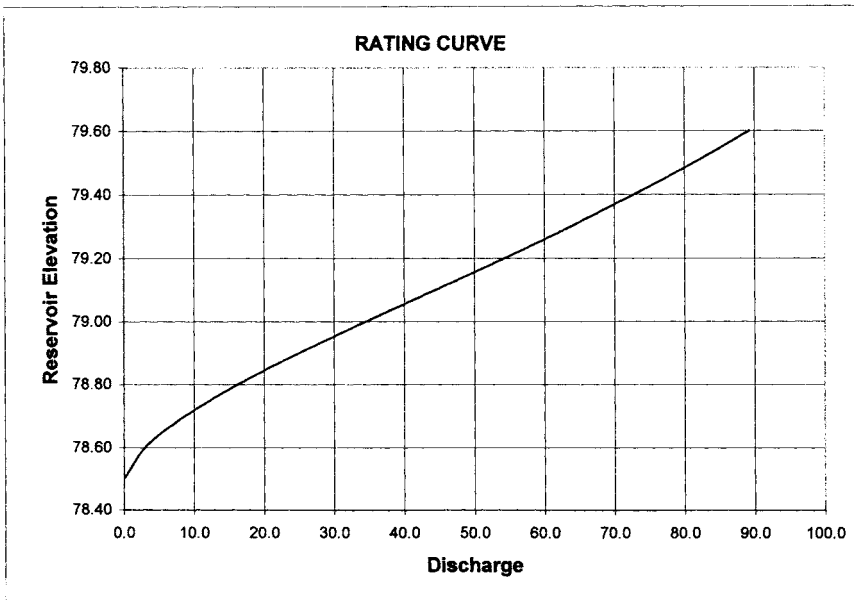
Qmax 89.3 m³/s

COEFFICIENTS

Column	2.00
Cd lower	0.42
Cd Upper	0.47
Cd	0.44
Efficacy	2.59

RATING CURVE

HEAD	H/P	Clower	Cupper	Cd	Q	RES
1.10	0.44	0.42	0.47	0.44	89.3	79.60
0.99	0.40	0.44	0.49	0.46	80.5	79.49
0.88	0.35	0.47	0.51	0.49	71.1	79.38
0.77	0.31	0.50	0.53	0.51	61.0	79.27
0.66	0.26	0.52	0.55	0.53	50.4	79.16
0.55	0.22	0.54	0.56	0.55	39.5	79.05
0.44	0.18	0.55	0.57	0.56	28.8	78.94
0.33	0.13	0.56	0.56	0.56	18.8	78.83
0.22	0.09	0.55	0.55	0.55	10.1	78.72
0.11	0.04	0.53	0.53	0.53	3.4	78.61
0.00	0.00	0.49	0.49	0.49	0.0	78.50



Discharge Coefficient Table Tullis et al. (1995)

	Angle wall makes with centerline α							
	6	8	12	15	18	25	35	90
A0	0.49	0.49	0.49	0.49	0.49	0.49	0.49	0.49
A1	-0.24	1.08	1.06	1.00	1.32	1.51	1.69	1.46
A2	-1.20	-5.27	-4.43	-3.57	-4.13	-3.83	-4.05	-2.56
A3	2.17	6.79	5.18	3.82	4.24	3.40	3.62	1.44
A4	-1.03	-2.83	-1.97	-1.38	-1.50	-1.05	-1.10	

This page intentionally left blank

Chapter 9

Sedimentation and Ice

Sedimentation Fundamentals

The sedimentation characteristics of labyrinth weirs are important for canals that carry large suspended loads or for spillways that have erodible upstream slopes. The concern about upstream deposition is warranted, because Taylor (1968) found that an upstream apron has a significant effect on the discharge characteristics of labyrinth weirs. He tested apron ratios, which are defined as Y_a/P , in Figure 1, of 0.50 and 0.75 for a variety of magnification ratios. The downstream apron ratio is defined similarly.

Taylor found that the effect increases as the magnification increases. The decrease in the discharge coefficient for a magnification ratio of 8 is shown in Figure 2.

Although some labyrinth weirs have been designed with aprons, Taylor's results can also be used to estimate the effect of sediment deposition in the space between the upstream labyrinth walls. Three studies are described below. Boardman is an example of sedimentation that can be expected because of bank erosion upstream of a spillway. The other two examples are studies of labyrinth weirs located in canals. Hellsgate has the possibility of retaining boulders from an alluvial stream. The Garland Canal transports a high bed and suspended sediment load.

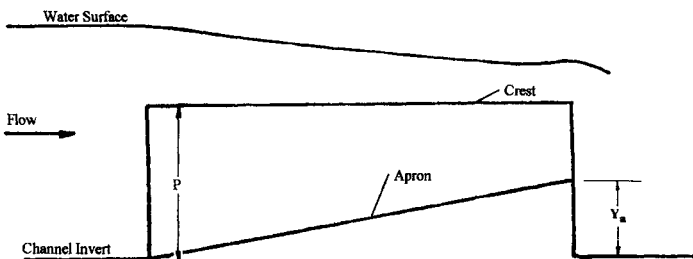


Figure 1. Apron Definition Sketch

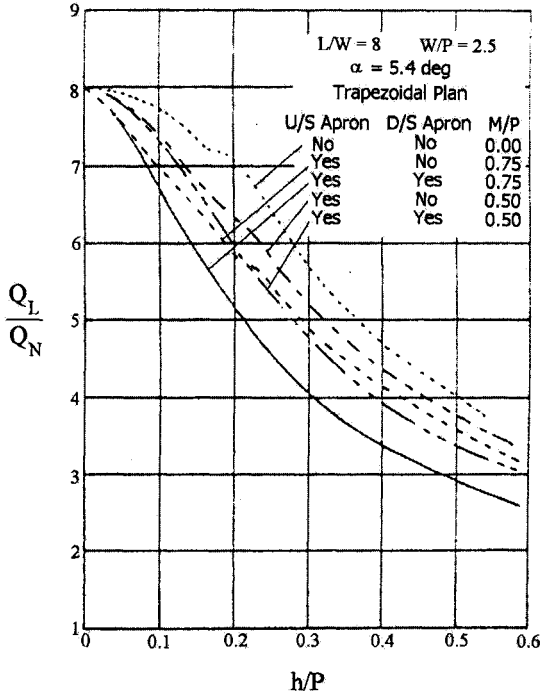


Figure 2. Effect of Upstream and Downstream Aprons on Discharge, from Taylor, G., (1968). "The performance of labyrinth weirs." PhD thesis, University of Nottingham, Nottingham, England.

Boardman

Babb (1976) investigated the effects of sedimentation on the Boardman labyrinth because a large erodible bank existed upstream of the structure. Two tests were conducted, as shown in Figure 3. The first consisted of dumping fine sand with a mean diameter of 0.14 mm into a reservoir upstream of the labyrinth. The second used coarse sand with a mean diameter of 1.77 mm. With the fine sand, approximately 2/3 of the material passed over the weir. The remaining sand was deposited in the low-velocity zones upstream of the labyrinth, and a small amount remained in the space between the sidewalls. Most of the coarse sand was deposited upstream of the labyrinth, with a small amount collecting within the weir.

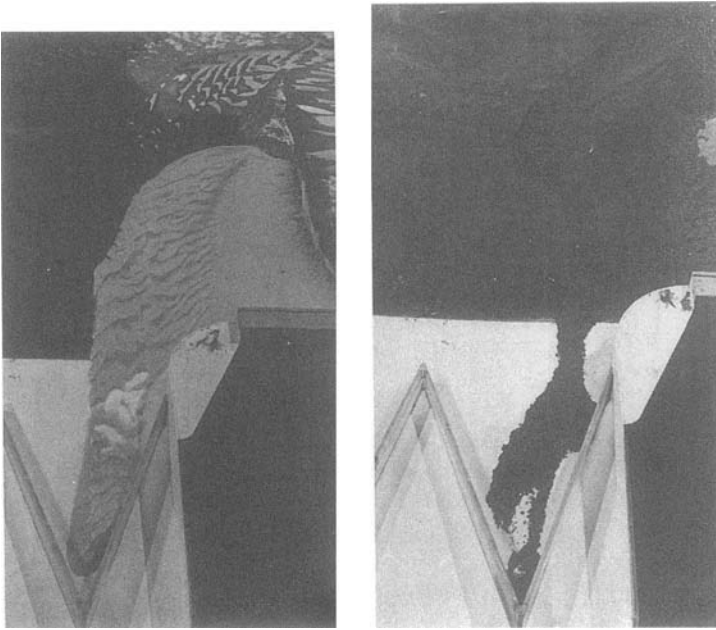


Figure 3. Sedimentation Tests at Boardman Labyrinth, from Babb, A.F., (1976). "Hydraulic model study of the Boardman Reservoir spillway." R.L. Albrook Hydraulic Laboratory, Washington State University, Pullman, Wash., May., permission from Albrook Hydraulic Laboratory.

In projects located within an alluvial stream or in those that transport high degrees of sediment, the sediment may deposit upstream of the labyrinth during low flows. Therefore, model studies have been conducted to determine if the sediment will be transported downstream at high flows. Two studies of this kind were conducted at Colorado State University under the direction of Tudor Engineering. The first of these studies was for the Hellsgate Project, located in Colorado. Although a labyrinth was studied for this project, another solution was adopted. The second study was for the Garland Canal Power Project, located in the Shoshone Irrigation District near Powell, Wyoming. This canal carries substantial quantities of sediment.

Hellsgate

The Hellsgate model study is interesting because the weir was filled completely with gravel that corresponded to 100-mm diameter cobbles in the prototype. Then the amount of scour from the crest level surface was observed. After only 6.3 minutes (prototype time), the scour developed, as shown in Figure 4. The head corresponded to an h/P of approximately 0.1. The sidewall height of the weir is 2.12 m. The scour is below the sidewalls in Figure 4 because a floor slab was not used in the model studies.

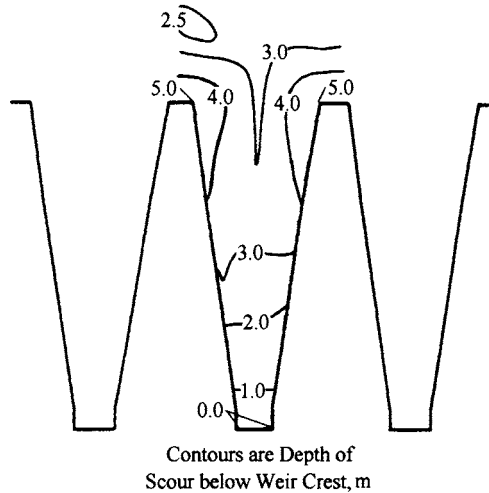


Figure 4. Scour Upstream of Labyrinth - Hellsgate.

For a head corresponding to an h/P of approximately 0.4, the scouring action was extremely violent. These tests showed that the weir is capable of removing sediment from the bays and the approach channel.

Garland Power Canal

The main purpose of the weir is to provide a constant head for a turbine bypass that is located in the upstream channel, as shown in Figure 5.

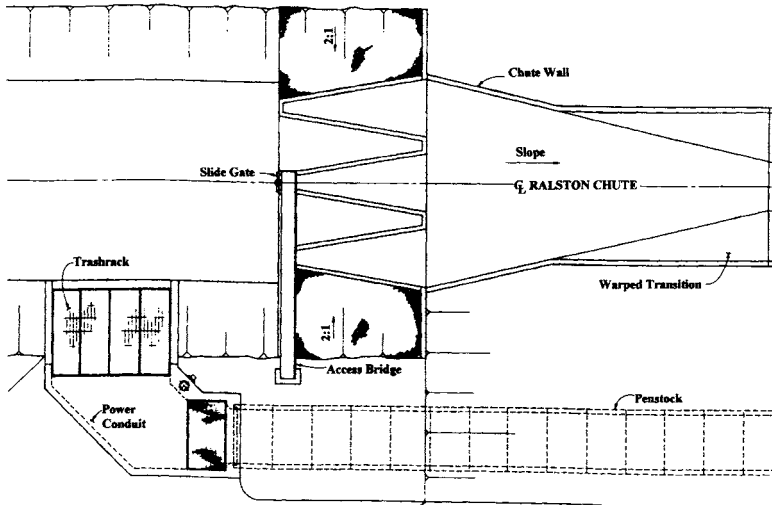


Figure 5. Plan of Labyrinth weir - Shoshone Irrigation District

On the Shoshone Irrigation, the flows are so low and the sediment load is so high that the labyrinth fills with sediment. The sediment forms a wedge that begins at the invert on the upstream end of the weir and extends almost to the lip at the downstream end of the weir. For this case, the apron ratio is approximately 0.95. This project is operated such that the design discharge rarely passes over the weir. As a result, the sediment in the weir is of little concern. Figure 6 shows the flow with the sediment almost at the lip of the weir.

Originally, a vertical slide gate was provided on the upstream apex of the center weir to sluice the sediment downstream. This has not proven to be necessary, because the weir is self-cleaning when it passes large flows.

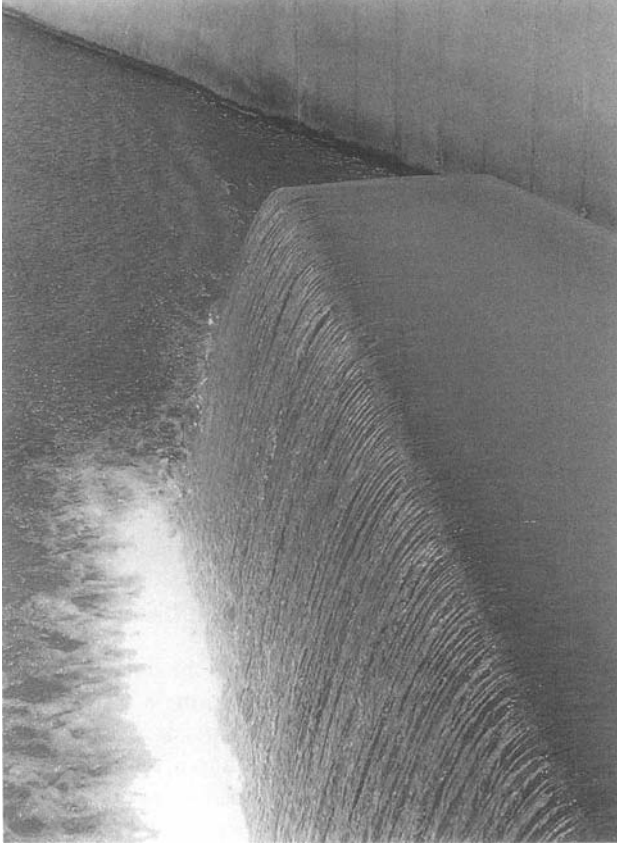


Figure 6. Sediment at Downstream Lip of Weir, Shoshone Irrigation

Conclusions

Sediment studies on Boardman, Hellsgate, and the Garland Power Canal have all shown that the labyrinth weir is self-cleaning. That is, any sediment that deposits in the bays during low flows will be scoured out by the violent turbulent action at the downstream apex during high flows.

Ice

Ice presents a special set of problems in cold climates. One problem is the pressure on the walls of the labyrinth. URS uses a loading on the walls of $49,000 \text{ kg/m}^2$ ($10,000 \text{ lb/ft}^2$). One method of relieving the pressure on the walls is to provide a mechanism to break the ice sheet upstream of the labyrinth. This was done at the Tongue River Dam in the United States, as shown in Figure 7. A sloping wall was constructed upstream of the labyrinth. As the reservoir elevation varies, the walls will cause the ice sheet to break. The breakup of the ice sheet will relieve the

pressures on the walls and facilitate the motion of the ice over the labyrinth if it spills. So far, the reservoir has never risen to the level of the upstream apron during a winter season. Flows over the structure with low heads have not produced any noticeable problems with nappe vibration.



Figure 7. Ice Breaking Piers - Tongue River Dam, USA

This page intentionally left blank

Chapter 10

Aeration

Introduction

As water quality issues become more important, the behavior of labyrinth weirs in aerating or de-aerating the flow needs to be considered. Turbulent flow that occurs with falling water has the capability of driving the upstream flow toward saturation conditions. That is, if the upstream flow is supersaturated, the falling water will detrain air from the water. Similarly, if the upstream flow is not saturated or has a so-called "oxygen demand," then the falling water will entrain air. Because the length of a labyrinth weir is greater than the length of a straight weir, a labyrinth weir would be expected to be an efficient device in improving water quality. Wilhelms et al. (1993) presented a review of the equations that are available for a straight weir. Hauser (1996) described methods to design both linear and labyrinth aerating weirs.

Wormleaton and Soufiani (1998) and Wormleaton and Tsang (2000) conducted aeration studies on labyrinth weirs. Their tests were made with one straight, five rectangular, and one triangular weir, as shown in Figure 1.

The width of the channel in the tests was 240 mm, and the weir heights varied between 500 and 1,500 mm.

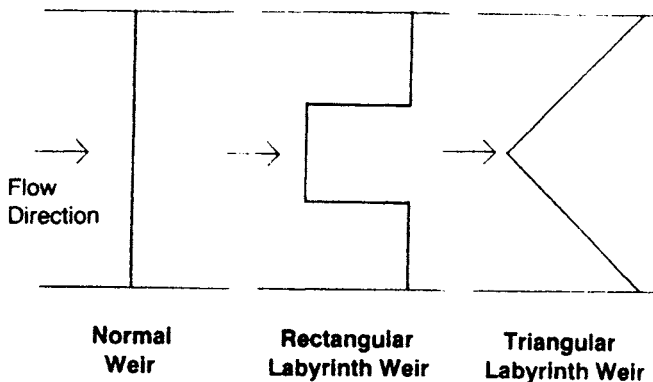


Figure 1. Weirs tested by Wormleaton et al.

Theory

The aeration process at a weir is often described by a deficit ratio, r , defined as

$$r = \frac{C_s - C_u}{C_s - C_{ds}} = e^{\left(\frac{k_t A_c t_c}{V_a}\right)} \quad (1)$$

in which C_s = the saturated concentration; C_u = the upstream concentration; C_{ds} = the downstream concentration; k_t = the bulk liquid film coefficient for the air-water interface; A_c = the contact area; t_c = the time the air bubbles remain in the water (contact time); and V_a = the volume of air entrained. The concentrations are measured either in terms of oxygen or in terms of air. A common assumption is that the oxygen-to-air concentration in the atmosphere remains constant when the air is dissolved in the water. However, this assumption is not always true. The value of r ranges between 1, for no aeration, and ∞ , for completely saturated downstream conditions.

The quantities of A_c , t_c , and V_a are difficult to impossible to measure. In addition, they are affected by the fall height, the nature of the falling jet, and the depth of the downstream pool. Alternatively, the deficit ratio can be determined from measurements upstream and downstream from the structure. Expressing the deficit ratio in terms of efficiency simplifies the measurements in which efficiency, E , is defined as

$$E = 1 - \frac{1}{r} = \frac{C_{ds} - C_u}{C_s - C_u} \quad (2)$$

The efficiency ranges between 0%, for no aeration, and 100%, for total downstream saturation.

Falling Jet Types

Ervine and Falvey (1987) showed that the structure of a circular jet falling through the atmosphere is influenced by the length of the fall and the turbulence at the source of the jet. Tsang (1987) adapted this description to describe rectangular jets flowing

over labyrinth weirs. The four types of impact types defined by Tsang are shown in Figure 2.

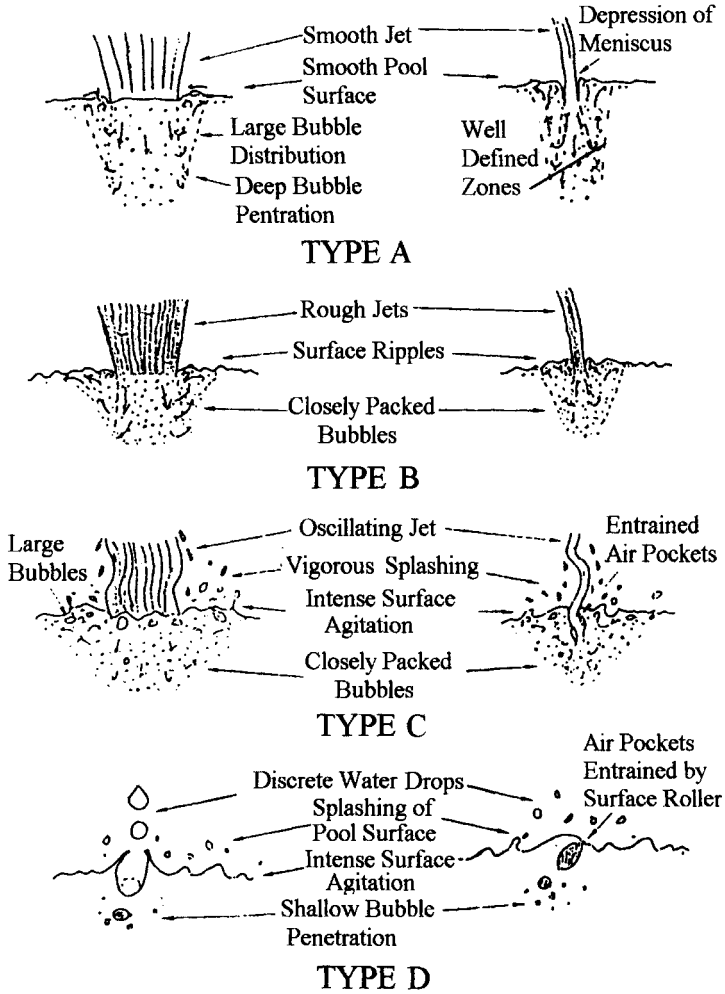


Figure 2. Jet Impact in the Downstream Pool from Wormleaton, P.R., and Tsang, C.C., (2000). "Aeration performance of rectangular planform labyrinth weirs." *American Society of Civil Engineering, Journal of Environmental Engineering*, 127(5), 456-465., permission from ASCE

Wormleaton and Tsang (2000) found that for drop heights of less than 900 mm, the jet was smooth (Type A) and, although the penetration of the bubbles was deep, the

efficiency was small. As the drop height increased, the efficiency also increased. However, when the fall height exceeded some critical value, the jet broke up into discrete water droplets, as shown is Type D in figure 2.

Performance

Because the concentration is a function of temperature, the efficiencies need to be referenced to a standard temperature. This is done using the equation of Tebbott et al. (1977)

$$\frac{r_T - 1}{r_{20} - 1} = \frac{E_T(1 - E_{20})}{E_{20}(1 - E_T)} = [1 + \alpha_d(T - 20)] \quad (3)$$

in which the subscript T = the measured temperature; and the subscript 20 = 20 ° C. The best fit for the constant is α_d is 0.0355 °C⁻¹.

Figure 3 from Wormleaton and Tsang (2000) shows that a rectangular labyrinth weir is more efficient than a triangular shape and that the triangular shape is better than a linear weir.

The performance of the rectangular weir is better than that of triangular plan forms at higher discharges because interference increases with the triangular plan form. This observation is important because it shows the effect of interference on the aeration efficiency of triangular weirs.

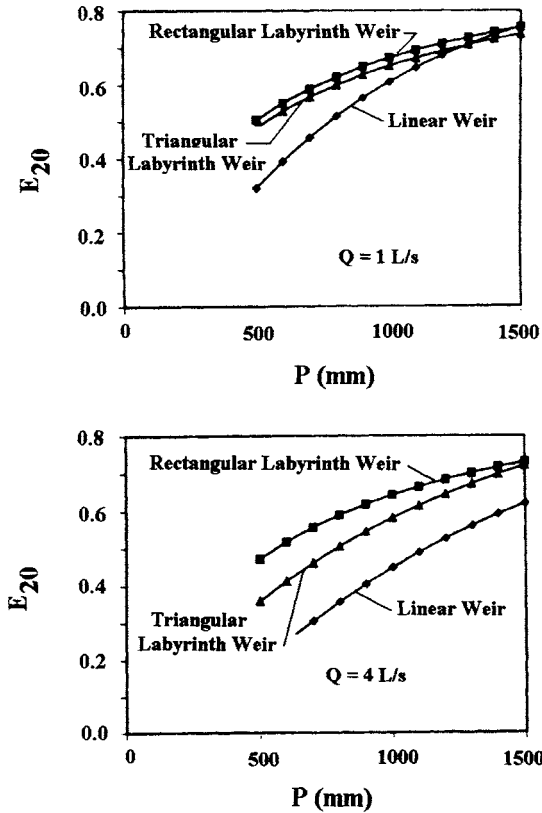


Figure 3. Comparison of Aeration Efficiencies as a Function of Discharge from Wormleaton, P.R., and Tsang, C.C., (2000). "Aeration performance of rectangular planform labyrinth weirs." *American Society of Civil Engineering, Journal of Environmental Engineering*, 127(5), 456-465.

Conclusions

- These studies show that a rectangular weir is more efficient than a triangular weir and that a triangular weir is more efficient than a straight weir in improving the downstream air or oxygen concentration.
- For fall heights greater than 1,500 mm and small discharges, all weirs tend to have an efficiency of about 70%.
- For higher discharges, the labyrinth weirs tend to approach an efficiency of 70% for fall heights greater than 1,500 mm. This value is dependent on the

downstream pool depth and may not be as high as 70% with large bubble-penetration depths.

- Interference becomes significant with triangular weirs as the flow rate increases.

Chapter 11

Special Cases

Introduction

As shown in Chapter 8, Design - Aspect Ratio, a triangular shape is the most efficient plan form of a labyrinth weir. However, the rectangular plan form can also be found in engineering applications. Two of the more significant cases using an almost rectangular plan form are Fusegates™ and sheet piling. Both of these have a smaller discharge coefficient than does the triangular form, but they serve a very practical purpose.

Some labyrinth spillways are designed to not only increase the flow rate for a given reservoir level but to also be used as detention structures. For example, flash floods are characterized by large peak inflows with a small volume. Detention structures are designed with sufficient capacity to detain the flood while simultaneously letting the water drain out of the structure slowly over an extended period of time.

Fusegates™

Fusegates™ were developed in France by Hydroplus® as a method of increasing both spillway and reservoir capacity. A Fusegate™ consists of a bucket that sits on a flat spillway, as shown in Figure 1. When several gates are placed next to each other on a spillway crest, their plan form has the shape of a trapezoidal labyrinth weir. An open chamber exists underneath the bucket. A well provides water into this open chamber. If the water surface gets high enough, water flows into the well and pressurizes the open chamber. This pressurization is sufficient to cause the Fusegate™ to rotate about lugs on the downstream side of the gate. The height of the wells is set so that one gate after another will tip as the water level in the reservoir rises. No two adjacent gates tip. This allows each gate to tip away from the rubber seals that are mounted on selected gates.

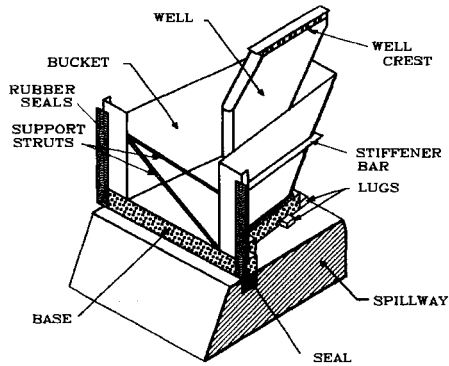


Figure 1. Individual Fusegate™ from Falvey, H.T., and Treille, P., (1995). "Hydraulics and design of fusegates." *Journal of Hydraulic Engineering*, 121(7), 512-518., permission from ASCE

Hydroplus® has developed three standard Fusegate™ designs. These are the Wide Low Head, the Narrow Low Head, and the Wide High Head, as shown in Figures 2 to 4.

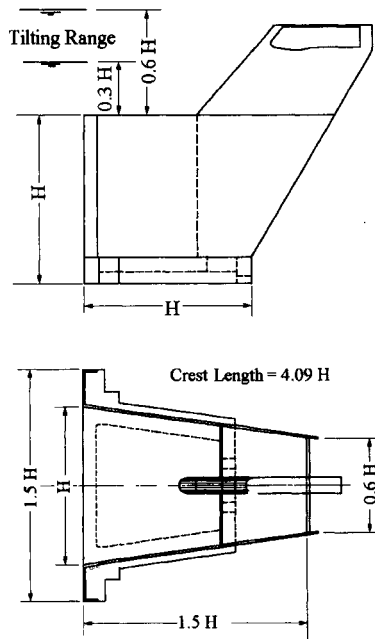


Figure 2. Wide Low Head Fusegate (WLH) from Falvey, H.T., and Treille, P., (1995). "Hydraulics and design of fusegates." *Journal of Hydraulic Engineering*, 121(7), 512-518., permission from ASCE

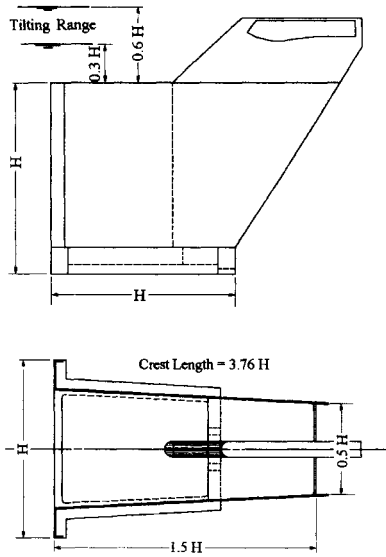


Figure 3. Narrow Low Head Fusegate (NLH) from Falvey, H.T., and Treille, P., (1995). "Hydraulics and design of fusegates." *Journal of Hydraulic Engineering*, 121(7), 512-518., permission from ASCE

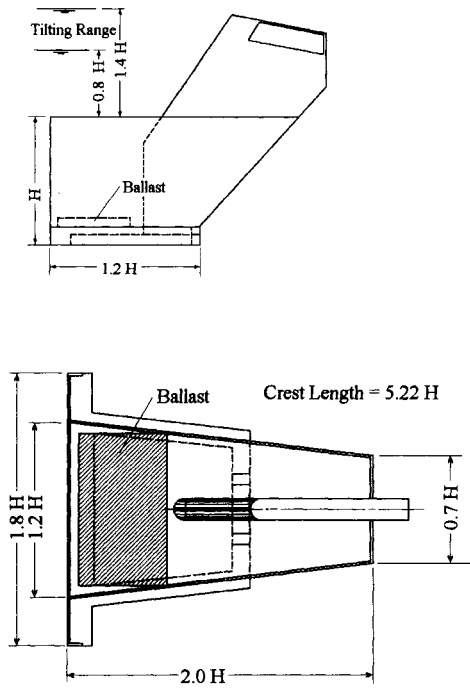


Figure 4. Wide High Head Fusegate (WHH) from Falvey, H.T., and Treille, P., (1995). "Hydraulics and design of fusegates." *Journal of Hydraulic Engineering*, 121(7), 512-518., permission from ASCE

Falvey and Treille (1995) analyzed the discharge over a labyrinth weir made up of Fusegates™. They used the conventional expression for flow over a straight weir as given by

$$Q_L = \frac{2}{3} \sqrt{2 \cdot g} \cdot C_g \cdot L \cdot h^{3/2} \tag{1}$$

in which C_g = the discharge coefficient for the Fusegates; L = the developed length of the weir crest; and h = the upstream head. For a sharp crested weir, the value of the discharge coefficient is given by Rehbock (1929) as

$$C_r = 0.605 + 0.08 \frac{h}{P} + \frac{1}{305 \cdot h(ft)} \tag{2}$$

The discharge coefficients for the three Fusegates™ are shown in Figure 5, along with the curves of Rehbock (1913). The curves clearly show that the discharge coefficient decreases as the labyrinth weir becomes more rectangular.

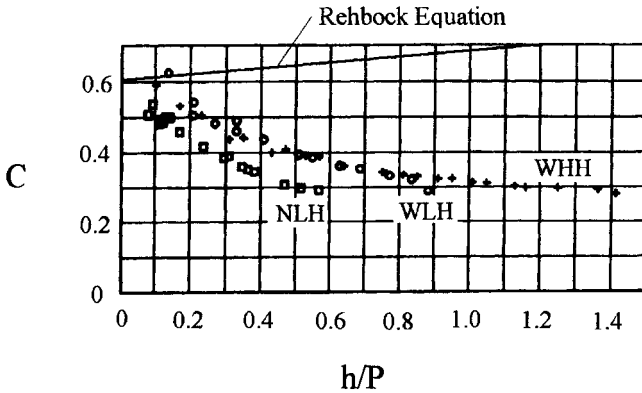


Figure 5. Discharge Coefficients for the Fusegates™ from Falvey, H.T., and Treille, P., (1995). "Hydraulics and design of fusegates." *Journal of Hydraulic Engineering*, 121(7), 512-518. with permission of ASCE.

The discharge coefficient in Equations 1 and 2 (neglecting the last term) can be expressed in the English system as

$$\frac{2}{3}\sqrt{2 \cdot g} \cdot 0.605 = 3.24 \tag{3}$$

and

$$\frac{2}{3}\sqrt{2 \cdot g} \cdot 0.08 = 0.43 \tag{4}$$

in which $g = 32.2 \text{ ft/sec}^2$.

These values are essentially identical to the Kindsvater and Carter (1959) values given in equation 6, Chapter Design Curves.

Detention Dams

An example of a detention structure is the Flamingo Detention Dam. It provides flood protection for Las Vegas, Nevada. Floods in the western United States are characterized by high peak flows of short duration. Therefore, the detention structures are designed to retain the entire flood. At the same time, they are provided with an orifice that slowly releases the water into the downstream channel. The plan of the Flamingo Detention Dam is shown in Figure 6.

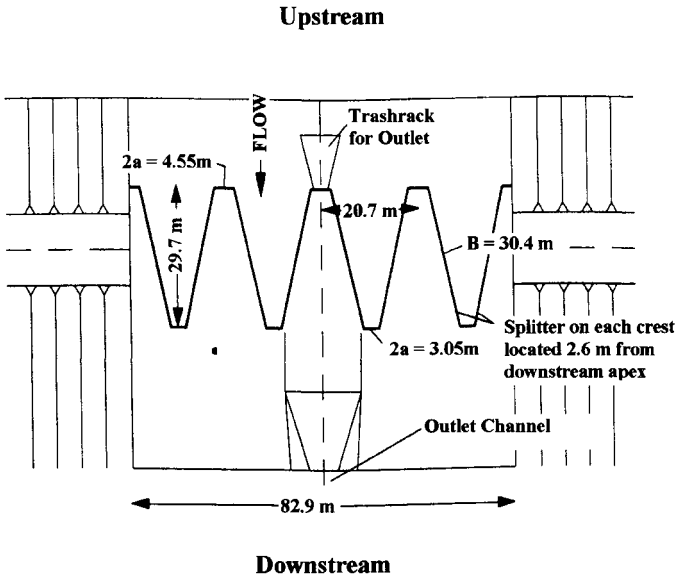


Figure 6. Plan of Flamingo Detention Structure

The dam partially retains flows with a discharge of less than the 100-year flood and releases the water slowly through a 2.44-m wide by 2.13-m high rectangular orifice located in the center of the spillway, as shown in Figure 7. The orifice is not gated.

A baffled apron drop provides energy dissipation downstream of the orifice, as shown in Figure 8. Flow splitters can be seen on the downstream end of each sidewall.

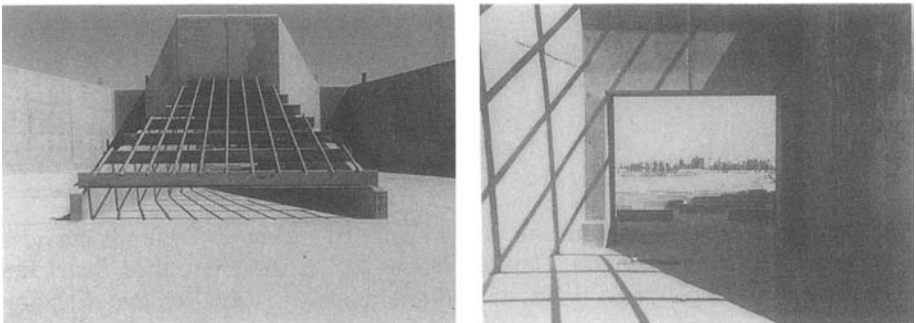


Figure 7. Trashrack and Rectangular Orifice

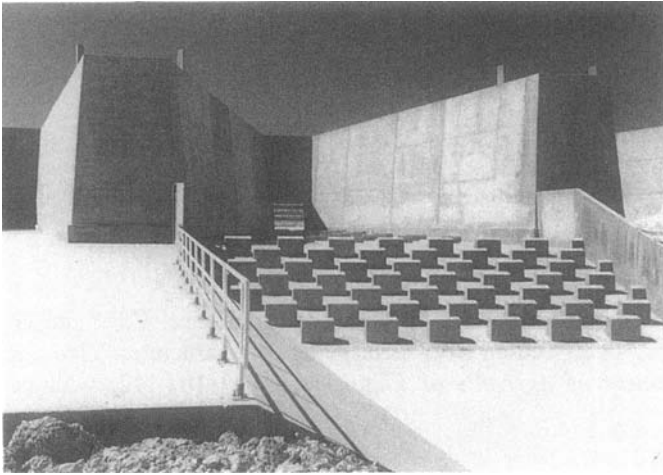


Figure 8. Baffled Apron Drop

For larger floods, the water passes both through the orifice and over the labyrinth spillway.

Sheet Piling

Rice and Gwinn (1981) studied the use of Z-section steel sheet piling for drop structures. The sheet piling has the shape of a labyrinth weir when it is put together, as shown in Figure 9.

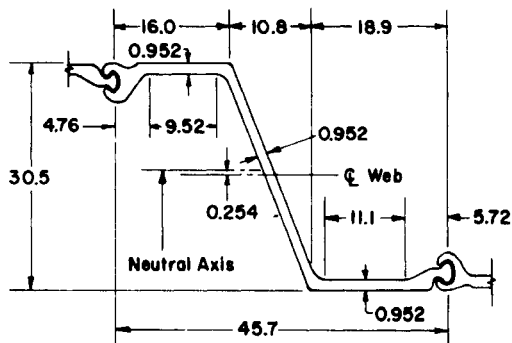


Figure 9. Z-Section Steel Sheet Piling, Dimensions in mm. from Rice, C.E., and Gwinn, W.R., (1981). "Rating of Z-section, steel-sheet piling drop structures." *Transactions of the American Society of Agricultural Engineers*, 24(1) 107-112. with permission of ASAE.

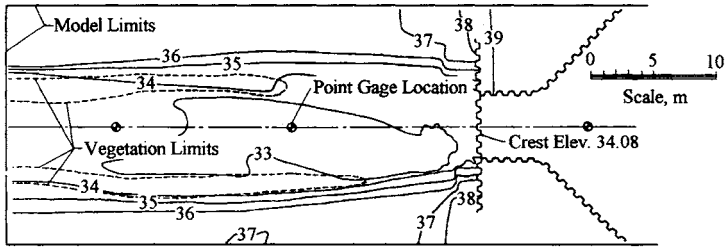


Figure 10. Prototype Layout and Topography from Rice, C.E., and Gwinn, W.R., (1981). "Rating of Z-section, steel-sheet piling drop structures." *Transactions of the American Society of Agricultural Engineers*, 24(1) 107-112. with permission of ASAE.

This application is for a drop structure, therefore, the upstream side of the weir is filled almost to the crest of the structure. The model that was tested is shown in Figure 10.

Because the weir is essentially at the same elevation as the upstream invert, the discharge coefficient is given in terms of flow depth. The discharge coefficient is defined as

$$C_d = \frac{Q}{\frac{2}{3} \sqrt{2g} \cdot L \cdot h_u^{1.5}} \quad (5)$$

in which L = the developed length of the weir. The discharge coefficient is shown in Figure 11.

The submergence characteristics of the sheet piling obey the Villemonte (1947) equation, as shown in Figure 12.

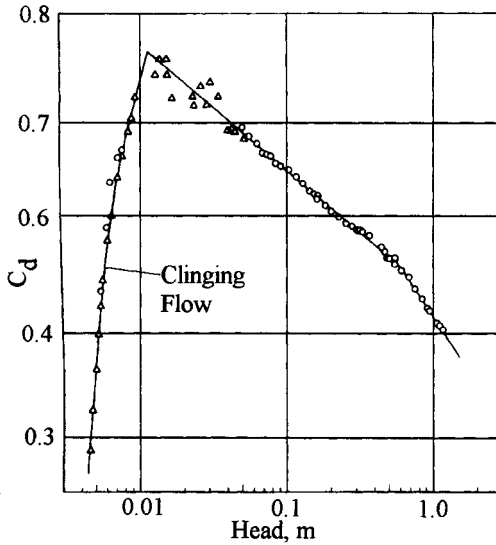


Figure 11. Discharge coefficient for Z-Shape Sheet Piling from Rice, C.E., and Gwinn, W.R., (1981). "Rating of Z-section, steel-sheet piling drop structures." *Transactions of the American Society of Agricultural Engineers*, 24(1) 107-112. with permission of ASAE.

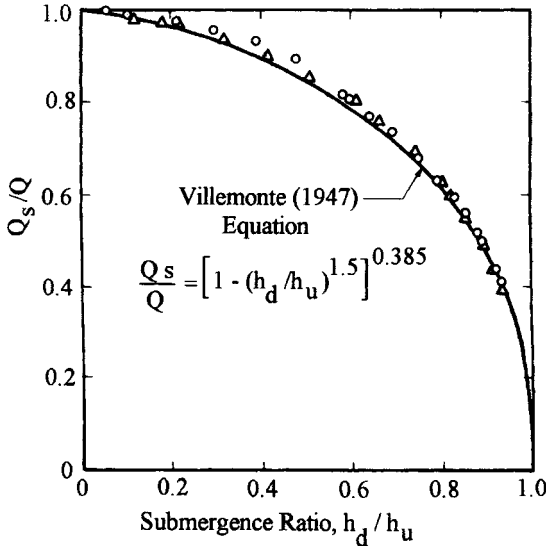


Figure 12. Submergence Characteristics for Sheet Piling from Rice, C.E., and Gwinn, W.R., (1981). "Rating of Z-section, steel-sheet piling drop structures." *Transactions of the American Society of Agricultural Engineers*, 24(1) 107-112. with permission from ASAE.

This page intentionally left blank

Chapter 12

Modeling Procedures

Introduction

Model studies are essential in the design of a project when the prototype conditions differ from conditions for which the design curves were developed. A careful analysis of scale effects is imperative if the model results are to be reliable. The design of a model-testing program should consider the pertinent variables so the results can be presented in a rational manner.

Chapter 2, Analytic Development, showed that the water surface profile on a labyrinth weir is a function of the following,

- Froude number, F ;
- Interference ratio, L_{de}/B ;
- Head to crest height ratio, H_o/P ; and
- Angle between the labyrinth wall and the centerline of the approach channel, α .

Because the discharge is related to the water surface profile, it should also be a function of these same parameters.

Two types of errors exist when conducting model studies: systematic and random errors. Systematic errors are always positive or negative, and they are the result of scale effects or the method of operation. Random errors are expressed as plus or minus root-mean-square values.

Systematic Errors

Scale Effects Caused by Surface Tension

The principal scale effect is caused by surface tension. This effect is described by a dimensionless parameter called the Weber number. It is the ratio of the inertial to the surface tension forces and is defined as

$$W = \frac{V}{\sqrt{\frac{\sigma}{\rho \cdot h}}} = \frac{\frac{2}{3} \sqrt{2 \cdot g \cdot h} \cdot C_d}{\sqrt{\frac{\sigma}{\rho}}} \quad (1)$$

in which V = the velocity; σ = the interfacial surface tension (0.0727N/m or 0.00498 lb/ft at 20 °C);

ρ = the density of water (1,000 kg/m³ or 1.94 slugs/ft³);

g = the acceleration of gravity (9.81 m/sec² or 32.2 ft/sec²);

h = the head on the weir; and

C_d = the discharge coefficient.

The effect of surface tension on the discharge coefficient can be determined from discharge coefficient over a sharp edged weir, as determined from the Rehbock (1929) equation, given in the metric system by

$$C_d = 0.605 + 0.08 \cdot \frac{h}{P} + \frac{1}{h} \quad (2)$$

The last term of this equation is a correction for the surface tension effect where h is measured in millimeters.

Table 1 shows the value of the Weber number for various heads over a weir in which the discharge coefficient is determined from Equation 2.

Table 1. Weber Number for a Sharp Crested Weir

P			h/P			
mm	inches	ft	0.1	0.3	0.5	0.7
2000	78.74	6.56	42.8	131.0	223.7	320.8
1000	39.37	3.28	21.6	65.7	112.0	160.6
600	23.62	1.97	13.1	39.6	67.4	96.5
300	11.81	0.98	6.7	19.9	33.8	48.4
200	7.87	0.66	4.6	13.4	22.7	32.4
100	3.94	0.33	2.5	6.9	11.5	16.4

For small heads and low weirs, the surface tension forces are large relative to the inertial forces. In the shaded range, surface tension effects are large, and the nappe will cling to the downstream face of the weir. This creates low pressures that artificially increase the discharge over the weir. The clinging nappe with small models is a scale effect that would not be observed in the prototype. For example,

Houston (1982) observed negative pressures on the downstream side of a weir for head ratios between 0 and 0.33 for a model weir height of 114 mm. In the prototype, the nappe would probably spring free for this range of heads.

The surface tension causes the discharge to be greater in the model than in the prototype by the amounts given in Table 2.

Table 2. Percent that the Model Over Predicts the Prototype Discharge

P			h/P			
mm	inches	ft	0.2	0.3	0.5	0.7
2000	78.74	6.56	0.4	0.3	0.2	0.1
1000	39.37	3.28	0.8	0.5	0.3	0.2
600	23.62	1.97	1.3	0.9	0.5	0.4
300	11.81	0.98	2.7	1.8	1.0	0.7
200	7.87	0.66	4.0	2.6	1.6	1.1
100	3.94	0.33	8.1	5.3	3.1	2.2

The values inside the shaded area represent an error of discharge that exceeds 5% over what would be observed in the prototype. Many model studies are conducted with weir heights of 150 mm and values for the h/P of approximately 0.2. Table 2 shows that these models overestimate the true discharge observed in the prototype.

Method of Operation

A physical model is normally operated by 1) setting an inflow to the model, 2) letting the flow stabilize, and 3) recording the discharge and reservoir elevation in the model. Theoretically, the flow will never stabilize because the reservoir level will continue to rise, although at an ever-slower rate. The equation for the rise in the reservoir level can be obtained by equating the change in the storage to the difference between the inflow and outflow rates from the reservoir. In dimensionless terms, the differential equation for the water level in the reservoir is given by

$$d\left(\frac{t \cdot Q_o}{A_r \cdot h_o}\right) = \frac{1}{1 - \left(\frac{h}{h_o}\right)^{3/2}} \cdot d\left(\frac{h}{h_o}\right) \quad (3)$$

in which Q_o = the inflow discharge; A_r = the reservoir area; h = the head at any time; h_o = the head over the weir at steady state; and t = time.

The solution to this differential equation is shown in Figure 1. A few representative values near final stabilization are shown in Table 3.

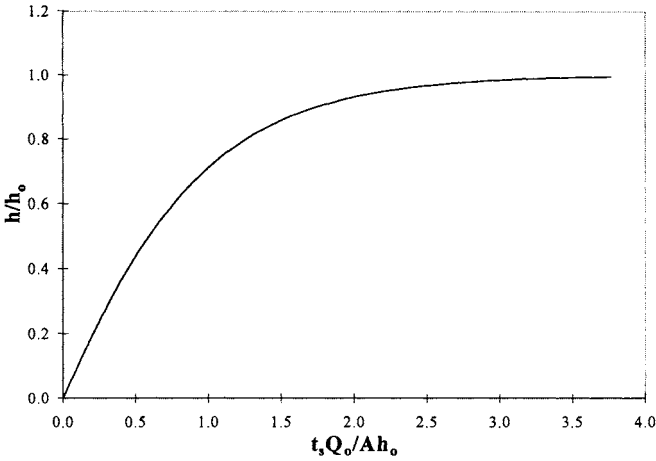


Figure 1. Time to Stabilize

Table 3. Values near Final Stabilization

H/h ₀	t _s Q ₀ /Ah ₀
.97	2.56
.98	2.93
.99	3.29
.999	5.41

For example, with a model reservoir area of 100 m² (1,080 ft²), a discharge of 60 L/sec (2.1 ft³/sec), and a head of 50 mm (0.16 ft), the model will take almost 5 minutes to reach 99% of the final depth.

$$t_s = 3.29 \cdot \frac{100 \cdot m^2 \cdot 0.05 \cdot m}{.06 \cdot m^3 \cdot sec^{-1}} = 4.6 \cdot min \tag{4}$$

Longer times are needed to stabilize as the discharge decreases or as the head and area increase.

Operating a model by increasing the head will result in predictions of discharge that are higher than will be observed in the prototype. Similarly, operating the model by decreasing the head will result in predictions that are lower than observed in the prototype. A good modeling technique is to make observations with both a rising and a falling water surface. The average of these will reduce or eliminate the systematic error resulting from operation.

Random Errors

The discharge equation for flow over any weir can be written as

$$Q = \frac{2}{3} \sqrt{2 \cdot g} \cdot C_d \cdot L \cdot h^{3/2} \quad (5)$$

in which C_d = the discharge coefficient; L = the weir length; and h = the head on the weir (upstream reservoir elevation minus weir crest elevation).

The discharge coefficient is primarily a function of the weir shape and the relative height of the head over the weir, h/P , where P is the height of the weir wall.

Taking the logarithm of both sides and differentiating the result gives

$$\frac{dC_d}{C_d} = \frac{dQ}{Q} + \frac{dL}{L} + \frac{3}{2} \cdot \frac{dh}{h} \quad (6)$$

Because the errors are expressed as plus or minus root-mean-square values, the error in the discharge coefficient is equal to the sum of the errors in discharge, length, and head. Of these, the contribution to the errors in head is 1.5 times greater than the errors of the other quantities.

The discharge is usually accurate to within 2%. The length of the weir can be measured to within an accuracy of $\pm 0.2\%$. Head is usually measured to within ± 0.3 mm (0.001 ft). Thus, although the discharge and length errors are constants, the error in head varies with the water surface elevation. Table 4 shows the percent error in determining the discharge coefficient for model weirs of various heights.

Table 4. Random Error in Discharge Coefficient

P (model)			h/P			
mm	inches	feet	0.1	0.3	0.5	0.7
2000	78.74	6.56	2.4	2.3	2.2	2.2
1000	39.37	3.28	2.7	2.4	2.3	2.3
600	23.62	1.97	3.0	2.5	2.4	2.3
300	11.81	0.98	3.7	2.7	2.5	2.4
200	7.87	0.66	4.5	3.0	2.7	2.5
100	3.94	0.33	6.7	3.7	3.1	2.8

Table 4 shows that the error in determining the discharge coefficient is large for small values of relative heads on the weir and for small weir heights.

Conclusions

- Because of surface tension effects and random errors, model tests should be conducted with wall heights of 300 mm (11.8 in.) or greater and relative heads (h/P) on the weir of greater than 0.2. The error in the discharge coefficient that is determined from a model test would be large for small wall heights and small relative heads on the weir.
- Design curves based on model studies should be used with caution. For relative heads less than 0.3, the test curves will overpredict the prototype discharge coefficients by more than 5%. The random errors in the discharge coefficient can be expected to be on the order of 8% or greater.
- The weir height in a model should not be less than 100 mm. Even with a height of 100 mm, the data are susceptible to significant errors for heads with an H_0/P of less than 0.3. To obtain accurate values for smaller heads, a minimum weir height of 200 mm is recommended.

Application

A model study is conducted to learn details about a specific flow condition. In many cases, tests at two or more scales are needed to completely investigate specific details. The type of model and the scales used are determined by the physical capabilities of the test facility. For example, if a model is needed to investigate the effect of the approach flow conditions, the maximum discharge characteristics, and the downstream channel for a labyrinth spillway, then a rather large physical model is often required. Because of limitations in laboratory space and in pumping capacity, a small model may be required. This means that the scale ratio will be large. However, if the discharge characteristics at small heads and the effects of nappe oscillation are to be studied, then a large model is required. This requires that only a portion of the entire installation be simulated. Special care must be exercised to ensure that the approach flow conditions are properly reproduced in a sectional representation of the installation.

Examples of small models that investigate the overall flow conditions are the simulations of Broadman, Ute, Ritschard, and Bartlett's Ferry labyrinth spillways. Examples of sectional models are the investigations of Taylor (1968) and Tullis (1993). The sectional models give valuable information about ideal discharge characteristics for different crest shapes and labyrinth weir configurations. The discharge curves are based on sectional models in a rectangular channel. However, they cannot accurately represent the effects of approach flow conditions that exist with labyrinth spillways, such as Kizilcapinar or Ohau.

Design and research engineers are faced with having to interpret the results of a specific model investigation very carefully. For example, conclusions concerning nappe oscillations and aeration cannot be reached using small models. In addition, the discharge characteristics obtained from small models are subject to large systematic

and random errors. If costs dictate that only one simulation of an installation can be studied, then the model should be made as large as possible. Tables 1, 2, and 4 indicate that the absolute weir height should not be less than 100 mm unless only the maximum discharge characteristics are of interest (i.e., head ratios, H_o/P , > 0.4). Because the average weir height for the installations listed in Appendix A is about 4 m, the smallest practical model scale should be on the order of 1:40.

Case Study

Model studies were conducted by the Corps of Engineers on the Prado labyrinth spillway to investigate the effects of the geometry on the overall operation of the proposed labyrinth spillway (Copeland and Fletcher 2000). Of primary concern were the discharge characteristics at the maximum head and the flow in the downstream chute. The investigations included a section of the upstream reservoir, the chute, and the downstream river channel, as shown in Figure 2.

To fit within the space available for the study and to have enough flow capacity to supply the model, a model scale of 1:50 was chosen. This results in a model weir height of 201 mm, which is large enough to avoid scale effects at the maximum water depths. This weir height is too small to investigate the nappe oscillation and surging effect that occur at small H_o/P ratios.

The study revealed the importance of carefully considering both the upstream flow conditions and the effects of interference. Some of the conclusions below are based on information that was not known at the time of the model investigations.

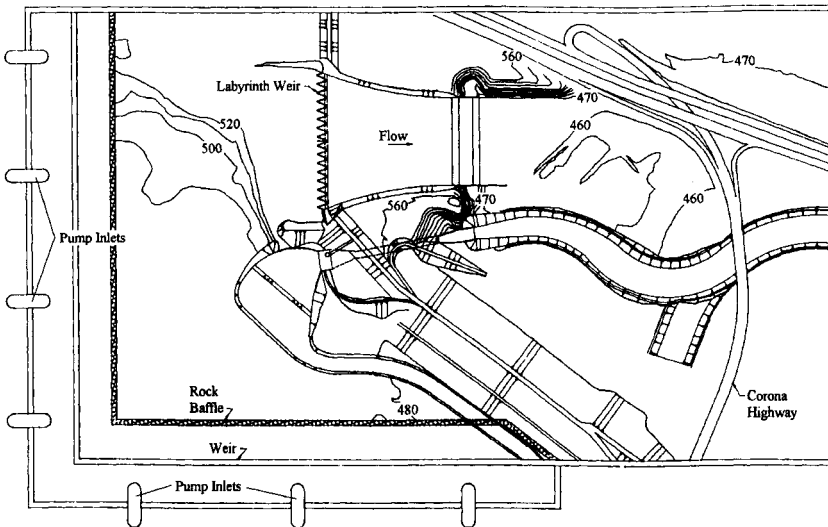


Figure 2. Model Layout for Prado Spillway Investigations with permission of US Army Corps of Engineers.

A depth-averaged numerical study of the approach flow in the reservoir was conducted to ensure that the physical model dimensions were large enough to correctly simulate the reservoir. The numerical model approximates the two-dimensional Navier-Stokes equations and includes the effects of the reservoir bathymetry. The agreement between velocities measured in the model and those predicted by the mathematical model were within $\pm 8\%$. The mathematical model investigation was also used to ensure that the flow into the model was properly simulated. The velocity vectors on the periphery of the model were adjusted to match the mathematically predicted values by varying the losses between the 7-inlet pipes and the interior of the model with a rock baffle.

The mathematical model also showed that a straight alignment of the labyrinth crest was not optimum with respect to the approach flow conditions. As shown in Figure 3, very high velocities approach the labyrinth from both abutments at large angles to the crest alignment. The effect of the non-uniform approach flow is to decrease the discharge coefficient for the labyrinth. The point of computation is at the base of the vector arrow.

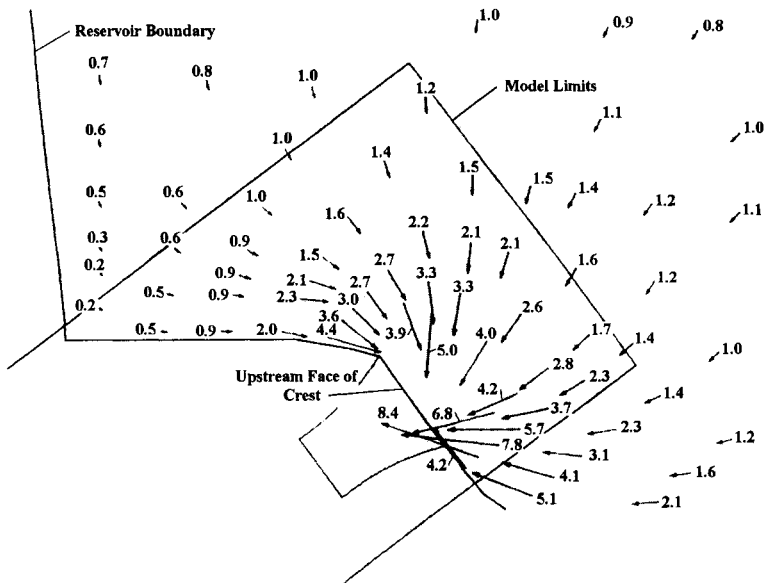


Figure 3. Numerical flow simulation of approach velocities at Prado spillway with permission of US Army Corps of Engineers.

The significant dimensions for the Prado spillway are

Cycle width, W_c	20.32 m
Weir height, P	10.06 m
Number of cycles, n	15
Sidewall length, B	22.64 m
Sidewall angle, α	23.5 °
Maximum head, H_o	8.2 m
Maximum discharge, Q_o	24,070 m ³ /sec
$W_o/P = 2.02$ $L/W_c = 2.52$ $L_d/B = 0.68$ $H_o/P = 0.82$	

The H_o/P criterion of 0.7 is exceeded for this spillway, but the W_o/P ratio meets the criterion of Taylor (1968), in which W_o/P is greater than 2, and the aspect ratio criterion of Lux (1993), in which L/W_c is greater than 2. Therefore, it is expected that the design curves would slightly overpredict the flow rate for this spillway. However, as shown in Figure 4, the discharge coefficient is about 20% lower than the Tullis et al (1995) design curves or 17% lower than the design curves of Lux and Hinchliff (1985).

Because of the lack of capacity, several modifications were made to the original design. The various modifications or types that are noted in Figure 4 and shown in Figure 5 refer to

- Type 1, a 0.3-m radius on the crest;
- Type 2, a 0.6-m radius on the weir crest;
- Type 3, filling the area behind an ogee crest placed downstream of the labyrinth with concrete;
- Type 4, removing the ogee crest;
- Type 5, blocking the overflow on the side embankments that were placed at the crest elevation; and
- Type 6, adding training walls to the embankments respectively.

Type 1 and 2 tests were conducted with an ogee crest at the end of the weirs. That is, with an elevation at the bottom of the weir at elevation 530 ft above sea level.

For depths with an H_o/P greater than 0.3, none of these modifications had a measurable effect on the discharge coefficient. Table 2 shows that the model will overpredict the discharge by between 3% and 5% for values of the H_o/P of less than 0.3. The random error from Table 4 is also between 3% and 5%. These estimates explain the scatter and the larger-than-expected values of the coefficients for small values of H_o/P , as shown in Figure 4.

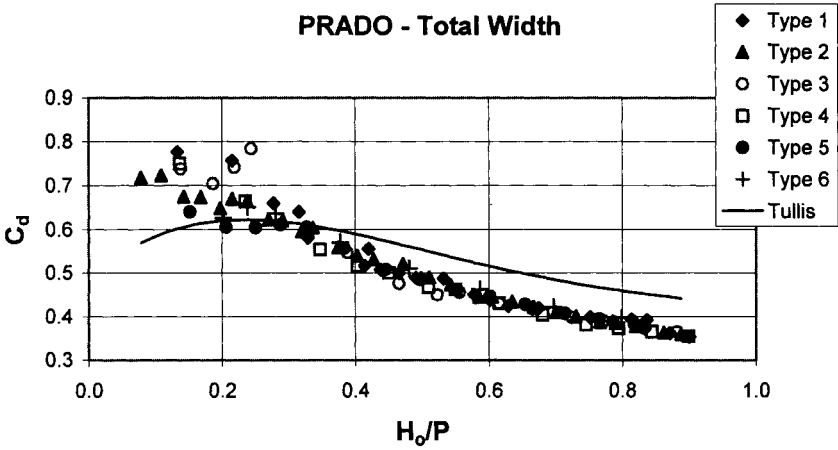


Figure 4. Discharge coefficient for Prado spillway, Copeland, R.R., and Fletcher, B.P., (2000).

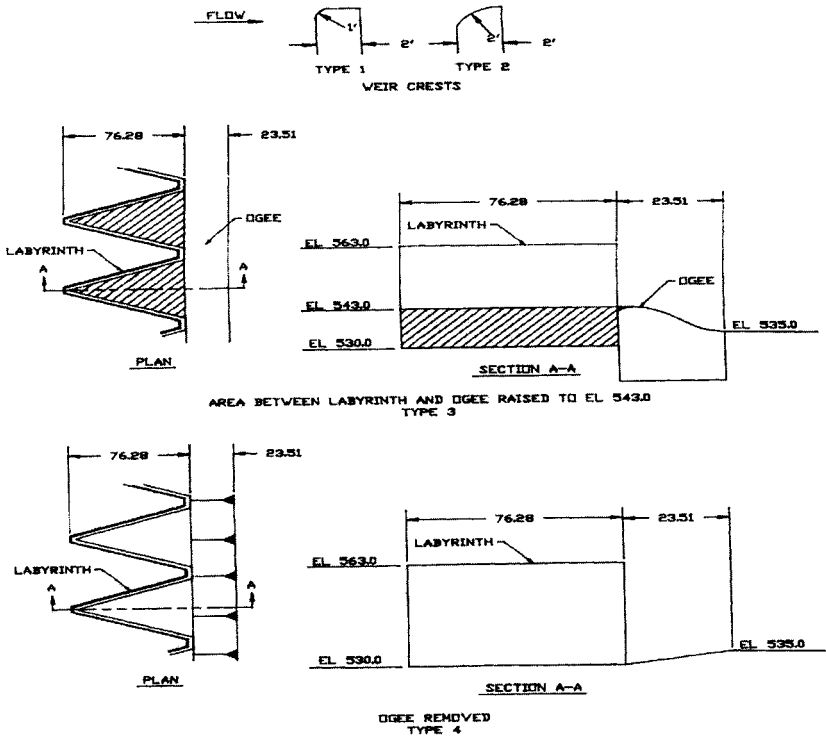


Figure 5. Type Definitions

Because some of the flow bypassed the labyrinth and passed over the embankments on each side of the weir, a separate study was made in which only a center section consisting of four weir cycles was blocked off to determine the discharge characteristics of the labyrinth sections. The coefficients for this study were also about 20% below the predicted values from Tullis (1994), as shown in Figure 6.

Two problems are identified in this case study. If the spillway alignment had been curved so that all the streamlines approached the spillway at right angles, the discharge coefficient would have been higher. However, the more significant problem is the interference. Figure 8 in Chapter 3, Nappe Interference, clearly shows that a ratio of effective disturbance length to crest length, L_d/B , is as high as 0.51. At a head having an H_o/P of 0.3, the interference length to the crest length, L_d/B , is approximately 0.25. The effect of interference is so great that factors such as crest shape, downstream blockage, and flow over the abutments have almost no effect on the discharge coefficient. A solution to this problem would be to increase the magnification or to decrease the number of cycles. Economics need to be considered because the size of the floor slab that supports the labyrinth walls increases as either the magnification increases or the number of cycles decreases. On the other hand, the large number of cycles with the existing design greatly improves the flow conditions in the downstream chute and eliminates the supercritical waves that would occur with fewer cycles.

This case study shows that the approach flow conditions to the labyrinth are important and that a mathematical model study of the reservoir can be beneficial in achieving the optimum alignment for the labyrinth crest. In addition, it shows that interference effects can overshadow all other effects even if the design satisfies the W_o/P criteria of Lux (1993) or Taylor (1968). In this case, the smaller footprint of the labyrinth spillway needs to be weighed against the loss in discharge capacity that is caused by the effects of interference. Finally, the example shows that a model study is essential if the design violates the criteria that are recommended in Chapter 8, Design.

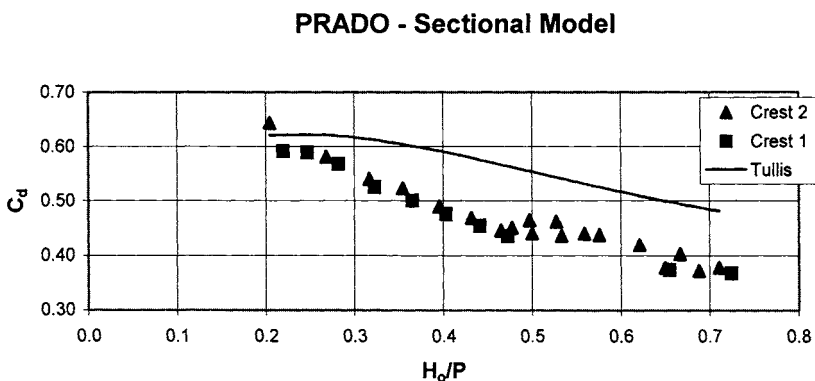


Figure 6. Discharge Coefficient with Center 4 Cycles, Data from Copeland, R.R., and Fletcher, B.P., (2000).

This page intentionally left blank

Appendix A

Prototype Labyrinth Spillways

This page intentionally left blank

Labyrinth Spillway Installations noted in the Literature

Name	Country	Year Built	Q m ³ /s	H ₀ m	P m	W m	L m	n	Source
Água Branca	Portugal		124	1.65	3.5	12.5	28.0	2	Quintel et al (2000)
Alfaiates	Portugal	1999	99	1.6	2.5	13.2	37.5	1	Quintel et al (2000)
Alijo	Portugal	1991	52	1.23	2.5*	8.7	21.05	1	Magalhães (1989)
Arcossó	Portugal	2001	85	1.25	2.5	13.3	16.68	1	Quintel et al (2000)
Avon	Australia	1970	1420	2.16	3.0	13.5	26.5	10	Darvis (1971)
Bartletts Ferry	USA	1983	5920	2.19	3.43	18.3	70.3	20.5	Mayer (1980)
Belia	Zaire		400	2.00	3.0/2.0	18.0	31.0	2	Magalhães (1989)
Beni Bahdel	Algeria	1944	1000	0.5		4	62.5	20	Afshar (1988)
Boardman	USA	1978	387	1.77	2.76*	18.3	53.5	2	Babb (1976)
Calde	Portugal	2001	21	0.6	2.5	7.4	28.19	1	Quintel et al (2000)
Carty	USA	1977	387	1.8	2.8/4.3	18.3	54.6	2	Afshar (1988)
Cimia	Italy	1982	1100	1.50	15.5	30.0	87.5	4	Lux/Hinchliff (1985)
Dungo	Angola	1985	576	2.40	4.3	9.7	28.6	4	Lux (1989)
Estancia	Venezuela	1967	661	3.01		32.0	65.0	1	Magalhães (1989)

* Sloped upstream apron. The minimum dimension at the upstream apex is given.

** Another type of spillway was constructed.

Name	Country	Year Built	Q m ³ /s	H _o m	P m	W m	L m	n	Source
Forestport	USA	1988	76	1.02	2.94	6.10	21.9	2	Lux (1989)
Garland Canal	USA	1982	25.5	0.37	1.40	4.57	19.6	3	Lux/Hincliff (1985)
Gema	Portugal		115	1.12	3.0*	12.5	30.0	2	Quintel et al (2000)
Harrezza	Algeria	1983	350	1.9	3.5*	9.7	28.6	3	Lux (1989)
Hyrum	USA		256	1.68	3.66	9.1	45.7	2	Lux (1989)
Influente	Mozambique	1985	60	1.00	1.60	4.15	24.76	3	Magalhães (1989)
Jutarnaiba	Brazil	1983	862	0.7					Afshar (1988)
Keddera	Algeria	1985	250	2.46	3.5*	8.9	26.3	2	Lux (1989)
Kizilcapinar	Turkey		2270	4.6	4.0	75.4	263.9	5	Yildiz (1996)
Mercer	USA	1972	239	1.83	4.57	5.49	17.6	4	CH2M Hill (1976)
Navet	Trinidad	1974	481	1.68	3.05	5.49	12.8	10	Phelps (1974)
Ohau C Canal	New Zealand	1980	540	1.08	2.50	6.25	37.5	12	Walsh (1980)
Pacoti	Brazil	1980	3400	2.72	4.0	8.0	41.52	15	Magalhães (1989)
Pisão	Portugal		50	1.0	3.5	8.0	200.0	1	Quintel et al (2000)
Quincy	USA	1973	26.5	2.13	3.96	13.6	26.5	4	Magalhães (1989)
Ritschard	USA	**	1555	2.74	3.05	83.8	411	9	Vermeyen (1991)

* Sloped upstream apron. The minimum dimension at the upstream apex is given.

** Another type of spillway was constructed.

Name	Country	Year Built	Q m ³ /s	H _o m	P m	W m	L m	n	Source
Rollins	USA	**	1841	2.74	3.35		472	9	Tullis (1995)
Saco	Brazil	1986	640	1.5		45	248.5		Quin et al (1988)
S. Domingos	Portugal	1993	160	1.84	3.0*	7.5	22.53	2	Magalhães (1989)
Sam Rayburn Lake	USA	1996	***		6.1	195.1	526.7	16	USCOLD Bulletin (1994)
Santa Justa	Portugal		285	1.35	3.00	10.5	67.4	2	Lux (1989)
Sarioglan	Turkey		490.7	1.06	3.0	70	358.4	7	Yildiz (1996)
Sarno	Algeria	1952	360	1.5	6.0		27.9	8	Afshar (1988)
Teja	Portugal	1995	61	1.05	2.0	12.0	36.0	1	Quintel et al (2000)
Ute	USA	1983	15570	5.79	9.14	18.3	73.7	14	Lux (1989)
Woronora	Australia	1941	1020	1.36	2.13	13.41	31.23	11	Afshar (1988)

* Sloped upstream apron. The minimum dimension at the upstream apex is given.

** Another type of spillway was constructed.

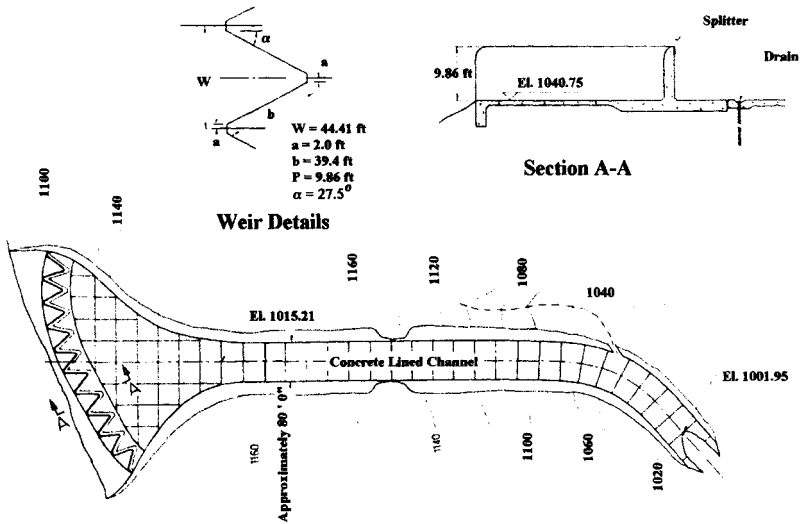
*** Distribution of heads and discharges restricted by Department of the Army after September 11, 2001.

Labyrinth Spillway Installations not noted in the Literature

Name	Country	Year Built	Q m ³ /s	H _o m	P m	W m	L m	n	Location
Flamingo	USA	1990	1591	2.23	7.32	95.1	67.4	4	Las Vegas, NV
Tongue River	USA								Decker, MT
Twin Lake	USA	1989	570	2.74	3.35	8.31	34.05	4	Buffalo, WY

The plan and profiles of a few of these installations are shown on the following pages to illustrate the varied configurations that have been used.

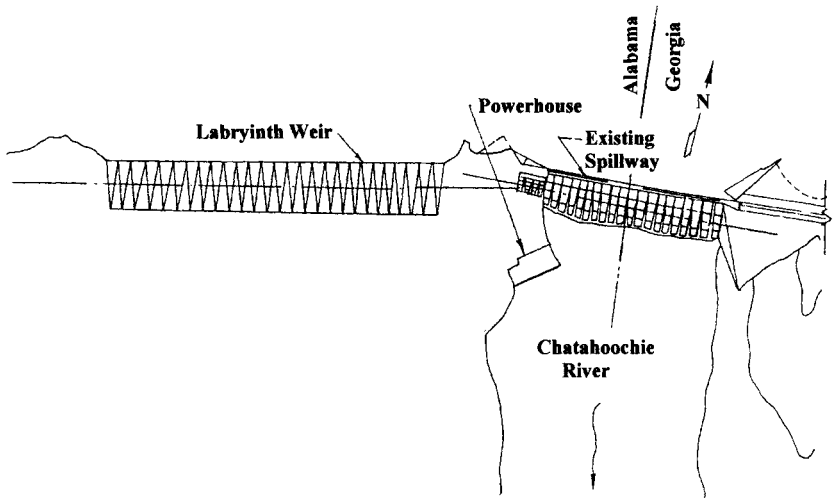
AVON



Avon Spillway - Australia

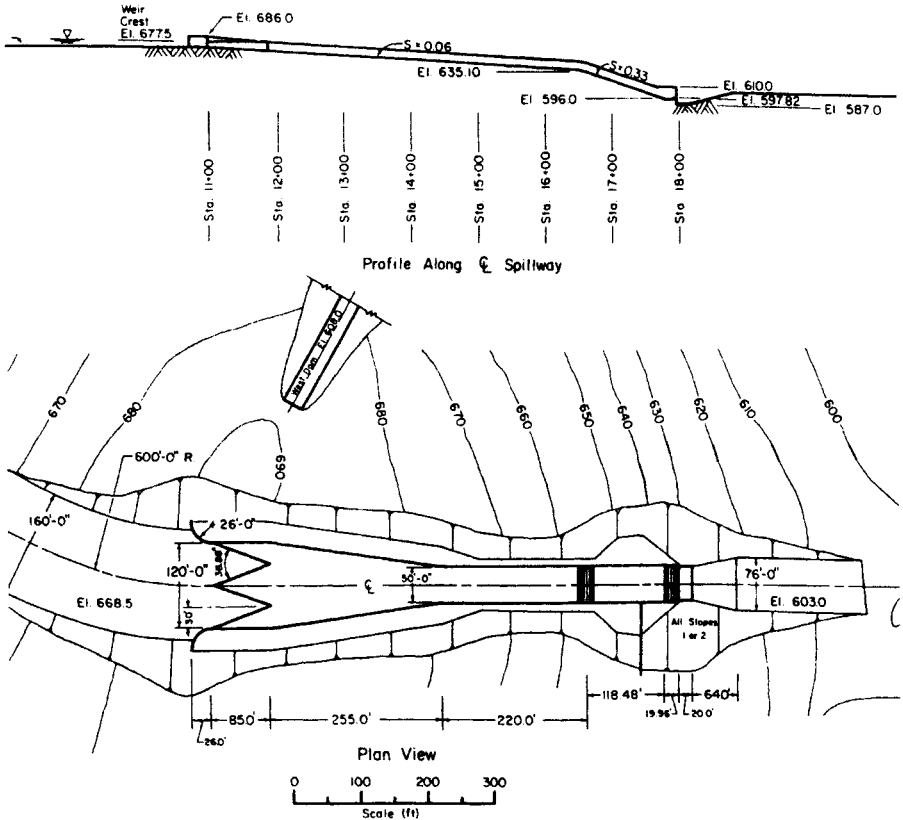
Avon spillway is unusual in that the labyrinth axis is curved in profile. In addition it is much wider than the downstream channel. Inlet conditions with this spillway are not significant because of the large number of cycles. Convergence and supercritical wavers in the channel need to be considered.

BARTLETTS FERRY



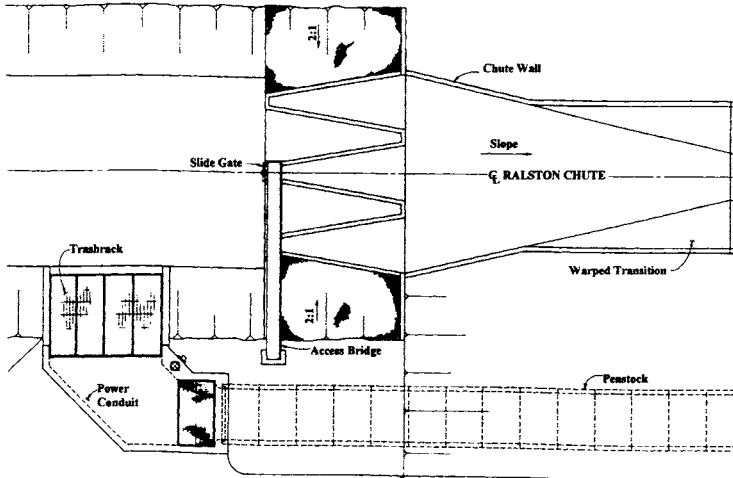
The labyrinth spillway is 1200 ft wide and consists of 40 cycles of triangular weirs. Due to the very wide spillway and the large number of cycles, supercritical waves in the downstream channel are not significant. Lateral flow at each embankment may decrease the predicted maximum discharge for this structure. An overall model of the installation or a numerical model of the reservoir should have been performed to determine if the inflow velocity vectors affect the discharge. Apparently only sectional models of one and two cycles were studied. As a result, the predicted discharge for the structure may be higher than that realized in nature.

BOARDMAN



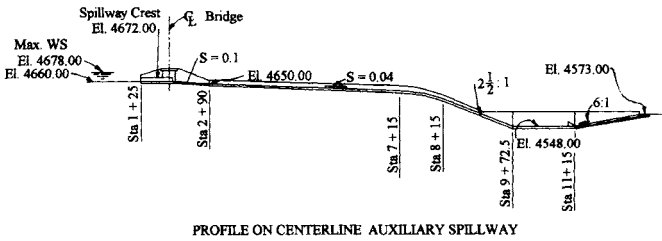
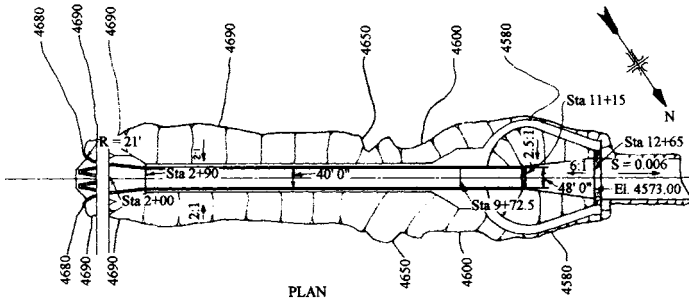
The entrance conditions to this spillway are very important because of the small number of cycles. Due to the small radius of curvature at the inlet, separation will occur on the walls leading to a smaller than expected maximum discharge. Supercritical waves in the channel are important. These were investigated in the model studies.

GARLAND CANAL



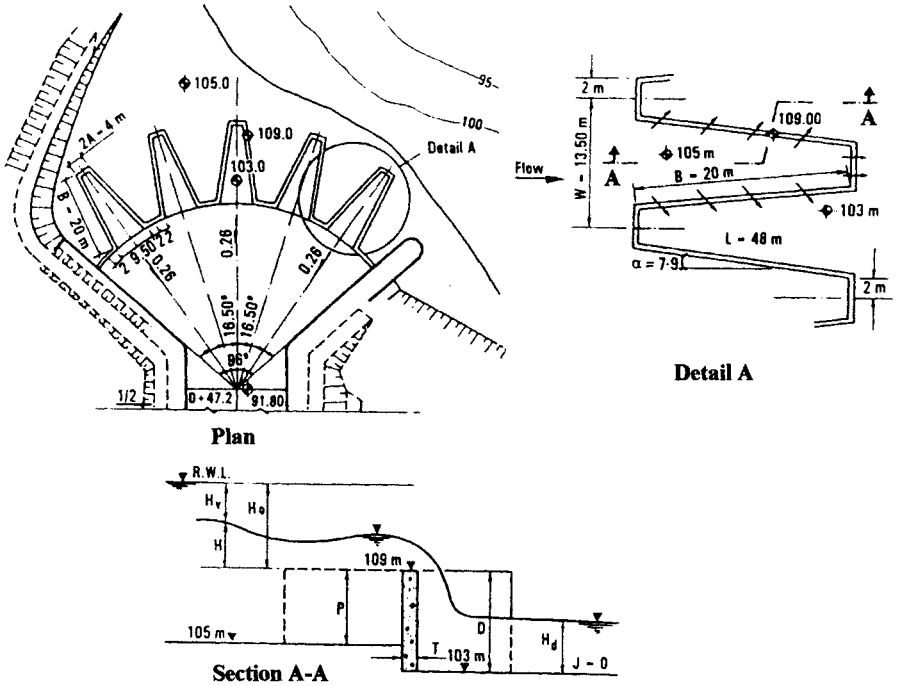
The structure is used to provide a constant head for a downstream turbine. The canal conveys large suspended sediment loads that deposit between the upstream sidewalls. During high flows the sediment is flushed out of the labyrinth. The sluice gate on the centerline of the canal was provided to pass the sediment downstream. Because of the sluicing action of the labyrinth, the sluice gate is not used. This structure required extensive numerical studies to develop the transition shape downstream of the labyrinth.

HYRUM



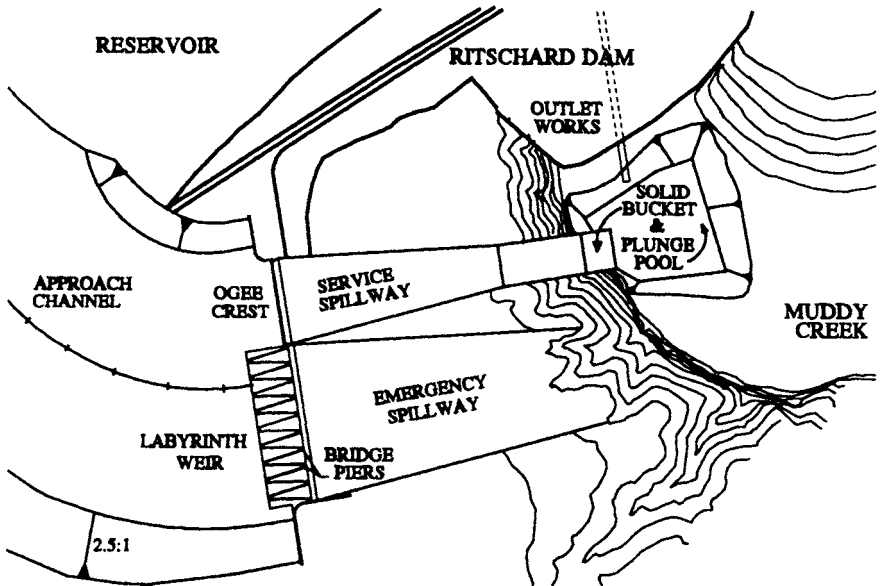
The inlet section to this spillway was developed by model studies that included changes to the location along the axis of the chute, varying the abutment conditions, and inverting the weir. Supercritical waves existed the entire length of the chute. To eliminate them a longer transition would have been necessary. As an alternative, higher chute walls were selected to be the most cost effective solution.

KIZILCAPINAR



This structure is unusual in that the axis of the labyrinth is curved. To reduce the tendency for submergence on the downstream side of the structure, the downstream invert was depressed. Extensive model studies were necessary to determine the best proportions for the weir height and the downstream invert elevation.

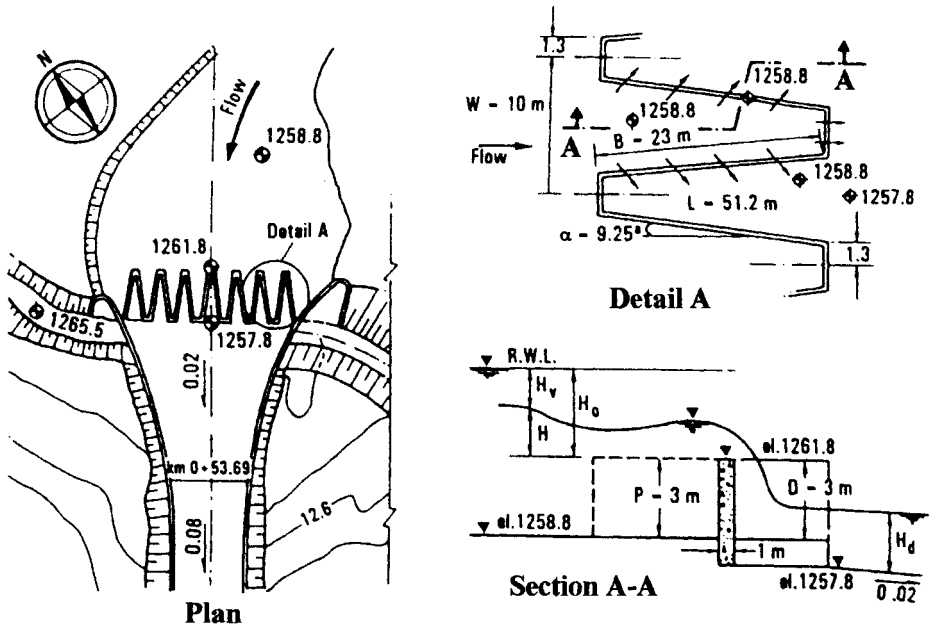
RITSCHARD



This structure was studied with a physical model. However, it was never built because the PMF was reduced after the model investigation. This structure is located at 2,300 m elevation. The original PMF was calculated from the PMP at sea level. However, since the amount of water that is contained in the atmosphere is less at 2,300 meters, the PMP could be reduced, which resulted in a lower PMF.

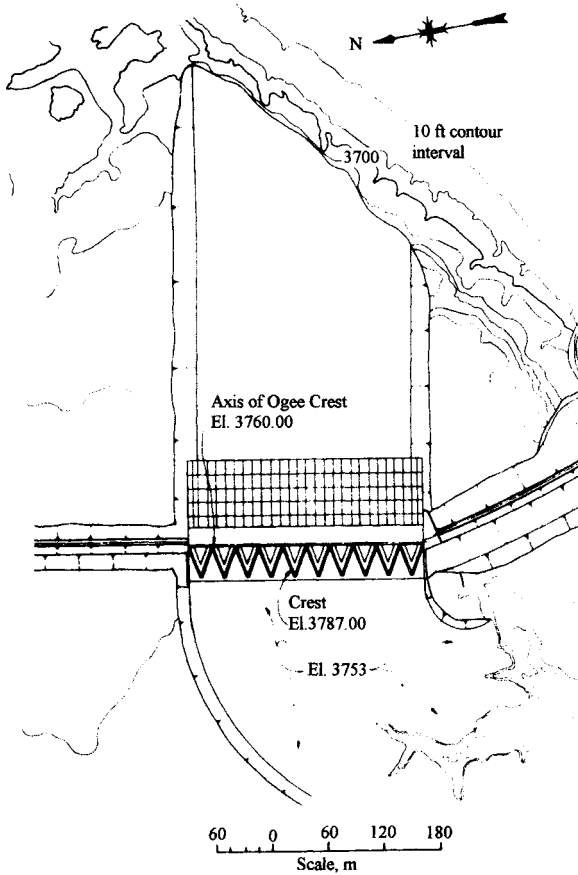
The approach flow conditions to the labyrinth are good. With a large number of cycles, supercritical waves in the downstream channel should interact with each other to produce an almost uniform flow depth where the discharge flows into Muddy Creek.

SARIOGLAN



This structure uses an expanded upstream section to increase the length of the spillway. The expanded section is joined to the downstream channel with a curved transition. A drop on the downstream side of the weir was provided to eliminate the tendency for submergence. The entire geometry shown in the plan view was simulated in a model to insure that the structure would perform as designed.

UTE



This installation placed a labyrinth weir immediately upstream of an existing ogee crest. The ogee crest was not removed. Flow disturbances were noted on each end of the spillway. Abutment modifications did not affect the discharge capacity. Supercritical waves in the downstream channel were not significant.

Appendix B

*Comparison of Labyrinth Spillways
with Curves of Tullis (1994)*

This page intentionally left blank

Name	Q	n	Wc	Lc	Ho	P	Ho/P	α	α_{max}	α/α_{max}	Cd	Cd Tullis	% Diff
Alijo	52	1	8.70	21.05	1.23	2.5	0.49	18.0	24.4	0.74	0.61	0.56	8.7
	52	1	8.70	21.05	1.23	3.0	0.41	18.0	24.4	0.74	0.61	0.59	3.8
Avon	1790	10	13.54	26.46	2.80	3.0	0.93	27.5	30.8	0.89	0.49	0.58	-18.6
	1420	10	13.54	26.46	2.16	3.0	0.72	27.5	30.8	0.89	0.57	0.63	-10.0
Bartletts Ferry	5920	20.5	18.30	70.30	2.19	3.4	0.64	*	15.1		0.43	0.43	-0.2
Boardman	387	2	18.30	54.60	1.80	2.8	0.64	19.4	19.6	0.99	0.50	0.52	-4.6
	387	2	18.30	54.60	1.80	4.3	0.42	19.4	19.6	0.99	0.50	0.62	-24.7
Cimia	1100	4	30.00	87.50	1.50	15.5	0.10	*	20.1		0.58	0.56	3.3
Dungo	576	4	9.73	28.56	2.40	3.5	0.69	15.2	19.9	0.76	0.46	0.43	7.5
	576	4	9.73	28.56	2.40	4.3	0.56	15.2	19.9	0.76	0.46	0.47	-2.3
Forestport	76	2	6.10	21.90	1.02	2.9	0.35	*	16.2		0.57	0.56	1.8
Garland Canal	25.5	3	4.57	19.60	0.37	1.4	0.26	*	13.5		0.65	0.56	14.2
Gema	148	2	12.50	30.00	1.32	2.5	0.53	19.0	24.6	0.77	0.55	0.56	-1.7
	148	2	12.50	30.00	1.32	3.0	0.44	19.0	24.6	0.77	0.55	0.60	-8.9
Harrezza	350	3	9.73	28.56	1.90	3.5	0.54	15.2	19.9	0.76	0.53	0.48	9.1
	350	3	9.73	28.56	1.90	4.3	0.44	16.2	19.9	0.81	0.53	0.52	2.5
Hyrum	256	2	9.14	45.72	1.68	3.7	0.46	8.9	11.5	0.77	0.44	0.42	4.0
Infulene	60	3	4.15	24.78	1.00	3.7	0.27	4.4	9.6	0.46	0.27	0.32	-17.1
Keddara	250	2	8.92	26.31	2.46	3.5	0.70	14.9	19.8	0.75	0.42	0.42	-0.7
	250	2	8.92	26.31	2.46	4.2	0.59	14.9	19.8	0.75	0.42	0.46	-10.3
Navet	481	10	5.49	12.80	1.68	3.1	0.55	23.6	25.4	0.93	0.58	0.62	-6.1
Oahu C Canal	540	12	6.25	37.50	1.08	2.5	0.43	*	9.6		0.36	0.44	-21.5
Pacoti	3400	15	8.00	41.52	2.72	4.0	0.68	10.0	11.1	0.90	0.41	0.34	17.5
Quincy	552	4	13.60	26.50	2.13	4.0	0.54	*	30.9		0.57	0.66	-16.3
Ritchard	1555	9	9.31	45.72	2.74	3.0	0.90	8.1	11.8	0.69	0.28	0.28	0.6
Rollins Dam	1841				2.74	3.4	0.82	9.2					
S. Domingos	160	2	7.50	22.53	1.84	3.0	0.61	13.3	19.4	0.68	0.48	0.42	12.8
	160	2	7.50	22.53	1.84	3.6	0.51	13.3	19.4	0.68	0.48	0.46	4.5
Santa Justa	285	2	10.50	67.40	1.35	3.0	0.45	4.0	9.0	0.45	0.46	0.28	38.7
Ute	15574	14	18.29	73.15	5.79	9.1	0.63	12.9	14.5	0.89	0.37	0.40	-8.2
Woronora	1020	11	13.41	31.23	1.36	2.2	0.62	22.8	25.4	0.90	0.63	0.58	8.5
												Average	-0.5
												RMS	13.0

This page intentionally left blank

Bibliography

Note: This Bibliography includes both references cited in the text and additional papers that may be of interest to the reader.

Ackers, P., (1957). "A theoretical consideration of side weirs as storm water overflows." *Proceedings of the Institution of Civil Engineers*, 6, 250-269.

Afshar, A., (1988). "The development of labyrinth weir design." *Water Power and Dam Construction*, 40(5), 36-39.

Afshar, A., and Mariño, M.A., (1990). "Determining optimum spillway capacity based on estimated flood distribution." *Water Power and Dam Construction*, 42(1), 44-53.

Afshar, A., and Mariño, M.A., (1990). "Optimizing spillway capacity with uncertainty in flood estimator," *J. Water Resources Planning and Management*, 116(6), 71-84.

Afshar, A., Barkhordary, A., and Mariño, M.A., (1994). "River diversion optimization under hydraulic and hydrologic uncertainties." *J. Water Resources Planning and Management*, 120(1), 36-47.

Allen, J.W., (1957). "The discharge of water over side weirs in circular pipes." *Proceedings of the Institution of Civil Engineers*, 6, 270-287.

Amanian, N., (1987). "Performance and design of labyrinth spillways." MSc thesis, Utah State University, Logan, Utah.

Aminipouri, B., and Valentine, E.M., (1994). "Numerical modeling of labyrinth spillway." *2nd International Conference on Hydraulic Modeling*, Stratford-upon-Avon, U.K., June.

Babb, A.F., (1976). "Hydraulic model study of the Boardman Reservoir spillway." R.L. Albrook Hydraulic Laboratory, Washington State University, Pullman, Wash., May.

Balmforth, D.J., (1981). "A mathematical model for spatially varied flow with decreasing discharge." *Engineering Software II, Proceedings of 2nd International Conference on Engineering Software*, CNL Publications, Ltd., London, England, 1094-1104.

Balmforth, D. J., and Sarginson, E.J, (1977). "Discussion of 'Experimental investigation of flow over side weirs,' by El-Hkashab and Smith." *American Society of Civil Engineering, Journal of Hydraulic Engineering*, 103(8), 941-943.

Balmforth, D. J., and Sarginson, E.J, (1983). "An experimental investigation of the discharge capacity of side weirs." *Proceedings of International Conference on the Hydraulic Aspects of Floods and Flood Control*, British Hydraulic Research Association, Fluid Engineering Center, Bedford, England, 171-180.

Benefield, L.D., Judkins, F.J., and Par, A.P., (1984). *Treatment plant hydraulics for environmental engineers*. Prentice Hall, Inc., Englewood Cliffs, N.J.

Borghei, S.M., Jalili, M.R., and Ghodsian, M., (1999). "Discharge coefficient for sharp-crested side weir in subcritical flow." *American Society of Civil Engineering, Journal of Hydraulic Engineering*, 125(10), 1051-1056.

Carter, F.J., (1970). "The strengthening of Avon Dam." *Journal of the Institution of Engineers*, Australia, June, 67-77.

Cassidy, J.J., Gardner, C.A., and Peacock, R.T., (1983). "Labyrinth-crest spillway – planning, design and construction." *Proceedings of the International Conference of the Hydraulic Aspects of Floods and Flood Control*, London, England, Sept., 59-80.

Cassidy, J.J., Gardner, C.A., and Peacock, R.T., (1985). "Boardman labyrinth crest spillway." *American Society of Civil Engineering, Journal of Hydraulic Engineering*, 111(3), 398-416.

Cassidy, J.J., Gardner, C.A., and Peacock, R.T., (1985). "Closure to 'Boardman labyrinth crest spillway.'" *American Society of Civil Engineering, Journal of Hydraulic Engineering*, 111(6), 808-819.

CH₂M-Hill, (1973). "Mercer Dam spillway model study." Dallas, OR, Mar. Internal Report

CH₂M-Hill, (1973), "Quincy terminal raw water storage," Aurora, CO., Internal Report.

Chandrasekhara, T.R., and Loganathan, V., (1985). "Discussion of 'Boardman labyrinth crest spillway.'" *American Society of Civil Engineering, Journal of Hydraulic Engineering*, 111(6), 808-819.

Chao, J.L., and Trussel, R.R., (1980). "Hydraulic design of flow distribution channels." *American Society of Civil Engineering, Journal of the Environmental Engineering Division*, 106(EE2), 321-334.

Coleman, G.S., and Smith, D., (1923). "The discharging capacity of side weirs." Selected Engineering Paper No. 6, Institution of Civil Engineers, London, England.

Collinge, V.K., (1957). "The discharge capacity of side weirs." *Proceedings of the Institution of Civil Engineers*, 6, 288-304.

Copeland, R.R., and Fletcher, B.P., (2000). "Model study of Prado Spillway, California, hydraulic model investigation." *Report ERDC/CHL TR-00-17*, U.S. Army Corps of Engineers, Research and Development Center, Sept.

Coulomb, R., de Saint Martin, J.M., and Nougauro, J., (1967). "Etude théorique de la réparation du débit le long d'un déversoir latéral." *Le Génie Civil*, 44(4), 311-316.

Darvas, L.A., (1971). "Discussion of 'Performance and design of labyrinth weirs,' by Hay and Taylor." *American Society of Civil Engineering, Journal of Hydraulic Engineering*, 97(80), 1246-1251.

De Marchi, G. (1943). "Saggio di teoria de funzionamento degle stamazzi laterali." *L'Energia Elettrica*, Rome, Italy, 11(11), 849-860.

El-Khashab, A.M.M., (1975). "Hydraulics of flow over side weirs." PhD thesis, University of Southampton, Southampton, England.

El-Khashab, A.M.M., and Smith, K.V.M, (1976). "Experimental investigations of flow over side weirs." *American Society of Civil Engineering, Journal of Hydraulic Engineering*, 102(9), 1255-1268.

Ervine, D.A., and Falvey, H.T., (1987). "Behavior of turbulent water jets in the atmosphere and in plunge pools," *Proceedings of the Institution of Civil Engineers*, Part 2, 83, 295-314.

Falvey, H.T., (1980). *Practical experiences with flow-induced vibrations*, edited by Naudascher, E., and Rockwell, D., Springer-Verlag, 386-398. Berlin/Heidelberg/New York.

Falvey, H.T., and Treille, P., (1995). "Hydraulics and design of fusegates." *Journal of Hydraulic Engineering*, 121(7), 512-518.

Francis, J.B., (1883). *Lowell hydraulic experiments*, 4th Ed., D. Van Norstrand, New York.

Frazer, W., (1957). "The behavior of side weirs in prismatic rectangular channels." *Proceedings of the Institution of Civil Engineers*, London England, 6(14), 305-327.

Garton, J.E., (1966). "Designing an automatic cutback furrow irrigation system." *Bulletin B-651*, Experimental Station, Oklahoma State University, Stillwater, Okla.

Gentiline, B., (1940). "Stramazzi con cresta a pianta obliqua e a zig-zag." *Memorie e Studi dell Istituto di Idraulica e Costruzioni Idrauliche del Regil Politecnico di Milano*, No. 48 (in Italian).

Guthrie-Brown, J., (19xx), *Hydro-electric engineering practice*, Blackie, London, England, 1, 586-587.

Hager, W.H., (1981). "Die hydraulik von verteilkanalen," MSc thesis, Federal Institute of Technology, Zurich, Switzerland (in German).

Hager, W.H., (1987). "Lateral outflow over side weirs." *American Society of Civil Engineering, Journal of Hydraulic Engineering*, 113(4), 491-504.

Hager, W.H., (1992). *Breitkroniges wehr*. Wasser, Energie, Luft, Baden Switzerland, 7/8, 152-155 (in German).

Hager, W.H., (1992). "Spillways, shockwaves and air entrainment." *Bulletin No. 81*, International Committee on Large Dams.

Hager, W.H., (1993). "Streichwehre mit kreisprofil," *GWF Wasser-Abwasser*, 134(4), 156-163 (in German)

Hager, W.H., and Hager, K., (1985). "Streamline curvature effects in distribution channels." *Proceedings of the Institution of Mechanical Engineers*, 199(3), 165-172.

- Hager, W.H., and Volkart, P.U., (1986). "Distribution channels." *American Society of Civil Engineering, Journal of Hydraulic Engineering*, 112(10), 935-952.
- Hall, G.W., (1962). "Discharge characteristics of broad-crested weirs using boundary-layer theory." *Proceedings of the Institution of Civil Engineers*, London, England, 22, 177-190.
- Harlock, J.H., (1956). "An investigation of the flow manifolds with open and closed ends." *Journal of the Royal Aeronautical Society*, London, England, 60, 749.
- Harshbarger, E.D., (1994). "Hydroplus fusegate evaluation." *Report No. WR28-1-900-259*, Tennessee Valley Authority.
- Hauser, G.E., (1996). "Design of aerating weirs." *EPRI Report TR-1039472694-17, Dec.* Prepared by TVA for the Electrical Power Research Institute, Palo Alto, Calif.
- Hay, N., and Taylor, G., (1969). "A computer model for the determination of the performance of labyrinth weirs." 13th Congress of the International Association for Hydraulic Research, Kyoto, Japan, Sept.
- Hay, N., and Taylor, G., (1970). "Performance and design of labyrinth weirs." *American Society of Civil Engineering, Journal of Hydraulic Engineering*, 96(11), 2337-2357.
- Hinchliff, D., and Houston, K.L., (1984). "Hydraulic design and application of labyrinth spillways." *Proceedings of 4th Annual USCOLD Lecture*, January.
- Hoffman, C.J., (1974), "Chapter IX Spillways," *Design of Small Dams*, United State Department of Interior, Bureau of Reclamation.
- Holley, E.R., (1989). "Discussion of 'Lateral outflow over side weirs,' by Hager," *American Society of Civil Engineering, Journal of Hydraulic Engineering*, Vol. 115(5), 682-688.
- Houston, K.L., (1982). "Hydraulic model study of Ute Dam labyrinth spillway." *Report No. GR-82-7*, U.S. Bureau of Reclamations, Denver, Colo.
- Houston, K.L., (1983). "Hydraulic model study of Hyrum Dam auxiliary labyrinth spillway." *Report No. GR 82-13*, U.S. Bureau of Reclamations, Denver, Colo.

- Houston, K.L., and DeAngelis, C.S., (1982). "A site specific study of a labyrinth spillway." *Proceedings Conference on Applying Research to Hydraulic Practice*, 86-95, Aug.
- Humphreys, A.S., (1969). "Mechanical structures for farm irrigation." *American Society of Civil Engineering, Journal of Irrigation and Drainage*, 94(4), 463-479.
- Indlekofer, H., and Rouvé, G., (1975). "Discharge over polygonal weirs." *American Society of Civil Engineering, Journal of the Hydraulics Division*, 101(HY3), 385-401.
- Ishikawa, T., (1984). "Water surface profile of stream with side overflow." *American Society of Civil Engineering, Journal of Hydraulic Engineering*, 110(2), 1830-1840.
- Jain, S., and Fischer, E.E., (1981). "Uniform flow over skew side weir." *American Society of Civil Engineering, Journal of Irrigation and Drainage*, 108(2), 163-166.
- Joseph, L., (1974). "Linear proportional weirs," MSc thesis, Concordia University, Montreal, Quebec, Canada.
- Kandaswamy, P.K., and Rouse, H., (1957). "Characteristics of flow over terminal weirs and sills." *American Society of Civil Engineering, Journal of Hydraulic Engineering*, 83(4), 1345-1 to 1345-11.
- Kindsvater, C.E., and Carter, R.W., (1959). "Discharge characteristics of rectangular thin-plate weirs." *American Society of Civil Engineering, Journal of Hydraulic Engineering*, 124, 772-822.
- Kosinsky, de V., (1969). "Etude expérimental de déversoirs latéraux." *Revue Universelle des Mines*, 199-211 (in French).
- Kotowski, A., (1990). "Modelversuche über regenüberläufe mit gefrosselterm ablauf." *GWF Wasser-Abwasser*, 131(3), 108-114 (in German).
- Kotowski, A., (2000). "Modelversuche über den regenüberläufe mit seitlichen streichwehren." *GWF Wasser-Abwasser*, 141(1), 47-55 (in German).
- Lux, F., (1984). "Discharge characteristics of labyrinth weirs." *Proceedings of Conference on Water for Resource Development*, Coeur d'Alene, ID, Aug, American Society of Civil Engineering.

- Lux, F. (1985). "Discussion on 'Boardman labyrinth crest spillway.'" *American Society of Civil Engineering, Journal of Hydraulic Engineering*, 111(6), 808-819.
- Lux, F., and Hinchliff, D.L., (1985). "Design and construction of labyrinth spillways." *15th Congress ICOLD, Vol. IV, Q59-R15*, Lausanne, Switzerland, 249-274.
- Lux, F., (1989), "Design and application of labyrinth weirs," *Design of Hydraulic Structures 89*, Edited by Alberson, M.L., and Kia, R.A., Balkema/Rotterdam/Brookfield.
- Lux, F., (1993). "Design methodologies for labyrinth weirs." *Proceedings Water Power 93*, Nashville, Tenn.
- Mayer, P.G., (1980). "Bartletts Ferry Project, labyrinth weir model studies." *Project No. E-20-610*, Georgia Institute of Technology, Atlanta, Ga., Oct.
- McNown, J.S., and Hsu, E., (1951). "Application of conformal mapping to divided flow." *Proceedings of the Midwestern Conference on Fluid Dynamics*, State University of Iowa, Ames, Iowa, Reprints in Engineering, Reprint No. 96, 143-154.
- Meeks, M.C., (1983). "The design and construction of Bartletts Ferry labyrinth weir spillway." *Occasional Paper*, Power Supply Engineering and Services Department, Georgia Power Company, Atlanta, Ga.
- Megalháes, A.P., (1985). "Labyrinth weir spillway." *Transactions of the 15th Congress ICOLD, Vol. VI, Q59-R24*, Lausanne, Switzerland, 395-407.
- Megalháes, A.P., Lorena, M., (1989). "Hydraulic design of labyrinth weirs." *Report No. 736*, National Laboratory of Civil Engineering, Lisbon, Portugal.
- Megalháes, A.P., and Melo, J.F., (1994). "Hydraulic model study of a large labyrinth weir spillway." *2nd International Conference on Hydraulic Modeling*, Stratford-upon-Avon, U.K., June.
- Metropolitan Water, Sewerage and Drainage Board, (1980). "Investigation into spillway discharge noise at Avon Dam." *ANCOLD Bulletin No. 57*, 31-36.
- Mitchell, J.M., (1890). "On the theory of free stream lines." *Philosophical Transactions of the Royal Society*, London, England, A181, 389.

Muralidhar, D., and Govida, Rao, N.S., (1963). "Discharge characteristics of weirs of finite crest width." *La Houille Blanche*, 5, 537-545.

Muslu, Y., and Tozluk, H., (1994). "Yan savaklarda akimin su yüzü profilini etkileven parametrelerle hesabi için nümerik bir yaklaşımlar." *8 Mühendislik Haftası*, S. Demirel Üniversitesi, Isparta, Turkey (in Turkish).

Nadesamoorthy, T., and Thomson, A., (1972). "Discussion of 'Spatially varied flow over side weirs' by Subramanya, K., and Awasthy, S.C." *American Society of Civil Engineering, Journal of Hydraulic Engineering*, 98(12), 2234-2235.

Naudascher, E., and Rockwell, D., (1994). *Flow induced vibrations - an engineering guide*, Balkema Press, Rotterdam/Brookfield.

Nimmo, W.H.R., (1928). "Side spillway for regulating diversion channels." *American Society of Civil Engineering Transactions*, 98(12), 2234-2235.

Oswalt, N.R., Buck, L.W., Helper, T.E., and Jackson, H.E., (1994). "Alternatives for overtopping protection of dams." American Society of Civil Engineering Task Committee on Overtopping Protection, ASCE Hydraulics Division.

Pinheiro, A.N., and Silva, I., (1999). "Discharge coefficient of side weirs. Experimental study and comparative analysis of different formulas," *XXVIII IAHR Proceedings*, Graz, Austria.

Parmley, W.C., (1905). "The Walworth Sewer, Cleveland Ohio." *American Society of Civil Engineering Transactions*, 55, 341.

Phelps, H.O., (1974). "Model study of labyrinth weir – Navet Pumped Storage Project." University of the West Indies, St. Augustine, Trinidad, West Indies, Mar.

Prakash, A., (1985). "Discussion on 'Boardman labyrinth crest spillway.'" *American Society of Civil Engineering, Journal of Hydraulic Engineering*, 111(6), 808-819.

Quin, J.T., Rezende, S.P., and Schrader, E.K., (1988). "Saco Dam - South America's first RCC dam." *Roller compacted concrete II*, edited by K.D. Hansen and L.K. Guice, American Society of Civil Engineering Conference on Concrete, Geotechnical and Engineering Materials, San Luis Obispo, Calif., 340-356.

Quintel, A.C., Pinheiro, A.N., Afonso, J.R., and Cordeiro, M.S., (2000). "Gated spillways and free flow spillways with long crests, Portuguese dams experience." *Proceedings of the 20th International Congress of Large Dams*, Beijing, China, Question 79.

Ramamurthy, A.S., and Carballada, L., (1977). "Lateral weir flow model." *Internal Report*, Civil Engineering Department, Concordia University, Montreal, Quebec, Canada.

Ramamurthy, A.S., and Carballada, L., (1980). "Lateral weir flow model," *American Society of Civil Engineering, Journal of Irrigation and Drainage*, 106(1), 9-25.

Ramamurthy, A.S., Subramanya, K., and Carballada, L., (1978). "Uniformly discharging lateral weirs." *American Society of Civil Engineering, Journal of Irrigation and Drainage*, 104(4), 399-412.

Ranga Raju, K.G., Pradas, B., and Gupta, S.K., (1979). "Side weir in rectangular channel." *American Society of Civil Engineering, Journal of Hydraulic Engineering*, 105(5), 547-544.

Rice, C.E., and Gwinn, W.R., (1981). "Rating of Z-section, steel-sheet piling drop structures." *Transactions of the American Society of Agricultural Engineers*, 24(1) 107-112.

Rao, S.S., Shukla, M.K., (1971). "Characteristics of flow over weirs of finite crest width." *American Society of Civil Engineering, Journal of Hydraulic Engineering*, 97(11), 1807-1816.

Rawn, A.M., Bouerman, F.R., and Brooks, N.H., (1960). "Diffusers for disposal of sewage in seawater." *American Society of Civil Engineering, Journal of Sanitary Engineering Division*, 86(2), 65.

Rehbock, T., (1929). "Wassermessung mit sharfkantigen uberfallwehren," *Zeitschrift des Vereins Deutscher Ingenieure*, 73, 343, May (in German).

Resendiz-Carrillo, D., and Lave, L.B., (1987). "Optimizing spillway capacity with an estimated distribution of floods." *Water Resources Research*, 23(11), 2043-2049.

Robertson, D.I., and McGhee, T.J., (1993). "Computer modeling of side-flow weirs." *American Society of Civil Engineering, Journal of Hydraulic Engineering*, 119(6), 989-1005.

Rouse, H., (1936). "Discharge characteristics of the free overfall." *Civil Engineering*, April.

Rouvé, G., and Indlekofer, H., (1974), "Abfluß über geradlinige Wehe mit halbkreisförmigem Überfallprofil," *Der Bauingenieur* 49,250-256, (in German).

Shukla, M.K., (1970). "Characteristics of flow over weirs of finite-crest width." Master of Technology Degree Thesis, Indian Institute of Technology, Kanpur, India.

Singer, J., (1964). "Square edged broad-crested weir as a flow measurement device." *Water and Water Engineering*, 68, 227-235, June.

Smith, K.V.H., (1973). "Computer programming for flow over side weirs." *American Society of Civil Engineering, Journal of Hydraulic Engineering*, 99(2), 227-235.

Subramanya, K., and Awasthy, S.C., (1972). "Spatially varied flow over side weirs." *American Society of Civil Engineering, Journal of Hydraulic Engineering*, 98(1), 1-10.

Sweeten, J.M., and Garton, J.E., (1970). "The hydraulics of an automated furrow irrigation system with rectangular side weir outlets." *Transactions of American Society of Agricultural Engineers*, 13(6), 747-751.

Sweeten, J.M., Garton, J.E., and Mink, A.L., (1980). "Hydraulic roughness of an irrigation channel with decreasing spatially varied flow." *Transactions of American Society of Agricultural Engineers*, 12(4), 466-470.

Tacail, F.G., Evans, B., and Babb, A., (1990). "Case study of a labyrinth spillway." *Canadian Journal of Civil Engineering*, 17, 1-7.

Taylor, G., (1968). "The performance of labyrinth weirs." PhD thesis, University of Nottingham, Nottingham, England.

Tebbutt, T.H.Y., Rajaratnam, S.K., and Essery, I.T.S., (1977). "Reaeration performance of a stepped cascade." *Journal of the Institute of Water Engineers*, 31, 285-297.

Thomas, H.H., (1976). *The engineering of large dams*, Parts I and II, John Wiley and Sons, Ltd., London, England.

- Tison, G., and Franson, T., (1963), "Essais sur déversoirs de forme polygonale en plan." *Review C. Tijdschrift*, Brussels, III(3), 38-51 (in French).
- Tozlu, H., (1994). "Yan savak akiminin hesabi için nümerik bir yaklasim." PhD thesis, Osmangazi Üniversitesi, Eskischir, Turkey. (in Turkish).
- Tsang, C., (1987), "Hydraulic and aeration performance of labyrinth weirs," PhD thesis, University of London, U.K.
- Tullis, J.P., (1993). "Standley Lake service spillway model study." *Hydraulic Report No. 341*, Utah State University Foundation, Utah Water Research Laboratory, Logan, Utah.
- Tullis, J.P., Nosratollah, A., and Waldron, D., (1995). "Design of labyrinth spillways. " *American Society of Civil Engineering, Journal of Hydraulic Engineering*, 121(3), 247-255.
- Uyumaz, A., (1997). "Side weir in U-shaped channels." *American Society of Civil Engineering, Journal of Hydraulic Engineering*, 123(7), 639-646.
- Uyumaz, A., and Smith, R.H., (1991). Design procedures for flow over side weirs." *American Society of Civil Engineering, Journal of Irrigation and Drainage*, 117(1), 79-90.
- Van Beesten, (1992), "Hydraulic structures in flood control systems," *Proceedings of the Institution of Civil Engineers, Civil Engineering*, 92, Feb., 30-38.
- Vermeyen, T., (1991). "Hydraulic model study of Ritschard Dam spillways." *Report No. R-91-08*, U.S. Bureau of Reclamations, Denver, Colo.
- Vigander, S., Elder, R.A., and Brooks, N.H., (1970). "Internal hydraulics of thermal discharge diffusers." *American Society of Civil Engineering, Journal of Hydraulic Engineering*, 96(2), 509.
- Villemonte, J.R., (1947). "Submerged weir discharge studies." *Engineering News Record*, 866, Dec.
- Vischer, D., (1960). "Allgemeine stau und senkungskurven an streichwehren." *Schweizerische Bauzeitung*, 49. (in German).

Waldron, D.R., (1994). "Design of labyrinth spillways." MSc thesis, Utah State University, Logan, Utah.

Walsh, J.M., and Jones, D.G., (1980). "Upper Waitake Power Development hydraulic model of Ohau C. Canal labyrinth side-weir." *Report No. 3-80/2*, Ministry of Public Works and Development, Central Laboratories, New Zealand, Mar.

Walters, R.C.S., (1962). *Dam geology*, Butterworths, London, England, 258.

Watt, W.E., and Wilson, K.C., (1987). "Allowance for risk and uncertainty in the optimal design of hydraulic structures." *Proceedings of the International Symposium on Risk and Reliability in Water Resources*, University of Waterloo, Waterloo, Ontario, Canada.

Wilhelms, S.C., Gulliver, J.S., and Parkhill, K. (1993). "Reaeration at low head hydraulic structures." *Technical Report No. W-93-2*, U.S. Waterways Experiment Station, U.S. Army Corps of Engineers, Vicksburg, MS.

Wormleaton, P.R., and Soufiani, E, (1998). "Aeration performance of triangular planform labyrinth weirs." *American Society of Civil Engineering, Journal of Environmental Engineering*, 124(8), 709-719.

Wormleaton, P.R., and Tsang, C.C., (2000). "Aeration performance of rectangular planform labyrinth weirs." *American Society of Civil Engineering, Journal of Environmental Engineering*, 127(5), 456-465.

Yen, B.C., and Wenzel, H.G., (1970). "Dynamic equations for steady spatially varied flow," *American Society of Civil Engineering, Journal of Hydraulic Engineering*, 96(3), 801-814.

Yildiz, D. and Uzecek, E., (1996). "Modeling the performance of labyrinth spillways." *Hydropower*, 3, 71-76.

Index

- aeration 6, 35, 41–42, 70, 103–108
apex ratio 81
approach flow conditions 82–84
aprons 64–66; detention dams 114
Arnwell Magna Spillway 65
atmospheric flow head 34
Avon Dam 24; design curves 57; design diagram 136; nappe vibration 69–74
- Bartletts Ferry Dam 27–28; design diagram 137
Boardman Dam 26–27; aprons 66; design curves 58; design diagram 138; pressure flow 35–36; sedimentation 95, 96–97; supercritical waves 61–62
- canals 6
cavity flow 34
chutes, downstream 61–68, 84
constant energy approach, for flow equations 9, 11
crests: applicability of design curves 56–59; jet interference 6; perpendicular flow 14; shape modifications 72–73; shapes 31–39, 82; *see also* specific crest shapes below
crests, flat 31; discharge coefficient 32–33
crests, half-round 31; discharge coefficient 32, 34–37
crests, nappe 31, 34; design curves 49, 59; discharge coefficient 32, 37–39
crests, ogee: *see* crests, nappe
crests, quarter-round 31; design curves 53; discharge coefficient 32, 33; labyrinth weirs 41–42
crests, sharp 31; design curves 45–46; discharge coefficient 32–33
- dams: Avon 24, 57, 69–74, 136; Bartletts Ferry 27–28, 137; Boardman 26–27, 35–36, 58, 61–62, 66, 95, 96–97, 138; detention 113–115; Flamingo Detention 113–115; Prado 25, 125–128; Ritschard 28, 142; Rollins 25–26; Tongue River 100–101; Ute 26, 63, 144; Woronora 24, 58, 70–72
design curves 41–59; applicability to crest shapes 56–59; applicability to labyrinth shapes 56–59; critique 56–59; dam model data 57–59; discharge coefficient 57; labyrinth weirs 44–59; nappe crests 49; quarter-round crests 53
design head 34, 37
design parameters: apex ratio 81; approach flow conditions 82–84; crest shapes 82; downstream chutes 84; headwater ratio 77; interference length ratio 82; labyrinth weirs 77–88; layout 84–87; magnification 78; sidewall angle 77, 78; vertical aspect ratio 77
design procedure: labyrinth weirs 88–93; spreadsheet 89–94
detention dams 113–115
discharge coefficient 13, 14–15, 16; crest shapes 31–39; design curves 57; flat-top crests 32–33; Fusegates 112; half-round crests 32, 34–37; labyrinth weirs 42–43, 87–88; nappe crests 32, 37–39; nappe interference 20; quarter-round crests 32, 33; relation to head 79–80; sharp crests 32–33; theoretical minimum value 32; upstream head 50
discharge computations 54–56
disturbance coefficient 20
disturbance lengths 20–23; defined 22
- efficacy 79–80
energy dissipation 6, 65, 114
errors, modeling: random errors 123; systematic errors 119–122
- falling jets 104–106; impact types 105
fish ladders 6
Flamingo Detention Dam 113–115
flow: aerated 6, 35, 41–42, 70, 103–108; approach conditions 82–84; cavity 34; directing using aprons 64–66; discharge equation 123; equations 9–11; instability 70; model studies 125–126, 129; stages 41–42; surging 74–75
flow splitter walls 63–64, 74–75, 114
Froude number 14, 119
Fusegates 5, 109–113; discharge coefficient 112
- Garland Canal 95, 98–99; design diagram 139
head 9; atmospheric flow 34; design 34, 37; nappe interference 20; nappe vibration 69; relation to discharge coefficient 79–80; total 9, 12, 28; upstream 33, 37, 43–44, 50
- headwater ratio 77
Hellsgate 95, 97–98
Hyrum spillway 140

- ice 100–101
- interference length ratio 82
- jet direction 9
- jets, falling 104–106; impact types 105
- Kizilcapinar spillway 141
- layout, labyrinth weir 84–87
- magnification 78
- model studies: *see* models
- modeling procedures: *see* models
- models 119–129; application 124–125; case study 125–129; design modification 127–128; model operation 121–122; model scale 125; operation 121–122; random errors 123; systematic errors 119–122
- momentum approach, for flow equations 9, 11
- nappes 6; interference 19–29; interference models 24–29; oscillation 69–76; vibration 69–74
- oscillations, nappes 69–76
- Prado Dam 25; discharge coefficient 128; model studies 125–128
- Quincy Spillway 63
- ratios: apex 81; headwater 77; interference length 82; magnification 78; vertical aspect 77
- reservoir head: *see* total head
- Ritschard Dam 28; design diagram 142
- Rollins Dam 25–26
- Sarioglan spillway 143
- sedimentation 95–100
- sheet piling 115–117
- sidewall angle 15; design parameters 77, 78; disturbance lengths 22; and efficacy parameter 79; and nappe interference 20–21; trapezoidal labyrinth weirs 78; triangular labyrinth weirs 78
- spillways 1–5; alignment 129; Arnwell Magna 65; capacity 6; Hyrum 140; Kizilcapinar 141; Quincy 63; Sarioglan 143; shapes 4–5; *see also* specific types below
- spillways, bathtub 3–4
- spillways, duckbill 1–2
- spillways, side channel 1–2; energy equations 11–13; flow equations 9–11; momentum equations 13–14
- splitter walls 63–64, 74–75, 114
- spreadsheet, for weir design procedure 89–94
- submergence 67–68
- supercritical waves 61–64
- surface tension 119–121
- surging flow 74–75
- Tongue River Dam 100–101
- total head 9, 12, 28
- upstream head 33, 37; defined 43–44; discharge coefficient 50
- Ute Dam 26; design diagram 144; supercritical waves 63
- vibrations, nappe 69–74
- walls, flow splitter 63–64, 74–75, 114
- waves, supercritical 61–64
- Weber number 119; sharp crests 120
- weirs 1–5; streamlines 6
- weirs, labyrinth 4–6; apex ratio 81; applicability of design curves 56–59; approach flow conditions 82–84; case study 125–129; crest shapes 82; design curves 44–59, 147; design parameters 77–88; design procedure 88–93; dimensions 84–86; discharge coefficient 42–43, 87–88; downstream chutes 84; flow 6; flow equations 16; headwater ratio 77; interference length ratio 82; layout 84–87; magnification 78; magnification ratio 78; nappe interference 24–29; prototypes 133–144; quarter-round crests 41–42; rectangular 42, 80; shapes 42; sidewall angle 77, 78; special cases 109–117; submergence 67–68; vertical aspect ratio 77; volume computations 86–87; *see also* specific labyrinth shapes below
- weirs, linear 31–39
- weirs, rectangular: efficacy parameter 80; performance 106
- weirs, skew 15–16
- weirs, trapezoidal 42–43; design curves 46, 50, 52, 59; efficacy parameter 80; sidewall angle 78
- weirs, triangular 42–43; apex ratio 81; design curves 45, 50–51, 59; efficacy parameter 79; performance 106; sidewall angle 78
- Woronora Dam 24; design curves 58; nappe vibration 70–72